

AL/OE-TR-1994-0141



ULTRASHORT PULSE LASER EFFECTS IN THE PRIMATE EYE

Clarence P. Cain
Gary D. Noojin
David J. Stolarski

The Analytical Sciences Corporation (TASC)
San Antonio, Texas

Cynthia A. Toth
Duke University Eye Center
Durham, North Carolina

Cheryl D. DiCarlo, Captain, USAF

Veterinary Science Division
Brooks Air Force Base, Texas

William P. Roach, Captain, USAF
Cindy D. Stein, First Lieutenant, USAF

OCCUPATIONAL AND ENVIRONMENTAL HEALTH DIRECTORATE
Optical Radiation Division
8111 18th Street
Brooks Air Force Base, Texas 78235-5215

November 1994

DTIC QUALITY INSPECTED 5

Interim Report for Period March 1993 - June 1994

Approved for public release; distribution is unlimited.

AIR FORCE MATERIEL COMMAND
BROOKS AIR FORCE BASE, TEXAS

19950524 002

NOTICES

When Government drawings, specifications, or other data are used for any purpose other than in connection with a definitely Government-related procurement, the United States Government incurs no responsibility or any obligation whatsoever. The fact that the Government may have formulated or in any way supplied the said drawings, specifications, or other data, is not to be regarded by implication, or otherwise in any manner construed, as licensing the holder or any other person or corporation; or as conveying any rights or permission to manufacture, use, or sell any patented invention that may in any way be related thereto.

The animals involved in this study were procured, maintained and used in accordance with the Animal Welfare Act and the "Guide for the Care and Use of Laboratory Animals" prepared by the Institute of Laboratory Animal Resources - National Research Council.

The Office of Public Affairs has reviewed this report, and it is releasable to the National Technical Information Service, where it will be available to the general public, including foreign nationals.

This report has been reviewed and approved for publication.

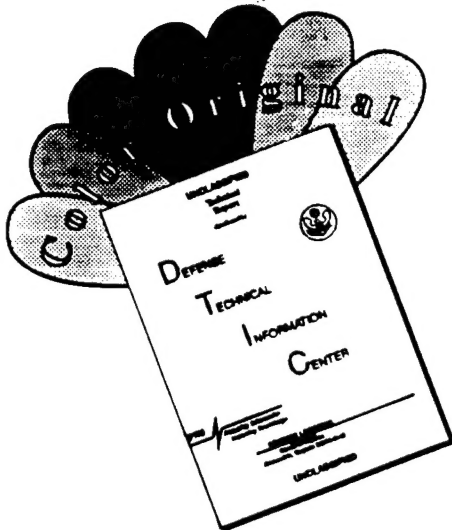
Government agencies and their contractors registered with Defense Technical Information Center (DTIC) should direct requests for copies to: DTIC, Building 5, Cameron Station, Alexandria VA 22304-6145.

Non-Government agencies may purchase copies of this report from: National Technical Information Service (NTIS), 5285 Port Royal Road, Springfield VA 22161-2103.



ROBERT M. CARTLEDGE, Lt Col, USAF, BSC
Chief, Optical Radiation Division

DISCLAIMER NOTICE



THIS DOCUMENT IS BEST
QUALITY AVAILABLE. THE COPY
FURNISHED TO DTIC CONTAINED
A SIGNIFICANT NUMBER OF
COLOR PAGES WHICH DO NOT
REPRODUCE LEGIBLY ON BLACK
AND WHITE MICROFICHE.

REPORT DOCUMENTATION PAGE

Form Approved
OMB No. 0704-0188

Public reporting burden for this collection of information is estimated to average 1 hour per response, including the time for reviewing instructions, searching existing data sources, gathering and maintaining the data needed, and completing and reviewing the collection of information. Send comments regarding this burden estimate or any other aspect of this collection of information, including suggestions for reducing this burden, to Washington Headquarters Services, Directorate for Information Operations and Reports, 1215 Jefferson Davis Highway, Suite 1204, Arlington, VA 22202-4302, and to the Office of Management and Budget, Paperwork Reduction Project (0704-0188), Washington, DC 20503.

1. AGENCY USE ONLY (Leave blank)	2. REPORT DATE	3. REPORT TYPE AND DATES COVERED	
	November 1994	Interim - March 1993 - June 1994	
4. TITLE AND SUBTITLE		5. FUNDING NUMBERS	
UltraSHORT Pulse Laser Effects in the Primate Eye		C - F33615-92-C-0017 PE - 62202F PR - 2312 TA - A1 WU - 01	
6. AUTHOR(S)		8. PERFORMING ORGANIZATION REPORT NUMBER	
Clarence Cain, Gary Noojin, David Stolarski, Cynthia Toth, Cheryl DiCarlo, William Roach, and Cindy Stein			
7. PERFORMING ORGANIZATION NAME(S) AND ADDRESS(ES)		9. SPONSORING/MONITORING AGENCY NAME(S) AND ADDRESS(ES)	
TASC, Incorporated 750 East Mulberry Suite 302 San Antonio, TX 78212-3159		Armstrong Laboratory Occupational and Environmental Health Directorate Optical Radiation Division 8111 18th Street Brooks Air Force Base, Tx 78235-5114	
11. SUPPLEMENTARY NOTES		10. SPONSORING/MONITORING AGENCY REPORT NUMBER	
		AL/OE-TR-1994-0141	
12a. DISTRIBUTION/AVAILABILITY STATEMENT		12b. DISTRIBUTION CODE	
Approved for public release; distribution is unlimited.			
13. ABSTRACT (Maximum 200 words)			
Minimum visible lesion (MVL) threshold measurements at the retina for rhesus monkey eyes are reported for femtosecond, picosecond, and nanosecond single laser pulses using visible wavelengths. Estimates of the dose causing 50% probability for damage (ED_{50}) are calculated for 1-hour and 24-hours postexposure as well as the 95% fiducial intervals for ED_{50} . The ED_{50} values are found to be dependent on both wavelength and pulsedwidth, and for a single wavelength are, in general, lower for short pulsedwidths, with the exception of values at the shortest pulsedwidth of 90 fs at 580 nm. At 90 fs the ED_{50} dosages were noted to increase slightly when compared with the 3-ps and 600-fs values, all three delivered at 580-nm wavelength. The 4-ns ED_{50} value was more than double the value at 60 ps delivered at 532-nm wavelength. Fluorescein angiography was accomplished at 1-hour and 24-hours postexposure and did not demonstrate lower threshold for damage, which has been the case for MVLs created with longer pulse duration (greater than 1 ns) or for rabbit eyes at the same pulsedwidths as measured in our laboratory.			
14. SUBJECT TERMS		15. NUMBER OF PAGES	
Eyes; Femtosecond; Minimum visible lesions; Pulsedwidth; Nanosecond; Picosecond; Rhesus monkey; Wavelength		126	
16. PRICE CODE			
17. SECURITY CLASSIFICATION OF REPORT	18. SECURITY CLASSIFICATION OF THIS PAGE	19. SECURITY CLASSIFICATION OF ABSTRACT	20. LIMITATION OF ABSTRACT
Unclassified	Unclassified	Unclassified	UL

TABLE OF CONTENTS

	Page
ACKNOWLEDGMENTS	v
INTRODUCTION	1
METHODS.....	2
Experimental Systems	2
<i>In Vivo</i> Model.....	3
<i>In Vivo</i> Preparation.....	3
Statistical Analysis	5
RESULTS.....	6
Visible Lesion Thresholds	6
Hemorrhagic Lesion Thresholds.....	8
DISCUSSION.....	10
CONCLUSION.....	13
REFERENCES	15
APPENDIX A.....	17
APPENDIX B	101

Accesion For	
NTIS	CRA&I
DTIC	TAB
Unannounced	
Justification	
By	
Distribution /	
Availability Codes	
Dist	Avail and / or Special
A-1	

FIGURES

Figure No.		Page
1	Schematic of the ultrashort laser pulse system and laser delivery system.....	2
2	The L-shaped grid pattern is placed as a marker grid at the edge of the macular region.....	5
3	Retinal Maximum Permissible Exposure for ANSI Z136.1-1993	14

TABLES

Table No.		Page
1	Minimum visible lesions threshold	6
2	Fluorescein angiography minimim visible lesion threshold	8
3	Hemorrhagic lesions produced in rhesus monkey eyes for all pulsewidths and pulse energies	9

ACKNOWLEDGMENTS

We wish to thank Drs. Frank E. Cheney, Jr. and Leon N. McLin, Jr., of AL/OEO, for their careful refraction of the animal eyes.

INTRODUCTION

The National Laser Safety Standard, ANSI Z136.1-1993¹, defines a maximum permissible exposure (MPE) for the retina from visible and near-infrared laser radiation. This standard applies to pulse durations down to 1 nanosecond (ns); it is based on retinal injury studies conducted on primate eyes for continuous-wave and pulsed laser systems with pulsedwidths greater than 2 ns. The few retinal studies that have been reported for pulsedwidths less than 1 ns in the rhesus monkey eyes²⁻⁶ were almost all for picosecond (ps) pulsedwidths. Two studies have been reported for femtosecond (fs) pulses in rabbits. In one study, Birngruber et al.⁷ measured the 50% probability for damage (ED₅₀) visible threshold dosage in chinchilla gray rabbit eyes for 80-fs pulsedwidths at 625 nanometers (nm). In the other study, Toth et al.⁸ reported damage thresholds for 90-fs pulsedwidths at 580 nm in the dutch-belted rabbit.

This study utilizes rhesus monkey⁹ eyes to determine the ED₅₀ threshold doses necessary to create visible lesions in the macular region for various pulsedwidths from 4 ns down to 90 fs. Our goal in this study was to evaluate retinal damage thresholds for single pulsedwidths in the rhesus monkey fundus. Further, our goal was to acquire urgently needed data to assess potential human retinal hazards that could be applied to new national laser safety standards for subnanosecond laser systems operating in the visible and near-infrared spectral regions. We have determined the threshold dosages for visible lesions for pulsedwidths of 90 and 600 fs and 3 ps at 580 nm and for pulsedwidths of 60 ps and 4 ns at 532 nm. These subnanosecond laser ocular tissue interaction studies are critical in identifying hazards to the human eye and in considering future clinical applications in laser surgery. Such studies also provide new insight into the biological information of intense electromagnetic fields. In our work, we define a "visible lesion" as a visible change in the fundus readily seen by at least two observers. Both observers must agree that the change in the fundus is actually a lesion before that exposure site is counted as a positive event. A minimum visible lesion (MVL) then is defined as a change in the fundus due to laser insult just minimally visible by the two observers, either ophthalmoscopically or from photographs of fluorescein angiography (FA).

In an earlier study we had determined the ED₅₀ MVL dosages for dutch-belted rabbit eyes^{8,10,11} from 5 ns down to 90 fs; herein we present our findings for the rhesus monkey eyes.⁶ For the present primate study we found a notably lower threshold for MVLs compared with our rabbit studies. These results are important in providing eye safety information because laser systems capable of producing subnanosecond pulses are in widespread use throughout the research, medical, and military communities. The low energy required for intraretinal hemorrhages was identified although subretinal hemorrhages were similarly difficult to create (or more so than in the rabbit). These studies demonstrate that the rabbit model cannot be extrapolated to predict human ocular injury.

METHODS

Experimental Systems

The ultrashort pulse laser system shown in Figure 1 produces a range of pulsewidths, wavelengths, and energy levels with relative ease of reconfiguration. It produces single pulses with an adjustable pulse repetition rate between single pulses and 10 pulses per second (pps). All pulses generated can have energies greater than 100 microjoules (μJ). This system consists of a dye laser pumped by a mode-locked (82 megahertz (MHz)), pulse-compressed, frequency-doubled neodymium:yttrium-aluminum-garnet (Nd:YAG) laser. The dye laser output is amplified by a three-stage pulse dye amplifier (PDA) which is pumped by a seeded, frequency-doubled Nd:YAG regenerative amplifier. Pulsewidths are measured by an INRAD Slow Scan Autocorrelator. The pulses from the PDA can also be compressed to achieve below 100-fs pulses by chirping the pulses before amplifying and rephasing the spectrally broadened pulse in time thereby giving rise to the compressed pulse afterwards. The PDA pulsewidths range between 3 ps and 90 fs at 580 nm. Pulses of 60 ps and 4 ns at 532 nm are generated by the seeded Nd:YAG regenerative amplifier or the Nd:YAG Q-switched laser.

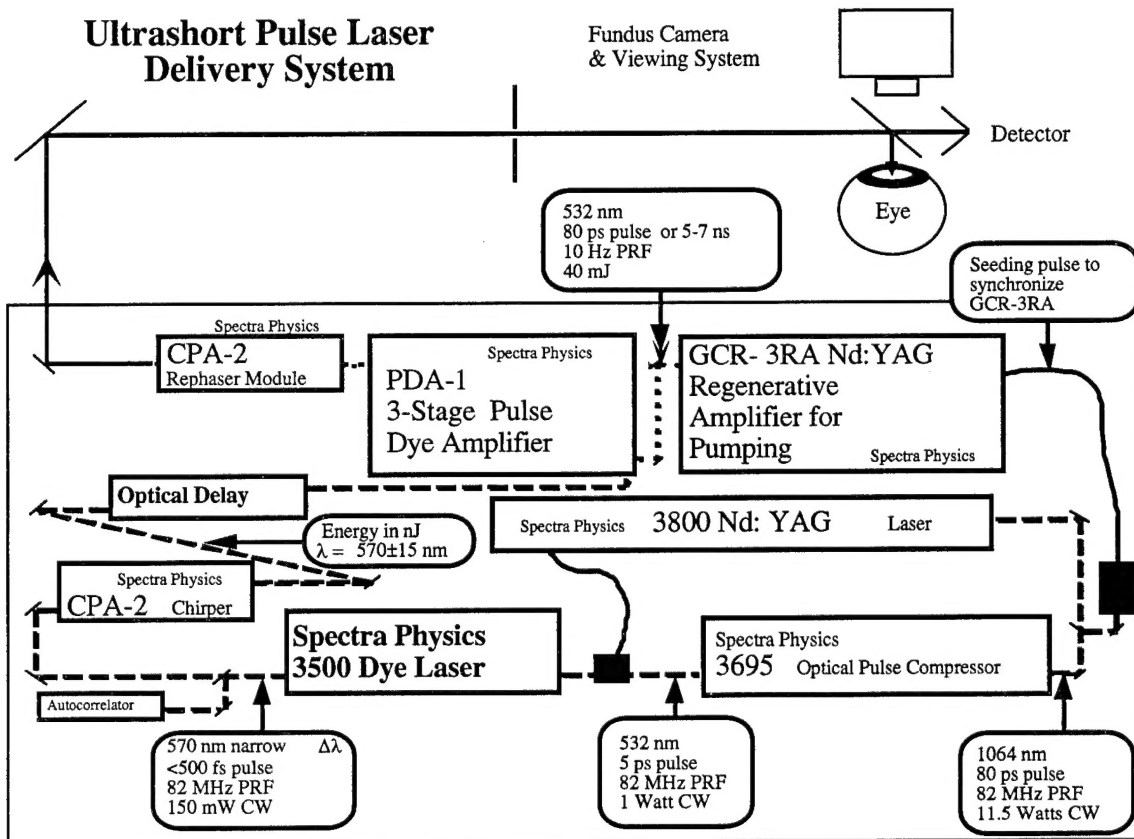


FIGURE 1. Schematic of the ultrashort laser pulse system and laser pulse delivery system.

The incident laser beam was apertured to provide a uniform spatial profile with a beam diameter of 2.5 millimeters (mm) for delivery to the corneal surface. Single pulses were delivered to monkey eyes by deflecting the beam off a glass beamsplitter (Figure 1) mounted on a Zeiss fundus camera; the beamsplitter path was adjusted such that the deflected beam was collinear with the optical axis of the fundus camera. These 580-nm beamsplitters have antireflective coatings that minimize second surface reflections and prevent double pulse generation. For suprathreshold experiments at 90 fs, the incident beam aperture was opened to 5 mm and the glass beamsplitter was replaced by a front surface mirror. The laser beam path length from aperture to incident corneal surface was 1 meter. The beam divergence was ~ 0.5 milliradian. The unamplified 580-nm mode-locked beam at 82 MHz from the pulsed dye amplifier was used to align retinal exposure sites. The output of the dye laser, 300-fs pulsewidths with 82 MHz at 580 nm and 20 to 30 milliwatts (mW), was shuttered between 100 and 200 milliseconds (ms) and used for producing retinal marker lesions.

The monkey cornea was positioned approximately 1 centimeter (cm) in front of the beamsplitter with the retina in the focal plane of the fundus camera. The single pulse was split by the 580-nm beamsplitter so that the reflected pulse could be sent to the eye while the transmitted pulse could be measured and its energy value recorded for each exposure to the eye. The reflected/transmitted (R/T) ratio was measured at the beginning and end of each session to ensure that its value did not change. Energies and ratios were measured by a joulemeter/ratiometer (Molelectron JD2000 or an OM4001) with one detector (Molelectron J3-09 or J4-09) at the eye position calibrated against a second detector intersecting the fraction of the beam being transmitted. Throughout this report "laser energy delivered" is the energy delivered to the corneal surface as described above and without any contact lens or other device to control the image size delivered to the retina within the eye.

In Vivo Model

Mature rhesus monkeys from 2.2 to 6.9 kilograms (kg) were maintained under standard laboratory conditions (12 hours light, 12 hours dark). Rhesus monkeys were screened preexposure to ensure that no eye was more than one-half diopter from being emmetropic. All procedures were performed during the light cycle. The treatment and procedures used in this study conformed to the use of Animals in Research and Federal Guidelines and the research protocol USAFSAM Protocol RZV-91-04¹².

In Vivo Preparation

Rhesus monkeys were chemically restrained using 10 milligrams (mg)/kg ketamine hydrochloride (HCl) intramuscularly. Once restrained, 0.16 mg atropine sulfate was administered subcutaneously. Two drops of proparacaine HCl 0.5%, phenylephrine HCl 2.5%, and tropicamide 1% were each administered to both eyes. Under ketamine restraint, the monkey had intravenous catheters placed for administration of warmed

lactated Ringer's solution (10 milliliters (ml)/kg/hour (hr) flow rate) and for administration of propofol. An initial induction dose of propofol (5 mg/kg) was administered to effect. The state of anesthesia was maintained in the monkey using 0.2 - 0.5 mg/kg/hr of propofol via syringe pump. The monkey was intubated with a cuffed endotracheal tube. A peribulbar injection of 2% lidocaine was administered to reduce extraocular muscular movement. The monkey was securely restrained in a prone position on an adjustable stage for the fundus photography, laser exposure, and FA. Prior to FA, 0.6 ml of Fluorescite 10% (Alcon Laboratories) was administered intravenously. The monkey's blood pressure and pulse were continuously monitored throughout the experimental protocol. The monkey's normal body temperature was maintained by the use of circulating hot water blankets.

Baseline fundus photography was performed prior to laser exposures. The eyelids were held open with a wire lid speculum, and the cornea was moistened throughout the procedures with 0.9% saline solution. The retina was viewed with a modified fundus camera through a glass beamsplitter. All macular exposures (15 to 30) were delivered to each eye, without any contact lens, in a rectangular grid pattern in the macular region of the fundus. Visible marker lesions (created by shuttered exposures of the dye laser output at 82 MHz) marked the exposure grid in columns and rows. To aid in localizing the exposure sites, an L-shaped grid pattern of marker lesions was placed around the edge of the macular region prior to the MVL exposures as shown in Figure 2. As seen within the grid pattern, there are small whitish spots just visible to the naked eye which are representative of MVLs used in the database to determine ED₅₀ values. These laser exposures were delivered at 90 fs, 580 nm, with energy variations between 0.1 and 10 μ J per pulse and were placed within the grid pattern, centered over the macular region for both the left (OS) and right (OD) eyes of our subjects.

Suprathreshold lesions (greater than 10 μ J) were placed extramacularly and away from the threshold grid so that a wider scattered pattern would avoid overlapping of lesions. A minimum of two examiners evaluated all eyes at 1-hr and 24-hr postexposure. Visible lesions at a given exposure site were reported only if the two examiners identified a lesion. Fundus photography and FA were performed at 1-hr and 24-hr postexposure. Fundus photographs of ophthalmoscopically visible lesions and FAs were evaluated for lesion presentation. Two eyes were exposed with a grid of nine shots for each pulselwidth and enucleated after 1- and 24-hr postexposure for histopathological evaluations. The results of the histopathology study of the lesions will be published in a later treatise.

Fundus photography (including FA) and observations of lesion formation by the researchers were performed by monocular viewing through the Zeiss fundus camera optical system. Thus the optics were not changed between fundus viewing and photography, and viewing and photography were performed interchangeably. Photographs for FA were taken immediately before the dye injection and continued at intervals of a few seconds until five minutes had elapsed, thus providing a sequence of photographs for the development of fluorescein leakage. After fluorescein injection and

angiography, in (most) animals, lesions were also assessed for fluorescence by viewing through the camera system with excitation and barrier filter in place. However, fluorescein leakage for the smaller lesions could not be identified by this method and it was not used for this paper.

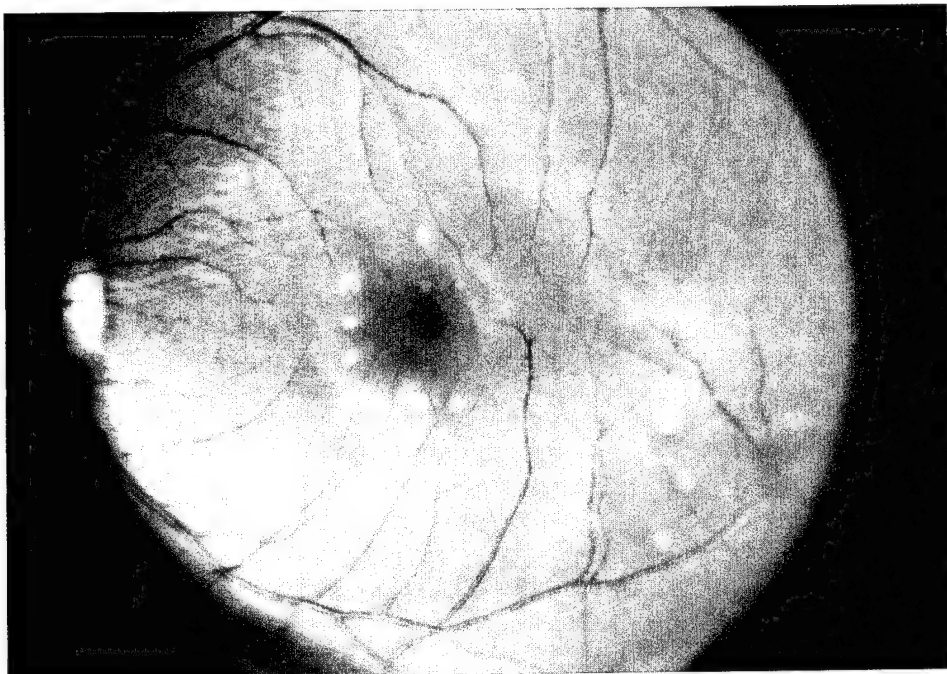


FIGURE 2. The L-shaped pattern is placed as a marker grid at the edge of the macular region. Within the grid pattern, whitish visible lesions were created using 90 fs, 580 nm, and 0.1 to 10 μ J energy pulses in the rhesus monkey eye.

Statistical Analysis

The Probit Procedure¹³ was used to estimate the ED₅₀ dose for creating an MVL in the retina for 4-ns, 60-ps, 3-ps, 600-fs, and 90-fs pulsewidths and to estimate the 95% confidence intervals for the ED₅₀s. Enough data was taken to ensure that the fiducial limits were reasonably narrow. The probit procedure was used for the ophthalmoscopically visible lesion data at 1 and 24 hr and for the data from the FAs. Table 1 includes the 1- and 24-hr estimated doses for ED₅₀ thresholds along with the slope of the probit curve for the 24-hr reading. Also included are the number of subjects, number of eyes, and total exposures for each pulsewidth delivered. Appendix A contains the complete SAS-Probit analyses for each of the five pulsewidths together with the ordered raw data and the predicted probabilities values from 0.01 to 0.99 inclusive. The program titled SAS-PC PROBIT.NOojin is included for the PC version of SAS also so that any new data may be analyzed using the identical procedure.

RESULTS

Visible Lesion Thresholds

For the pulsedwidths generated at 532 nm (4 ns and 60 ps), not all of the lesions developed during the first hour, and exposures at 60 ps took longer to develop than did the 4-ns exposures. The number of lesions observed increased by 25% at 4 ns and by 32% at 60 ps between the 1- and 24-hr postexposure readings. Consequently, the calculated 24-hr ED₅₀ threshold dosages had to be reduced considerably for both pulsedwidths as listed in Table 1. This table includes the 1- and 24-hr estimated doses for ED₅₀ thresholds with the 95% fiducial intervals along with the slope of the probit curve for the 24-hr reading. The slope is calculated using the ED₈₅ and ED₅₀ points to obtain the values listed at each pulsedwidth. Also included are the number of subjects, number of eyes, and total exposures for each pulsedwidth. The retinal response to minimal exposures was consistently a pale gray to white lesion increasing in whiteness and in size as energy increased in all exposures. Exposures with energies ranging from (0.03 - 6.6 μ J) for both pulsedwidths were placed macularly. For the 4-ns study, two eyes from two different monkeys were used for a total of 50 exposures in the macular region. At 60 ps, five eyes from five different monkeys were exposed, with 88 total exposures in the macula. Color fundus photographs for the these pulsedwidths showing typical lesions in the macular region are included in Appendix B.

TABLE 1. Minimum Visible Lesions Threshold - ED₅₀ for Rhesus Monkeys at the 95% Confidence Level with Fiducial Limits in Parentheses.

PULSEDWIDTH	1 HOUR READING ED ₅₀ (μ J)	24 HOUR READING ED ₅₀ (μ J)	SLOPE OF PROBIT CURVE
4 ns 2 Subjects, 2 Eyes, 50 Exposures	1.5 (0.75 - 8.93)	0.9 (0.60 - 1.35)	2.68
60 ps 5 Subjects, 5 Eyes, 88 Exposures	0.66 (0.46 - 1.05)	0.43 (0.32 - 0.54)	3.03
3 ps 4 Subjects, 4 Eyes, 68 Exposures	0.68 (0.40 - 0.91)	0.58 (0.31 - 0.83)	2.61
600 fs 5 Subjects, 6 Eyes, 112 Exposures	0.60 (0.43 - 0.84)	0.26 (0.21 - 0.31)	4.11
90 fs 5 Subjects, 7 Eyes, 122 Exposures	1.18 (0.83 - 2.09)	0.43 (0.27 - 0.60)	1.58

For the pulsedwidths evaluated at 580 nm (3 ps, 600 fs, and 90 fs), the delay in the appearance of a visible lesion to minimal retinal laser exposures depended on the pulse energy and on the pulsedwidth. The retinal response to these exposures was consistently a pale gray to white lesion increasing in whiteness and in size as energy increased as before. At 3 ps, threshold retinal lesions were visible almost immediately; 98% were visible after only 1 hr. The range of energies (0.45 μ J to 1.43 μ J) producing a visible lesion did not change between the 1- and 24-hr evaluations. Color fundus photographs for typical lesions at these three pulsedwidths are included in Appendix B.

For 600-fs pulsedwidths, the time required for a lesion to appear increased significantly; only half were visible after 10 minutes. From the 1-hr reading to the 24-hr reading, we observed an increase of 30% in the number of visible lesions at a given exposure level. The MVL ED₅₀ threshold dosage calculated for 24 hr was less than half the value calculated for 1 hr. Also, the range of pulse energies from minimum-to-maximum (minimum lesion to maximum no-lesion) decreased significantly from the 1-hr reading to the 24-hr reading (0.22 μ J - 3.0 μ J to 0.17 μ J - 0.45 μ J).

At 90-fs pulsedwidths, the delay in appearance of visible lesions past the 1-hr reading was even more pronounced, and the calculated ED₅₀ values were larger than the 600-fs values for both the 1-hr and 24-hr calculations. Again, the ED₅₀ dosage calculated at 24 hr was less than half the value at 1 hr, showing that a large number of lesions (28) developed between 1 hr and 24 hr. In fact, a 48% increase in the number of visible lesions (58 to 86) occurred at the 24-hr reading. The range of energies from minimum-to-maximum did not change significantly during the 24-hr postexposure examinations (0.16 μ J-1.8 μ J to 0.10 μ J-1.4 μ J). Above 1.4 μ J, all energies delivered showed visible lesion development. Out of 122 data points taken at 90 fs within the macula, 94 exposures were within the energy range of 0.1 μ J to 1.4 μ J, and 49 lesions developed within 24 hours. For 3 ps, four monkeys and four eyes were used for a total of 68 exposures. For 600 and 90 fs, six monkeys were used for each pulsedwidth with six eyes exposed with 112 exposures and seven eyes exposed with 122 exposures respectively as listed in Table 1.

In our studies, FA appeared to be much less sensitive in identifying retinal lesions than determining the lesions ophthalmoscopically. This insensitivity occurred across all readings for our pulsedwidths, wavelengths, and observation times. At 3 ps, the fluorescein angiography visible lesion (FAVL) ED₅₀ value dropped from 2.8 μ J at 1 hr to 1.3 μ J at the 24-hr readings. However the FAVL ED₅₀ values were much higher than the ophthalmoscopically determined MVLs. For the 600-fs pulses, the FAVL ED₅₀ value dropped from 3.7 μ J to 1.5 μ J after 24 hr. These values are six times higher than the MVLs read funduscopically. In each case the 24-hr reading was lower than the 1-hr reading. This was not the case with 90 fs, where the 24-hr calculated FAVL ED₅₀ thresholds were more than 1.6 times the value at 1 hr and more than 6.7 times the MVL ED₅₀ value. Using FA as an endpoint, the trend of more lesions showing up after 24 hr dramatically reversed at 90 fs, and many of the lesions counted after 1 hr simply disappeared during the post 24-hr FA evaluation. Although, the number of

funduscopically visible lesions increased from 58 to 86 at 24-hr postexposure, the number of lesions showing up on FA decreased from 43 at 1 hr down to 25 after 24 hr. The data for our FA work are given in Table 2 along with the MVL ED₅₀ values for comparison. Black and white fundus photographs for the FA have been included in Appendix B for all 5 pulsewidths for each primate eye which have color fundus photographs showing visible lesions.

TABLE 2. Fluorescein Angiogram Minimum Visible Lesion Threshold - FAVL ED₅₀ for the Rhesus Monkey Compared to ED₅₀ MVL.

PULSEWIDTH		1 HOUR READING (μ J)	24 HOUR READING (μ J)
4 ns 532 nm	FAVL	*	1.8 (1.2 - 3.7)
	MVL	1.5	0.9
60 ps 532 nm	FAVL	1.9 (1.1 - 10.1)	1.5 (0.98 - 4.4)
	MVL	0.66	0.43
3 ps 580 nm	FAVL	2.8 (2.1 - 4.7)	1.3 (1.0 - 1.6)
	MVL	0.68	0.58
600 fs 580 nm	FAVL	3.7 (2.5 - 6.3)	1.5 (1.2 - 2.0)
	MVL	0.60	0.26
90 fs 580 nm	FAVL	1.9 (1.2 - 5.1)	2.9 (1.6 - 13.6)
	MVL	1.18	0.43

*Data not at 95% confidence level.

Hemorrhagic Lesion Thresholds

In the rhesus monkey, laser exposures at 90 fs were directed to the macula for lesions created with energies under 10 μ J. All laser exposures exceeding this value were directed away from the macula, most of which were directed nasal to the optic disc, and a few were directed outside the temporal arcades. Of the 122 exposures (0.01 to 9.3 μ J) delivered to the macula at 90 fs, seven hemorrhagic lesions were produced with 0.83 to 4.8 μ J energy (2 to 11 times MVL ED₅₀ of 0.43 μ J). While delivering energy within the macular grid pattern, the laser would infrequently intersect the network of retinal microvessels. Macular hemorrhagic lesions were seen only when the exposure site coincided with a small blood vessel. The area of the hemorrhages was approximately 50 to 250 micrometers (μ m) in diameter (estimated relative to the optic nerve and vessel size in photographs), and they were either thin with lacy margins or very slightly thickened with smooth round margins. The hemorrhage location appeared to be intraretinal for several lesions; however, without stereo imaging, it was difficult to differentiate small intraretinal versus subretinal hemorrhages. With FA, the blood from the macular hemorrhages blocked fluorescence from both the underlying retinal vessel and the choroid.

At one of the sites there was late fluorescein leakage from the margin of the hemorrhage. While many hemorrhages appeared almost immediately, three hemorrhages in one eye, not visible immediately after laser exposure, developed within 1 hr and increased in size over the next 24 hr. These same hemorrhagic lesions were not visible ophthalmoscopically, 29 days after laser exposure. All data for hemorrhagic versus nonhemorrhagic lesions has been summarized in Table 3 for all exposures and pulsewidths.

TABLE 3. Hemorrhagic Lesions Produced in Rhesus Monkey Eyes for all Pulsewidths and Pulse Energies.

PULSEWIDTH	ENERGY DELIVERED TO CORNEA (μ J)	HEMO. LESIONS	NONHEMO. LESIONS	TOTAL LESIONS	TOTAL EXPOS.
90 fs	0.01- 9.3 ext.macular - (14 - 105)	7 5	63 17	70 22	122 (22)
600 fs	0.02 - 15.5 ext.macular -(2)	7 3	64	71	112 (3)
3 ps	0.03 - 11.4	6	41	47	68
60 ps	0.03 - 6.6	1	49	50	88
4 ns	0.09 - 5.0	0	25	25	50

Of 21 suprathreshold energy exposures (14 to 105 μ J) at 90 fs and 580 nm placed outside the macula, five hemorrhagic lesions were produced by energies ranging from 38 to 105 μ J. One of these lesions demonstrated a very faint (less than 50 μ m) red lesion ringed by a white chorioretinal lesion. Three lesions were probably subretinal hemorrhages (although intraretinal blood leakage from retinal vasculature is possible) of approximately 50 to 100 μ m diameter with a rim of white chorioretinal thickening. One laser site (81 μ J) over a retinal venule demonstrated an immediate retinal hemorrhage which enlarged over 24 hr. With FA, the injured retinal vessel demonstrated leakage within the area of blocked fluorescence from the hemorrhage.

Sixteen suprathreshold lesions (14 to 82 μ J) were nonhemorrhagic even though the laser energy for several of these was delivered directly to overlying retinal blood vessels. The lesions were white and, as with rabbit lesions⁸, their size increased as pulse energy increased.

For the 600-fs pulses, a total of 112 exposures were placed within the macula, all had energies between 0.02 μ J and 15.5 μ J. Seven of fourteen exposures with energies ranging from 3.6 μ J to 15.5 μ J, produced hemorrhagic lesions in the macular region. Three exposures with energies of 2.1 μ J were placed nasal to the optic disc and all three produced hemorrhages. All lesions produced at this pulsedwidth appeared to be in intraretinal vessels; none were believed to be choroidal hemorrhages. Similar results were found at 3-ps pulses where six hemorrhagic lesions were produced in the macula by energies ranging from 1.6 μ J to 11.4 μ J; all were intraretinal hemorrhagic lesions. All hemorrhagic lesions produced in the macula were counted as positive lesions in the MVL data pool because they were always visible funduscopically.

At the 4-ns pulsedwidth there were no hemorrhages produced for pulse energies ranging up to 5 μ J within the macular area. At the 60-ps pulsedwidth, there was only one hemorrhage produced with 6.6 μ J intraretinally; no attempt was made to produce hemorrhages with suprathreshold doses. Of the 88 total exposures for 60 ps and 532 nm, only one pulse had an energy greater than 4.1 μ J and it produced a hemorrhage. All pulses within the range of energies used (0.03 μ J - 6.6 μ J) for both pulsedwidths were placed within the macular area; no attempt was made to create hemorrhages within or outside of the macular area with suprathreshold energies.

DISCUSSION

We have determined the MVL thresholds for laser pulsedwidths from 4 ns down to 90 fs. As listed in Table 1, all ED₅₀ values are below 1.0 μ J with the exception of the 1-hr readings at 4 ns and 90 fs. In assessing the implications of retinal laser damage observed in this study, we consider biological and laser variables which impact the damage thresholds measured. The biological variables which affect ED₅₀ include species, ocular anatomy, retinal lesion location, retinal vasculature, pigmentation of the retinal pigment epithelium, and choroid. This study is the first to report lesions in primate eyes for pulsedwidths from 4 ns down to 90 fs; it is directly comparable to all other data reported for the primate eyes down to 6 ps, including the data from which the ANSI Z136.1-1993¹ standard is derived.

The laser variables which impact the determination of retinal damage thresholds include wavelength, pulse duration or pulsedwidth, beam diameter incident upon the cornea, beam profile, retinal spot size, beam divergence, and optics used in the pulse delivery. One benefit from our study is the evaluation of a wide range of laser pulsedwidths using the same species and delivery system. The change in MVL thresholds identified in our study for the five pulsedwidths and two wavelengths suggests that the calculated ED₅₀ thresholds depend not only on pulsedwidth, but on the wavelength as well, which one would expect to be the case.

For the two pulsedwidths at 532 nm, 4 ns and 60 ps, the number of lesions observed between the 1-hr reading and the 24-hr reading increased between 25% and 32% which

had the effect of lowering the MVL ED_{50} threshold doses calculated by probit analyses. At 4 ns, the threshold dose decreased from 1.5 μ J to 0.9 μ J after 24 hr while the value at 60 ps decreased from 0.66 μ J to 0.43 μ J after 24 hr. The slope of the probit curve increased from 2.68 to 3.03 when the pulsedwidth was reduced from 4 ns to 60 ps while the ED_{50} decreased from 0.9 μ J to 0.43 μ J, respectively. However, these slopes are larger than those reported by Lund and Beatrice¹⁴ (1.58 for the slope of the regression line defined as ED_{84}/ED_{50}) for doubled Nd:YAG pulses at 140-ns pulsedwidths.

Ophthalmoscopically, the time interval for development of retinal MVLs for the 580-nm wavelength increased significantly for 600 and 90 fs as with 4 ns and 60 ps, but this was not true for the 3-ps case. For 600 fs, there were 21 exposures between 0.17 and 3.0 μ J, which required more than 1 hr to develop out of a total of 112 exposures. These delayed lesions reduced the MVL ED_{50} threshold dosage calculations from 0.60 μ J (1 hr) to 0.26 μ J (24 hr) with reduced fiducial limits as well. At 90 fs, there was a 48% increase in the number of visible lesions after 24 hr as compared to the 1-hr reading. For 90 fs there was a total of 34 exposures, with dosages ranging between 0.10 and 2.0 μ J, which required longer than 1 hr to develop into visible lesions. These additional lesions reduced the calculated MVL ED_{50} threshold values from 1.18 μ J (1 hr) to 0.43 μ J (24 hr); there was a similar reduction in the fiducial limits.

The slope of the probit curve at 3 ps was almost identical to that at 4 ns, but then it changed greatly as the pulsedwidth was reduced down to 90 fs. The value at 600 fs was more than 150% (4.11) the value at 3 ps, but then the slope dropped to 60% of the 3 ps value at 90 fs. We attribute this large swing up and then down to the multiple effects of nonlinear propagation and self-focusing within the eye at these shortest pulsedwidths. Rockwell et al.^{15,16} have measured the nonlinear index of refraction in vitreous humor and they have developed a simplified model to predict the self-focusing effects for light propagating in the eye. Their model predicts a critical peak power within the laser pulse propagating through the vitreous at which the focused image collapses (beam collapse) into a filamentary propagating beam as predicted by Powell et al.¹⁷ When we compare the peak power in our pulses for the MVL ED_{50} value in Table 1, we find that the value at 600 fs is just below the critical peak power of 500 kilowatts (kW), and the value at 90 fs is an order of magnitude above the critical power. Thus we expect that the self-focusing effects without beam collapse at 600 fs should lower the threshold MVL ED_{50} values because of a smaller retinal image size. Also, it is possible for the beam to collapse at 90 fs; this collapse could cause nonlinear effects to occur within the vitreous or retinal layers. Laser-induced breakdown could occur anterior to the retina and produce a shock wave causing mechanical damage to the neural layer. This type of damage may prevent leakage and thus would not show up in FA which would increase the calculated threshold dose. Nonlinear effects due to beam collapse could also prevent some of the energy in the pulse from reaching the retina and increase the MVL ED_{50} threshold dose above those for longer pulsedwidths whose peak power levels are much lower than the critical power.

In search for a damage model which would fit our data, several models were considered and some were rejected outright because they could not adequately describe our findings. As an example, when we consider the thermal model usually ascribed to damage from longer pulsedwidths (i.e., greater than 1 ns), we calculated the temperature rise for all our pulsedwidths below 1 ns and found the ΔT to be 14°C or less. These calculations are based on an image diameter of $30 \mu\text{m}$ and a pigmented epithelium (PE) $10\text{-}\mu\text{m}$ thick with all of the energy reaching the retina being absorbed in this layer. Thus we reject the thermal model to describe our damage thresholds because the temperature-time history is not even close to being adequate to cause damage.

Photochemical damage processes as discussed by other researchers³⁻⁵ for the picosecond pulsedwidths appear to be possible damage mechanisms because of the latency of the development of lesions. In all cases our threshold dose at 24 hr was lower than at 1 hr which suggests either photochemical damage or possibly mechanical damage due to acoustic or shock waves. Our histopathological results will, when they become available, help us to better describe the damage mechanisms.

Another damage mechanism which we cannot reject, especially for the femtosecond pulses, is the possibility of direct membrane effects resulting from the intense electric fields associated with these pulses.^{4,5} The peak power going into the eye at the ED_{50} threshold at 90 fs was 5 megawatts (MW) and thus the peak irradiance at the retina was well up into the GW/cm^2 (gigawatts) range. With such extremely high retinal irradiances, retinal cell damage would be most likely to occur which would agree with the latency of the observed injury.

In determining ED_{50} threshold levels for rhesus monkeys, our FA studies did not show the sensitivity that our direct ophthalmoscopic examinations did. With probit calculations for the 1-and 24-hr readings for the five pulsedwidths studied, there were seven instances when the fiducial confidence intervals did not overlap, and only two in which they did. The exceptions were 90-fs thresholds at the 1-hr reading ($2.09 \mu\text{J}$ MVL versus $1.2 \mu\text{J}$ FAVL) and the 24-hr reading at 4 ns ($1.35 \mu\text{J}$ MVL versus $1.2 \mu\text{J}$ FAVL). However, the FA VL ED_{50} decreased between the 1- and 24-hr readings for all pulsedwidths with the exception of the 90 fs, for which it increased by almost 60%. Thus, many of the FA lesions visible at 1-hr postexposure at 90 fs disappeared and were not visible after 24 hr. These findings contrast with other FA work including our own in dutch-belted rabbits¹¹ where at 5 ps, 500 fs, and 90 fs the MVL to FA VL ratios for 1-hr postexposure were 1.2, 2.8, and 3.7, showing greater sensitivity in FAs respectively. The same procedure was used in determining our FAs for the rhesus monkey in this study. With observation, and with analysis of fundus photographs and FAs, we found FA to be unreliable in identifying the small, barely above threshold lesions at short pulsedwidths. The choroidal pattern of fluorescence could not be differentiated from the minimally fluorescent less-than-30-micron lesions in these cases. Also, we enlarged our FAs photographically by 5 to 1 in comparison to the strip photographs and found no significant change in our ability to read lesions.

Birngruber et al.⁷ noted fluorescein angiography to be more sensitive than observation of minimal short pulse laser lesions; however, they artificially maintained a constant lesion size of 50 microns in a rabbit eye. In addition, their fluorescein ED₅₀ was 0.75 μ J while our MVL ED₅₀ was only 0.43 μ J, a little more than half of their value for fluorescein and less than one-tenth of their visible lesion threshold of 4.5 μ J. This difference can be accounted for by the difference in image size as well as the different species (i.e, primate versus rabbit).

Borland et al.,¹⁸ with 15- and 40-ns lesions, noted a similar problem with FA of small laser lesions. As reported in 1978, the granular appearance of the fluorescein "was of the same order as the small size lesions: 10-30 microns," and "small image lesions were extremely difficult to identify at just suprathreshold exposure levels." When they plotted the regression lines of the probit curves, they identified a reduction in statistical reliability with FA because of the confusion between threshold lesions of small image size and the background grain of the choroidal flush for minimal image size exposures. In our study, not only do we have minimal size lesions in which we would expect a reduction of fluorescein reliability for the same reasons mentioned above, but we also have shorter pulse lesions which should produce less thermal area of damage. As Borland's group observed, thermal damage with disruption of zona occludentes and cell walls was associated with FA positive lesions. A histopathologic study of our ultrashort-pulse lesions will provide additional insight into our findings in the future.

CONCLUSION

Our data for the rhesus monkey can be compared with other published data as included in the database used to establish the ANSI Z136.1-1993¹ standard, shown in Figure 3. The only known data points for rhesus monkeys for pulsedwidths below 1 ns at visible wavelengths are also shown in Figure 3 (Goldman et al.³ and Bruckner and Taboada⁵). Because Goldman et al. did not do a probit study, our data is more directly comparable to the Bruckner and Taboada datum point at the 6-ps pulsedwidth. At 4 ns and below, our ED₅₀ thresholds for the 24-hr readings (within the circles) for rhesus monkeys show a slight downward trend until 90 fs is reached; then the estimated value becomes larger. This abrupt change in slope may be due to nonlinear effects such as self-focusing and/or beam collapse due to the high peak powers at 90 fs. The solid black line shown in Figure 3 represents the ANSI retinal MPE for pulsedwidths down to 1 ns which is 0.5 μ J/cm². Thus, 0.2 μ J at the cornea for a pulsedwidth of 1 ns is considered safe; however, one cannot extrapolate this safe level to pulsedwidths below 1 ns because our data includes nine visible lesions out of a total of 54 exposures at or below 0.2 μ J for pulsedwidths below 1 ps (90 fs and 600 fs). However, below 1 ns, ANSI recommends a constant irradiance for decreasing pulsedwidths and therefore at 100 fs, the safe limit would only be 20 picojoules (pJ), or more than four orders of magnitude below our MVL ED₅₀. It is obvious from Figure 3 that our MVL ED₅₀ thresholds are an order of magnitude or more below those in the databank for pulsedwidths longer than 1 ns and do not decrease with

Retinal Maximum Permissible Exposure

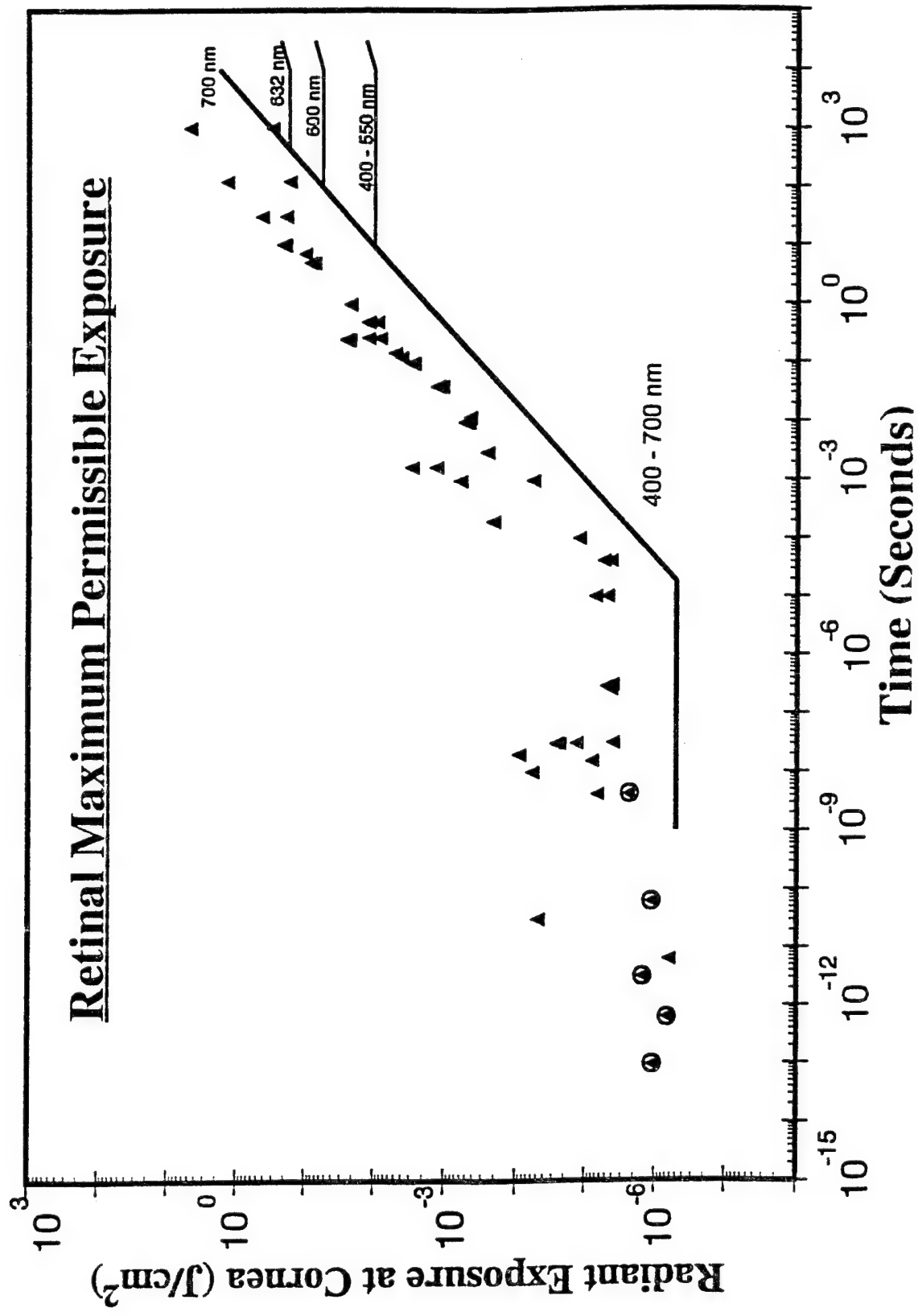


Figure 3. Retinal maximum permissible exposure for ANSI Z136.1-1993. The solid line indicates the current National Standard below which radiant exposure levels are considered safe. The triangles represent the database upon which the standard is determined and the circled triangles are from the present study.

pulsewidth to an appreciable extent. Therefore new interim standards could be set for picosecond and femtosecond laser pulsewidths which would relax somewhat the constant irradiance for decreasing pulsewidths ANSI recommendation. These interim standards could apply until the histological studies are completed and the damage mechanisms are fully understood. until the histological studies are completed and the damage mechanisms are fully understood. New standards are especially critical because laser systems which produce tens of millijoules per pulse below 100-fs pulsewidths are now commercially available. These pulses can have energies as much as five orders of magnitude greater than necessary to create visible lesions in the eye.

REFERENCES

1. ANSI Standard Z136.1. American national standard for the safe use of lasers. American National Standards Institute, Inc., New York, 1993.
2. Goldman AJ, Ham WT, Mueller HA. Mechanisms of retinal damage resulting from the exposure of rhesus monkeys to ultrashort laser pulses. *Exp Eye Res.* 1975;21:457-469.
3. Goldman AJ, Ham WT, Mueller HA. Ocular damage thresholds and mechanisms for ultrashort pulses of both visible and infrared laser radiation in the rhesus monkey. *Exp Eye Res.* 1977;24:45-56.
4. Taboada J, Gibbons WD. Retinal tissue damage induced by single ultrashort 1060 nm laser light pulses. *Appl Opt.* 1978;2871-2873.
5. Bruckner AP, Taboada J. Retinal tissue damage induced by 6 psec 530-nm laser light pulses. *Appl Opt.* 1982;21(3):365-367.
6. Roach WP, Toth CA, Stein CD, Noojin GD, Stolarski DJ, Cain CP. Minimum visible lesions from pico- and femtosecond laser pulses. *SPIE Proceedings* 1994; 2134 (Laser-Tissue Interaction V): 10-21.
7. Birngruber R, Puliafito CA, Gawande A, Lin W, Schoenkin R, Fujimoto JG. Femtosecond laser-tissue interactions: Retinal injury studies. *IEEE J Quant Electron.* 1987;QE 23(10):1836-1844.
8. Toth CA, Cain CP, Roach WP, Stein CD, Allen RG, Elliott WR, Zuchlich JA. Retinal effects of ultrashort laser pulses. *Invest Ophthalmol Vis Sci.* 1993;34(4):960.
9. Animals involved in this study were procured, maintained, and used in accordance with The Federal Animal Welfare Act, Public Law 89-544, 1966, as amended and the "Guide for the Care and Use of Laboratory Animals" NIH No. 86-23, Washington, D.C. 1986.

10. Zuchich JA, Elliott WR, Cain CP, Noojin GD, Roach WP, Rockwell BA, Toth CA. Ocular damage induced by ultrashort laser pulses. 1993;AL-TR-93-0099.
11. Toth CA, Cain CP, Stein CD, Noojin G, Stolarski D, Zuchich JA, Roach WP. Retinal effects of ultrashort laser pulses in the rabbit eye. (Submitted to *Invest Ophthalmol Vis Sci.* for publication, June 1994)
12. Roach WP, Cain CP, Toth CA, Stein CD. Ocular effects of ultrashort pulselength laser radiation. 1991;USAFSAM Protocol RZV-91-04.
13. SAS/STAT Probit Procedure, SAS Institute, Cary, NC 27513, 1994.
14. Lund DJ, Beatrice ES. Near infrared laser ocular bioeffects. *Health Phys.* 1989;56(5):631-636.
15. Rockwell BA, Roach WP, Rogers ME, Mayo MW, Toth CA. Nonlinear refraction in vitreous humor. *Opt Let.* 1993;18:1792-1794.
16. Rockwell BA, Roach WP, Rogers ME. Determination of self-focusing effects for light propagating in the eye. To appear in *SPIE Proceedings* 1994; 2134 (Laser-Tissue Interaction V).
17. Powell JA, Maloney JV, Newell AC, Albanese RA. Beam collapse as an explanation for anomalous ocular damage. *J Opt Soc Am B.* 1993;10(7):1230-1241.
18. Borland RG, Brennan DH, Marshall J, Viveash JP. The role of fluorescein angiography in the detection of laser-induced damage to the retina: A threshold study for Q-switched, neodymium and ruby lasers. *Exp Eye Res.* 1978;27:471-493.

APPENDIX A

This appendix contains the SAS-PC Probit Procedure program used in the data analysis and all minimum visible lesion data for all five pulsedwidths, both visible lesion data and fluorescein angiographic data. In addition to the raw data in ordered format, the probability plot and the predicted distribution of doses between 0.01 and 0.99 probability are included along with 95% confidence level for the fiducial intervals.

SAS-PC PROBIT.NOOJIN

```
filename testdata 'xxxx';
title 'xxxx';
data indata;
    infile testdata;
    input energy mvl;
run;

proc sort data = indata;
    by energy;
run;

proc print data = indata;
run;

proc sort data = indata;
    by desending energy;
run;

proc probit data = indata outest = mvldata order = data covout Hprob = 0.10 lackfit
log10 inversecl;
class mvl;
model mvl = energy / lackfit d = normal corrb covb inversecl;
output out = mdat prob = p xbeta = xB std = sd;
run;

goptions target=winprtg; /* grey-scale postscript */

goptions rotate = landscape;

proc gplot;
    axis logbase = 10 logstyle = power;
    plot mvl*energy p*energy / overlay;
run;
```

Probit Analysis

Data Set	Pulsewidth	Reading Time	Fluorescein Angiography
m90fs1h.dat	90 fs	1 hour	
m90fs24h.dat	90 fs	24 hour	
m90fs1hf.dat	90 fs	1 hour	FA
m90fs2hf.dat	90 fs	24 hour	FA
m600f1h.dat	600 fs	1 hour	
m600f2h.dat	600 fs	24 hour	
m600f1hf.dat	600 fs	1 hour	FA
m600f2hf.dat	500 fs	24 hour	FA
m3ps1h.dat	3 ps	1 hour	
m3ps24h.dat	3 ps	24 hour	
m3ps1hf.dat	3 ps	1 hour	FA
m3ps2hf.dat	3 ps	24 hour	FA
m60ps1h.dat	60 ps	1 hour	
m60ps2h.dat	60 ps	24 hour	
m60p1hf.dat	60 ps	1 hour	FA
m60p2hf.dat	60 ps	24 hour	FA
mon4ns1h.dat	4 ns	1 hour	
mon4ns2h.dat	4 ns	24 hour	
m4ns1hf.dat	4 ns	1 hour	FA
m4ns2hf.dat	4 ns	24 hour	FA

m90fs1h.dat

MV₀^L

0.9

0.8

0.7

0.6

0.5

0.4

0.3

0.2

0.1

0.0



OBS	ENERGY	MVL	OBS	ENERGY	MVL
1	0.01	0	62	0.61	0
2	0.03	0	63	0.62	0
3	0.04	0	64	0.63	0
4	0.05	0	65	0.65	0
5	0.08	0	66	0.67	0
6	0.08	0	67	0.71	0
7	0.10	0	68	0.74	0
8	0.10	0	69	0.74	0
9	0.11	0	70	0.77	1
10	0.12	0	71	0.78	1
11	0.12	0	72	0.78	0
12	0.16	1	73	0.83	1
13	0.17	0	74	0.83	0
14	0.18	0	75	0.84	1
15	0.19	0	76	0.84	0
16	0.20	0	77	0.90	0
17	0.20	0	78	0.91	1
18	0.21	0	79	0.91	0
19	0.22	0	80	0.93	0
20	0.22	0	81	1.00	0
21	0.22	0	82	1.00	0
22	0.24	1	83	1.00	0
23	0.24	0	84	1.00	0
24	0.24	1	85	1.00	0
25	0.25	0	86	1.00	0
26	0.25	0	87	1.00	1
27	0.27	0	88	1.00	0
28	0.27	0	89	1.05	0
29	0.29	1	90	1.07	1
30	0.30	0	91	1.10	1
31	0.30	0	92	1.10	0
32	0.30	0	93	1.10	0
33	0.30	0	94	1.10	0
34	0.31	0	95	1.10	0
35	0.33	0	96	1.10	0
36	0.33	0	97	1.10	0
37	0.36	1	98	1.20	1
38	0.36	1	99	1.30	1
39	0.38	1	100	1.30	1
40	0.42	0	101	1.40	0
41	0.42	0	102	1.60	0
42	0.46	0	103	1.68	1
43	0.46	0	104	1.70	1
44	0.50	0	105	1.80	0
45	0.50	0	106	1.82	0
46	0.51	1	107	1.89	1
47	0.52	0	108	1.90	1
48	0.52	0	109	2.00	1
49	0.52	0	110	2.00	0
50	0.56	1	111	2.10	1
51	0.57	0	112	2.10	1
52	0.57	1	113	2.20	1
53	0.58	1	114	2.30	1
54	0.58	1	115	2.40	1
55	0.58	0	116	2.44	1
56	0.58	1	117	4.20	1
57	0.59	0	118	4.30	1
58	0.59	0	119	4.30	1
59	0.60	1	120	4.80	1
60	0.60	0	121	7.20	1
61	0.60	0	122	9.30	1

Class Levels Values

MVL 2 1 0

Number of observations used = 122

Probit Procedure

Data Set =WORK.INDATA
Dependent Variable=MVL

Weighted Frequency Counts for the Ordered Response Categories

Level	Count
1	42
0	80

Log Likelihood for NORMAL -64.47120881

Goodness-of-Fit Tests

Statistic	Value	DF	Prob>Chi-Sq
Pearson Chi-Square	85.9111	71	0.1097
L.R. Chi-Square	88.4001	71	0.0792

Response Levels: 2 Number of Covariate Values: 73

NOTE: Since the chi-square is small ($p > 0.1000$), fiducial limits will be calculated using a t value of 1.96.

Variable	DF	Estimate	Std Err	ChiSquare	Pr>Chi	Label/Value
INTERCPT	1	-0.1187452	0.137547	0.745302	0.3880	Intercept
Log10(ENE)	1	1.66201977	0.364641	20.77504	0.0001	

Estimated Covariance Matrix

	INTERCPT	Log10(ENERG)
INTERCPT	0.018919	0.018826
Log10(ENERG)	0.018826	0.132963

Estimated Correlation Matrix

	INTERCPT	Log10(ENERG)
INTERCPT	1.000000	0.375352
Log10(ENERG)	0.375352	1.000000

Probit Model in Terms of Tolerance Distribution

	MU	SIGMA
	0.071446	0.601678

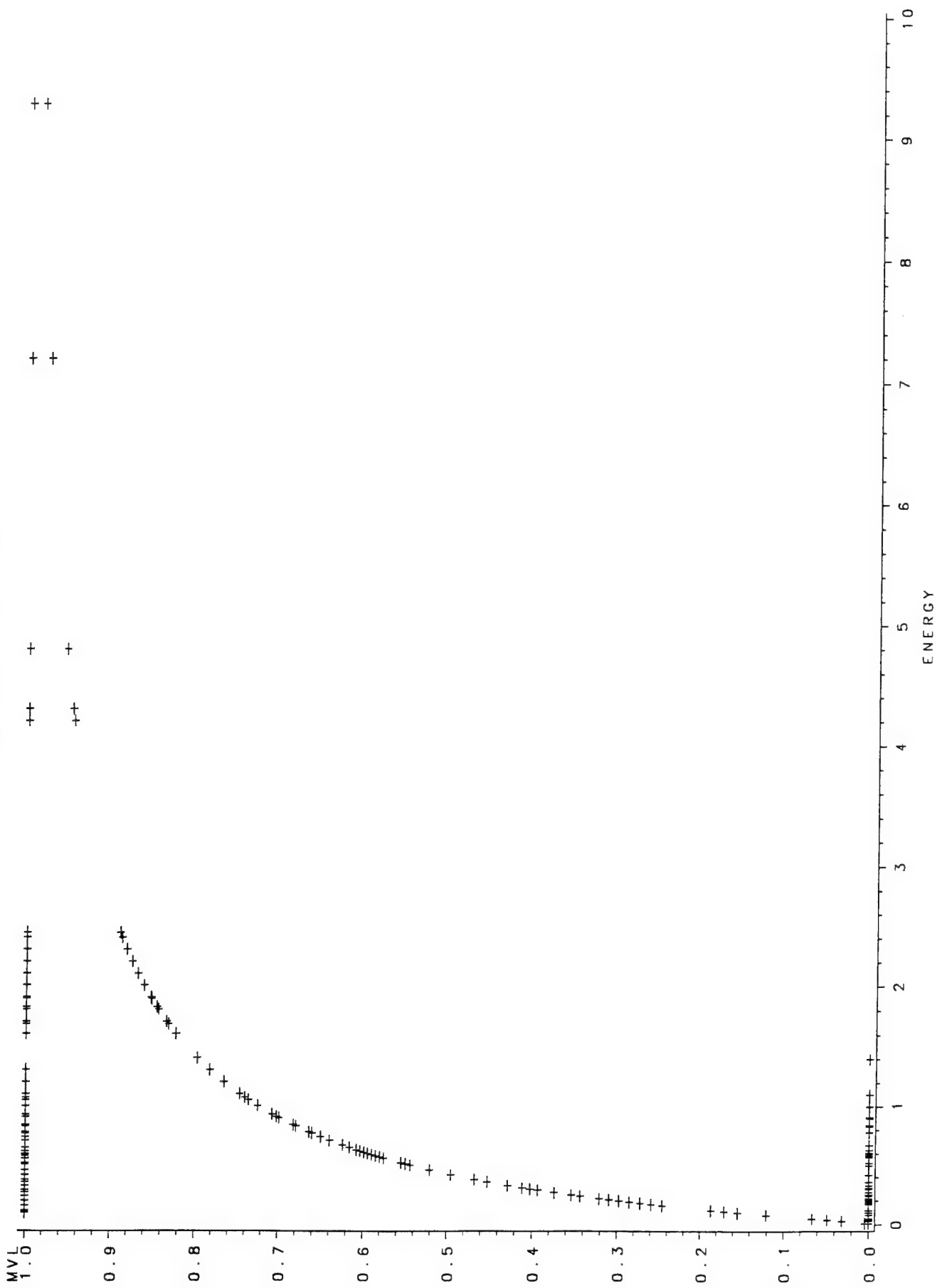
Estimated Covariance Matrix for Tolerance Parameters

	MU	SIGMA
MU	0.008069	0.006170
SIGMA	0.006170	0.017426

Probit Procedure
 Probit Analysis on ENERGY

Probability	ENERGY 95 Percent Fiducial Limits		
	Lower	Upper	
0.01	0.04696	0.00568	0.11229
0.02	0.06851	0.01094	0.14736
0.03	0.08706	0.01656	0.17533
0.04	0.10426	0.02259	0.20000
0.05	0.12072	0.02906	0.22277
0.06	0.13676	0.03599	0.24435
0.07	0.15258	0.04338	0.26513
0.08	0.16829	0.05125	0.28540
0.09	0.18397	0.05961	0.30534
0.10	0.19969	0.06847	0.32509
0.15	0.28044	0.12064	0.42455
0.20	0.36733	0.18671	0.53193
0.25	0.46304	0.26715	0.65617
0.30	0.57007	0.36107	0.80866
0.35	0.69121	0.46614	1.00500
0.40	0.82988	0.57968	1.26570
0.45	0.99046	0.70047	1.61675
0.50	1.17882	0.82960	2.09259
0.55	1.40299	0.97024	2.74280
0.60	1.67448	1.12725	3.64386
0.65	2.01041	1.30747	4.92029
0.70	2.43762	1.52084	6.78685
0.75	3.00104	1.78303	9.64226
0.80	3.78295	2.12114	14.30583
0.85	4.95502	2.58877	22.73010
0.90	6.95868	3.31546	40.83501
0.91	7.55350	3.51821	47.06081
0.92	8.25746	3.75201	54.91242
0.93	9.10745	4.02645	65.07591
0.94	10.16058	4.35599	78.67952
0.95	11.51113	4.76394	97.71743
0.96	13.32892	5.29106	126.07869
0.97	15.96164	6.01787	172.51476
0.98	20.28341	7.13783	261.84636
0.99	29.59086	9.33361	505.84282

m90fs24h.dat



OBS	ENERGY	MVL	OBS	ENERGY	MVL
1	0.01	0	62	0.61	0
2	0.03	0	63	0.62	1
3	0.04	0	64	0.63	0
4	0.05	0	65	0.65	1
5	0.08	0	66	0.67	0
6	0.08	0	67	0.71	1
7	0.10	0	68	0.74	1
8	0.10	1	69	0.74	1
9	0.11	1	70	0.77	1
10	0.12	0	71	0.78	1
11	0.12	1	72	0.78	0
12	0.16	1	73	0.83	1
13	0.17	0	74	0.83	0
14	0.18	0	75	0.84	1
15	0.19	0	76	0.84	0
16	0.20	0	77	0.90	0
17	0.20	1	78	0.91	1
18	0.21	0	79	0.91	0
19	0.22	0	80	0.93	1
20	0.22	0	81	1.00	1
21	0.22	0	82	1.00	1
22	0.24	1	83	1.00	0
23	0.24	0	84	1.00	0
24	0.24	1	85	1.00	1
25	0.25	0	86	1.00	1
26	0.25	0	87	1.00	1
27	0.27	1	88	1.00	0
28	0.27	0	89	1.05	1
29	0.29	1	90	1.07	1
30	0.30	0	91	1.10	1
31	0.30	0	92	1.10	0
32	0.30	0	93	1.10	1
33	0.30	0	94	1.10	1
34	0.31	0	95	1.10	1
35	0.33	0	96	1.10	0
36	0.33	1	97	1.10	0
37	0.36	1	98	1.20	1
38	0.36	0	99	1.30	1
39	0.38	1	100	1.30	1
40	0.42	1	101	1.40	0
41	0.42	0	102	1.60	1
42	0.46	1	103	1.68	1
43	0.46	1	104	1.70	1
44	0.50	0	105	1.80	1
45	0.50	0	106	1.82	1
46	0.51	1	107	1.89	1
47	0.52	0	108	1.90	1
48	0.52	0	109	2.00	1
49	0.52	1	110	2.00	1
50	0.56	1	111	2.10	1
51	0.57	0	112	2.10	1
52	0.57	0	113	2.20	1
53	0.58	1	114	2.30	1
54	0.58	1	115	2.40	1
55	0.58	0	116	2.44	1
56	0.58	1	117	4.20	1
57	0.59	0	118	4.30	1
58	0.59	1	119	4.30	1
59	0.60	1	120	4.80	1
60	0.60	1	121	7.20	1
61	0.60	0	122	9.30	1

Class	Levels	Values
MVL	2	1 0

Number of observations used = 122

Probit Procedure

Data Set =WORK.INDATA
Dependent Variable=MVL

Weighted Frequency Counts for the Ordered Response Categories

Level	Count
1	70
0	52

Log Likelihood for NORMAL -68.21446878

Goodness-of-Fit Tests

Statistic	Value	DF	Prob>Chi-Sq
Pearson Chi-Square	55.2443	71	0.9159
L.R. Chi-Square	67.0562	71	0.6107

Response Levels: 2 Number of Covariate Values: 73

NOTE: Since the chi-square is small ($p > 0.1000$), fiducial limits will be calculated using a t value of 1.96.

Variable	DF	Estimate	Std Err	ChiSquare	Pr>Chi	Label/Value
INTERCPT	1	0.59644115	0.152723	15.25198	0.0001	Intercept
Log10(ENE)	1	1.61456145	0.338641	22.73155	0.0001	

Estimated Covariance Matrix

	INTERCPT	Log10(ENERG)
INTERCPT	0.023324	0.030005
Log10(ENERG)	0.030005	0.114678

Estimated Correlation Matrix

	INTERCPT	Log10(ENERG)
INTERCPT	1.000000	0.580171
Log10(ENERG)	0.580171	1.000000

Probit Model in Terms of Tolerance Distribution

	MU	SIGMA
	-0.36941	0.619363

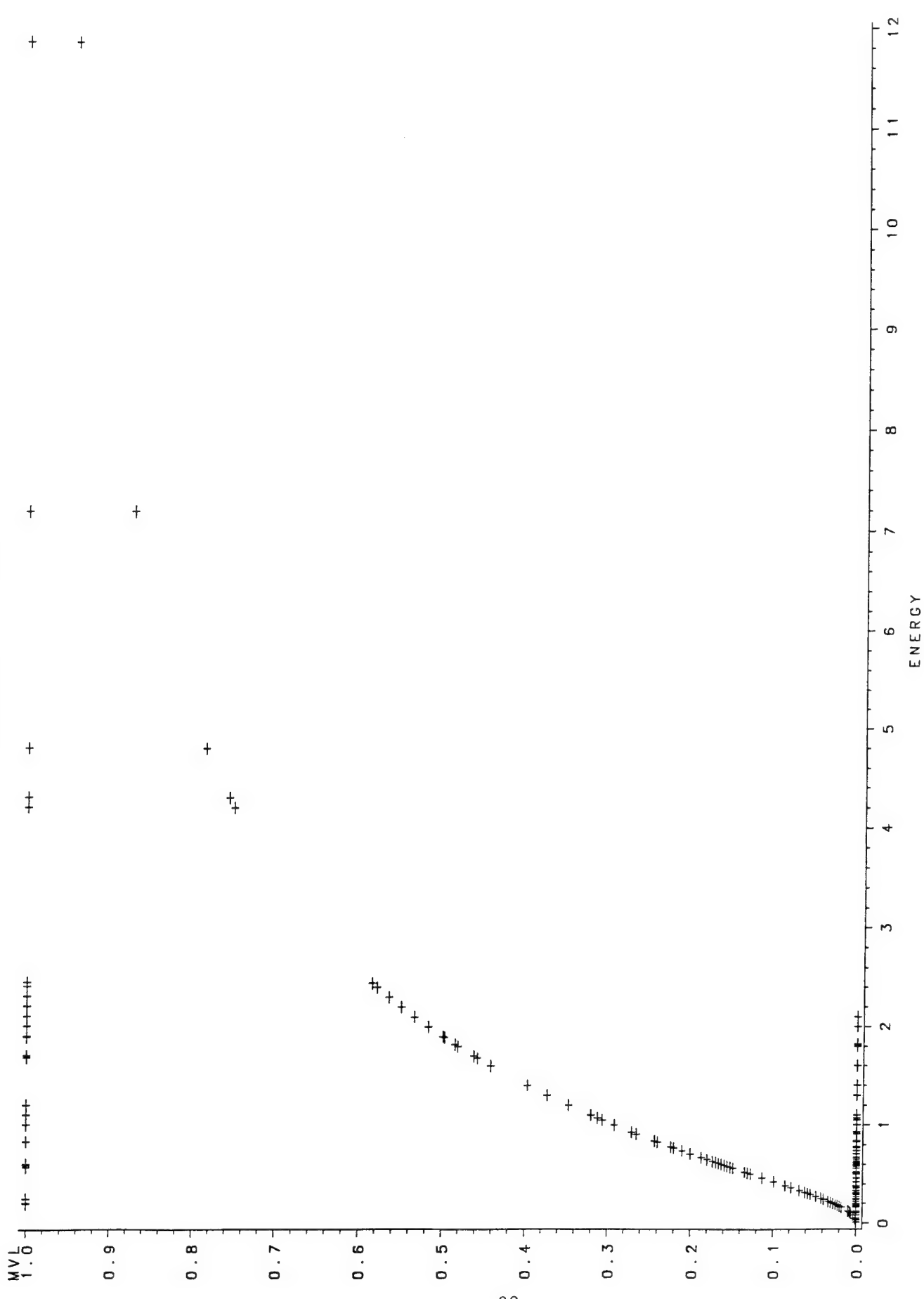
Estimated Covariance Matrix for Tolerance Parameters

	MU	SIGMA
MU	0.006447	-0.002936
SIGMA	-0.002936	0.016876

Probit Procedure
Probit Analysis on ENERGY

Probability	ENERGY 95 Percent Fiducial Limits		
	Lower	Upper	
0.01	0.01548	0.00123	0.04556
0.02	0.02283	0.00237	0.06031
0.03	0.02922	0.00360	0.07209
0.04	0.03518	0.00491	0.08249
0.05	0.04091	0.00633	0.09207
0.06	0.04652	0.00785	0.10112
0.07	0.05206	0.00948	0.10982
0.08	0.05759	0.01122	0.11826
0.09	0.06312	0.01308	0.12652
0.10	0.06868	0.01506	0.13466
0.15	0.09742	0.02692	0.17473
0.20	0.12862	0.04255	0.21573
0.25	0.16324	0.06276	0.25955
0.30	0.20220	0.08856	0.30792
0.35	0.24657	0.12110	0.36293
0.40	0.29763	0.16169	0.42756
0.45	0.35707	0.21165	0.50630
0.50	0.42716	0.27205	0.60630
0.55	0.51099	0.34357	0.73899
0.60	0.61306	0.42665	0.92240
0.65	0.74001	0.52240	1.18499
0.70	0.90236	0.63404	1.57369
0.75	1.11774	0.76850	2.17329
0.80	1.41859	0.93914	3.15624
0.85	1.87290	1.17292	4.93203
0.90	2.65664	1.53537	8.73905
0.91	2.89068	1.63665	10.04550
0.92	3.16837	1.75360	11.69153
0.93	3.50459	1.89109	13.81998
0.94	3.92244	2.05653	16.66553
0.95	4.46014	2.26187	20.64256
0.96	5.18677	2.52806	26.55836
0.97	6.24426	2.89666	36.22721
0.98	7.99103	3.46795	54.78670
0.99	11.78801	4.59817	105.31995

m90fs1hf.dat



OBS	ENERGY	MVL	OBS	ENERGY	MVL
1	0.01	0	62	0.60	0
2	0.03	0	63	0.60	1
3	0.04	0	64	0.61	0
4	0.05	0	65	0.62	0
5	0.08	0	66	0.63	0
6	0.08	0	67	0.65	0
7	0.08	0	68	0.67	0
8	0.10	0	69	0.71	0
9	0.10	0	70	0.74	0
10	0.11	0	71	0.74	0
11	0.12	0	72	0.77	0
12	0.12	0	73	0.78	0
13	0.16	0	74	0.78	0
14	0.17	0	75	0.83	1
15	0.18	0	76	0.83	0
16	0.18	0	77	0.84	0
17	0.19	0	78	0.84	0
18	0.20	0	79	0.91	0
19	0.20	1	80	0.91	0
20	0.21	1	81	0.93	0
21	0.22	0	82	1.00	0
22	0.22	0	83	1.00	0
23	0.22	0	84	1.00	0
24	0.24	0	85	1.00	1
25	0.24	0	86	1.00	0
26	0.24	0	87	1.00	0
27	0.25	1	88	1.00	0
28	0.25	0	89	1.00	0
29	0.27	0	90	1.05	0
30	0.27	0	91	1.07	0
31	0.29	0	92	1.10	0
32	0.30	0	93	1.10	0
33	0.30	0	94	1.10	0
34	0.30	0	95	1.10	1
35	0.30	0	96	1.10	0
36	0.31	0	97	1.10	0
37	0.33	0	98	1.10	0
38	0.33	0	99	1.20	1
39	0.36	0	100	1.30	0
40	0.36	0	101	1.30	0
41	0.38	0	102	1.40	0
42	0.42	0	103	1.60	0
43	0.42	0	104	1.68	1
44	0.46	0	105	1.70	1
45	0.46	0	106	1.80	0
46	0.50	0	107	1.82	0
47	0.50	0	108	1.89	1
48	0.51	0	109	1.90	1
49	0.52	0	110	2.00	1
50	0.52	0	111	2.00	0
51	0.52	0	112	2.10	1
52	0.56	0	113	2.10	0
53	0.57	1	114	2.20	1
54	0.57	1	115	2.30	1
55	0.58	0	116	2.40	1
56	0.58	0	117	2.44	1
57	0.58	0	118	4.20	1
58	0.58	0	119	4.30	1
59	0.59	0	120	4.30	1
60	0.59	1	121	4.80	1
61	0.60	0	122	7.20	1
			123	11.9	1

Class Levels Values

MVL 2 1 0

Number of observations used = 123

Probit Procedure

Data Set =WORK.INDATA
 Dependent Variable=MVL

Weighted Frequency Counts for the Ordered Response Categories

Level	Count
1	27
0	96

Log Likelihood for NORMAL -48.75607625

Goodness-of-Fit Tests

Statistic	Value	DF	Prob>Chi-Sq
Pearson Chi-Square	99.7159	70	0.0113
L.R. Chi-Square	65.2876	70	0.6372

Response Levels: 2 Number of Covariate Values: 72

WARNING: All variances and covariances have been multiplied by the heterogeneity factor H= 1.4245. Please check to be sure that the large chi-square (p < 0.0113) is not caused by systematic departure from the model. A t value of 1.9944 will be used in computing fiducial limits.

Variable	DF	Estimate	Std Err	ChiSquare	Pr>Chi	Label/Value
INTERCPT	1	-0.5476554	0.174725	9.824335	0.0017	Intercept
Log10(ENE)	1	1.96193346	0.497834	15.53097	0.0001	

Estimated Covariance Matrix

	INTERCPT	Log10(ENERG)
INTERCPT	0.030529	0.016302
Log10(ENERG)	0.016302	0.247839

Estimated Correlation Matrix

	INTERCPT	Log10(ENERG)
INTERCPT	1.000000	0.187413
Log10(ENERG)	0.187413	1.000000

Probit Model in Terms of Tolerance Distribution

MU	SIGMA
0.279141	0.509701

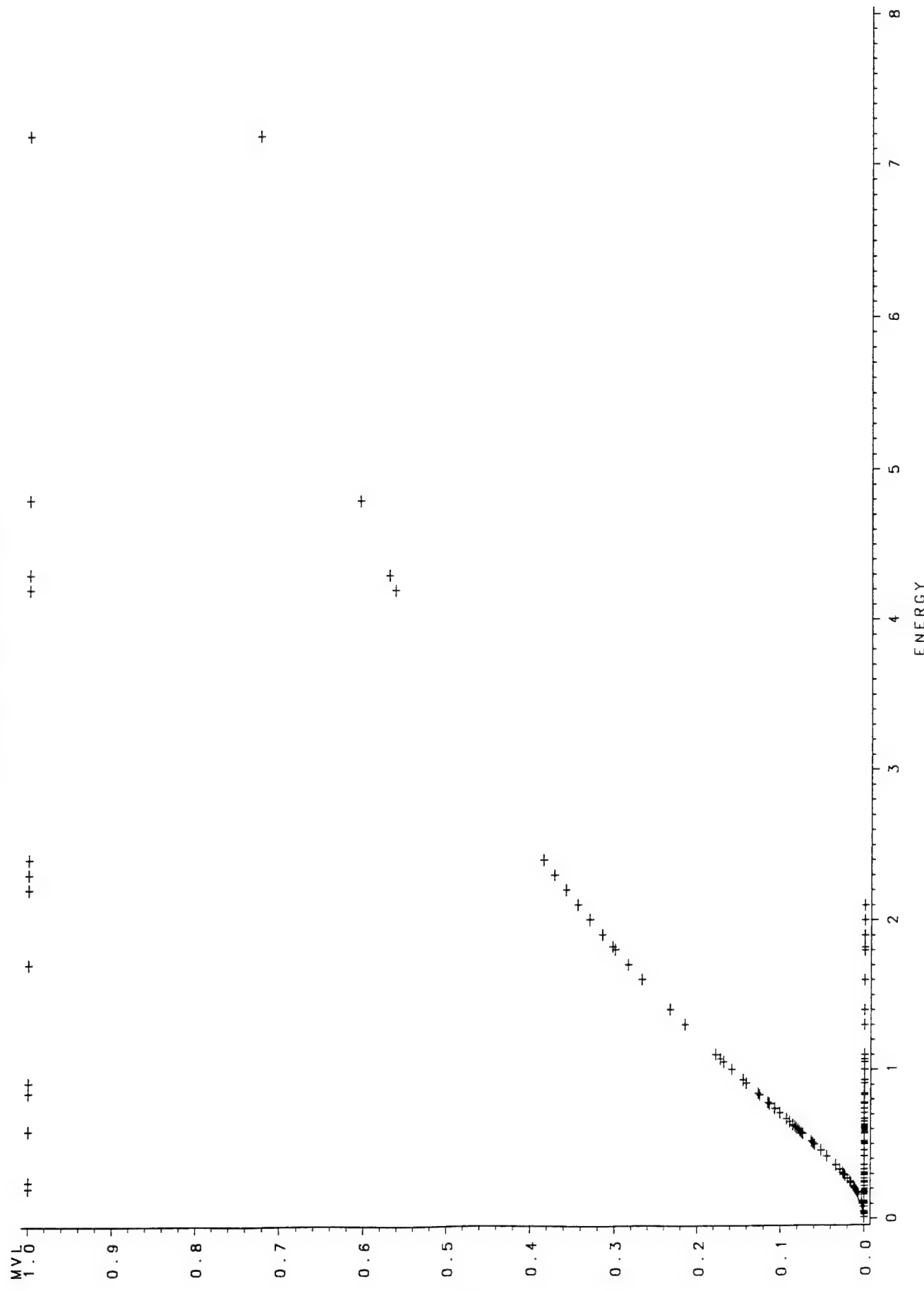
Estimated Covariance Matrix for Tolerance Parameters

MU	SIGMA
0.015313	0.011320
0.011320	0.016728

Probit Procedure
Probit Analysis on ENERGY

Probability	ENERGY 95 Percent Fiducial Limits		
	Lower	Upper	
0.01	0.12399	0.01575	0.25743
0.02	0.17074	0.02965	0.32305
0.03	0.20917	0.04418	0.37424
0.04	0.24368	0.05950	0.41894
0.05	0.27590	0.07567	0.46006
0.06	0.30667	0.09269	0.49904
0.07	0.33646	0.11056	0.53675
0.08	0.36557	0.12929	0.57378
0.09	0.39424	0.14884	0.61056
0.10	0.42260	0.16920	0.64742
0.15	0.56347	0.28189	0.84217
0.20	0.70822	0.40832	1.07509
0.25	0.86169	0.54131	1.37415
0.30	1.02767	0.67532	1.76870
0.35	1.20988	0.80864	2.29087
0.40	1.41257	0.94267	2.98025
0.45	1.64093	1.08025	3.89103
0.50	1.90169	1.22484	5.10167
0.55	2.20389	1.38039	6.72973
0.60	2.56019	1.55162	8.95757
0.65	2.98909	1.74478	12.08064
0.70	3.51907	1.96872	16.60505
0.75	4.19690	2.23719	23.46404
0.80	5.10641	2.57361	34.56179
0.85	6.41818	3.02343	54.40110
0.90	8.55754	3.69370	96.50552
0.91	9.17329	3.87551	110.87069
0.92	9.89253	4.08270	128.92483
0.93	10.74863	4.32277	152.20705
0.94	11.79263	4.60695	183.23983
0.95	13.10764	4.95310	226.46477
0.96	14.84115	5.39206	290.50590
0.97	17.28954	5.98377	394.66853
0.98	21.18064	6.86938	593.34197
0.99	29.16642	8.53248	1129

m90fs2hf.dat



OBS	ENERGY	MVL	OBS	ENERGY	MVL	OBS	ENERGY	MVL
1	0.01	0	62	0.65	0	123	41	1
2	0.03	0	63	0.67	0	124	42	1
3	0.04	0	64	0.71	0	125	43	1
4	0.05	0	65	0.74	0	126	43	1
5	0.08	0	66	0.74	0	127	47	1
6	0.08	0	67	0.77	0	128	52	1
7	0.10	0	68	0.78	0	129	71	1
8	0.10	0	69	0.78	0	130	81	1
9	0.11	0	70	0.83	0	131	82	1
10	0.12	0	71	0.83	0			
11	0.12	0	72	0.84	1			
12	0.16	0	73	0.84	0			
13	0.17	0	74	0.91	1			
14	0.18	0	75	0.91	0			
15	0.19	0	76	0.93	0			
16	0.20	0	77	1.00	0			
17	0.20	0	78	1.00	0			
18	0.21	1	79	1.00	0			
19	0.22	0	80	1.00	0			
20	0.22	0	81	1.00	0			
21	0.22	0	82	1.00	0			
22	0.24	0	83	1.00	0			
23	0.24	0	84	1.00	0			
24	0.24	0	85	1.05	0			
25	0.25	1	86	1.07	0			
26	0.25	0	87	1.10	0			
27	0.27	0	88	1.10	0			
28	0.27	0	89	1.10	0			
29	0.29	0	90	1.10	0			
30	0.30	0	91	1.10	0			
31	0.30	0	92	1.10	0			
32	0.30	0	93	1.10	0			
33	0.30	0	94	1.30	0			
34	0.31	0	95	1.30	0			
35	0.33	0	96	1.40	0			
36	0.33	0	97	1.60	0			
37	0.36	0	98	1.70	1			
38	0.36	0	99	1.80	0			
39	0.42	0	100	1.82	0			
40	0.42	0	101	1.90	0			
41	0.46	0	102	2.00	0			
42	0.46	0	103	2.00	0			
43	0.50	0	104	2.10	0			
44	0.50	0	105	2.10	0			
45	0.51	0	106	2.20	1			
46	0.52	0	107	2.30	1			
47	0.52	0	108	2.40	1			
48	0.52	0	109	4.20	1			
49	0.57	0	110	4.30	1			
50	0.57	0	111	4.30	1			
51	0.58	0	112	4.80	1			
52	0.58	0	113	7.20	1			
53	0.58	0	114	11.90	1			
54	0.59	0	115	14.00	1			
55	0.59	1	116	16.00	1			
56	0.60	0	117	22.00	1			
57	0.60	0	118	28.00	1			
58	0.60	0	119	37.00	1			
59	0.61	0	120	38.00	1			
60	0.62	0	121	38.00	1			
61	0.63	0	122	39.00	1			

Class Levels Values

MVL 2 . 1 0

Number of observations used = 131

Probit Procedure

Data Set =WORK.INDATA
 Dependent Variable=MVL

Weighted Frequency Counts for the Ordered Response Categories

Level	Count
1	32
0	99

Log Likelihood for NORMAL -32.91782956

Goodness-of-Fit Tests

Statistic	Value	DF	Prob>Chi-Sq
Pearson Chi-Square	195.4954	79	0.0000
L.R. Chi-Square	54.7453	79	0.9829

Response Levels: 2 Number of Covariate Values: 81

WARNING: All variances and covariances have been multiplied by the heterogeneity factor H= 2.4746. Please check to be sure that the large chi-square (p < 0.0001) is not caused by systematic departure from the model. A t value of 1.9905 will be used in computing fiducial limits.

Variable	DF	Estimate	Std Err	ChiSquare	Pr>Chi	Label/Value
INTERCPT	1	-0.9743068	0.270673	12.95694	0.0003	Intercept
Log10(ENE)	1	2.1200031	0.618372	11.75367	0.0006	

Estimated Covariance Matrix

	INTERCPT	Log10(ENERG)
INTERCPT	0.073264	-0.021317
Log10(ENERG)	-0.021317	0.382384

Estimated Correlation Matrix

	INTERCPT	Log10(ENERG)
INTERCPT	1.000000	-0.127361
Log10(ENERG)	-0.127361	1.000000

Probit Model in Terms of Tolerance Distribution

	MU	SIGMA
	0.459578	0.471697

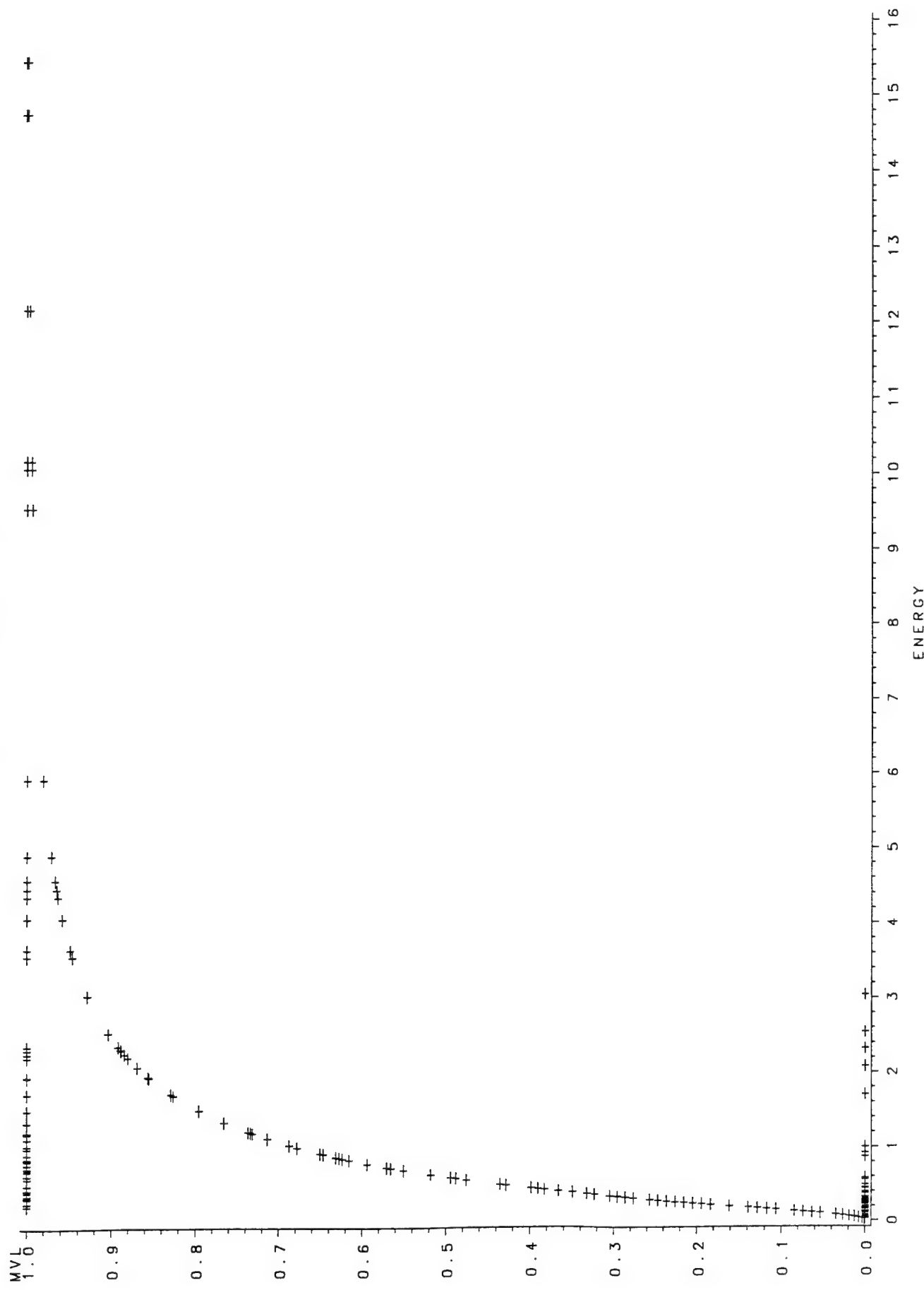
Estimated Covariance Matrix for Tolerance Parameters

	MU	SIGMA
MU	0.029911	0.016206
SIGMA	0.016206	0.018930

Probit Procedure
 Probit Analysis on ENERGY

Probability	ENERGY	95 Percent Fiducial Limits	
		Lower	Upper
0.01	0.23027	0.02128	0.49129
0.02	0.30962	0.04168	0.61265
0.03	0.37360	0.06342	0.70971
0.04	0.43031	0.08652	0.79674
0.05	0.48273	0.11094	0.87899
0.06	0.53235	0.13657	0.95914
0.07	0.58003	0.16335	1.03882
0.08	0.62634	0.19116	1.11919
0.09	0.67166	0.21990	1.20113
0.10	0.71626	0.24948	1.28537
0.15	0.93475	0.40647	1.76144
0.20	1.15501	0.57072	2.37524
0.25	1.38491	0.73526	3.18811
0.30	1.63012	0.89789	4.26913
0.35	1.89593	1.05958	5.70627
0.40	2.18814	1.22277	7.61994
0.45	2.51364	1.39053	10.18179
0.50	2.88123	1.56634	13.64410
0.55	3.30257	1.75425	18.38937
0.60	3.79386	1.95925	25.01943
0.65	4.37857	2.18795	34.52543
0.70	5.09256	2.44980	48.63723
0.75	5.99423	2.75938	70.61197
0.80	7.18735	3.14139	107.25357
0.85	8.88098	3.64322	175.09877
0.90	11.58998	4.37528	325.52729
0.91	12.35972	4.57106	378.29267
0.92	13.25399	4.79288	445.42693
0.93	14.31215	5.04827	533.17528
0.94	15.59411	5.34848	651.90056
0.95	17.19694	5.71129	820.10572
0.96	19.29177	6.16719	1074
0.97	22.21997	6.77507	1498
0.98	26.81181	7.67224	2331
0.99	36.05042	9.32268	4687

m600fh.dat



OBS	ENERGY	MVL	OBS	ENERGY	MVL
1	0.02	0	62	0.43	1
2	0.03	0	63	0.44	1
3	0.03	0	64	0.44	0
4	0.03	0	65	0.45	0
5	0.03	0	66	0.49	0
6	0.03	0	67	0.50	1
7	0.04	0	68	0.56	0
8	0.04	0	69	0.58	0
9	0.05	0	70	0.59	1
10	0.05	0	71	0.63	1
11	0.05	0	72	0.69	1
12	0.06	0	73	0.72	1
13	0.07	0	74	0.73	1
14	0.08	0	75	0.78	1
15	0.08	0	76	0.83	1
16	0.10	0	77	0.83	1
17	0.11	0	78	0.85	1
18	0.11	0	79	0.86	1
19	0.11	0	80	0.87	0
20	0.12	0	81	0.91	1
21	0.13	0	82	0.92	0
22	0.13	0	83	1.00	0
23	0.15	0	84	1.00	1
24	0.16	0	85	1.03	1
25	0.17	0	86	1.03	1
26	0.17	0	87	1.12	1
27	0.17	0	88	1.19	1
28	0.17	0	89	1.20	1
29	0.18	0	90	1.21	1
30	0.18	0	91	1.34	1
31	0.20	0	92	1.50	1
32	0.22	0	93	1.70	0
33	0.22	1	94	1.72	1
34	0.22	0	95	1.94	1
35	0.23	0	96	1.95	1
36	0.24	0	97	1.95	1
37	0.25	0	98	2.08	0
38	0.25	0	99	2.21	1
39	0.25	0	100	2.26	1
40	0.25	1	101	2.31	1
41	0.26	0	102	2.32	0
42	0.26	1	103	2.36	1
43	0.26	0	104	2.54	0
44	0.27	0	105	3.04	0
45	0.28	0	106	3.56	1
46	0.29	0	107	3.66	1
47	0.31	0	108	4.07	1
48	0.32	0	109	4.36	1
49	0.32	0	110	4.46	1
50	0.32	0	111	4.58	1
51	0.32	1	112	4.91	1
52	0.33	1	113	4.91	1
53	0.34	1	114	5.94	1
54	0.36	1	115	9.57	1
55	0.37	0	116	10.10	1
56	0.37	0	117	10.10	1
57	0.37	0	118	10.20	1
58	0.39	0	119	12.20	1
59	0.39	0	120	14.80	1
60	0.41	1	121	15.50	1
61	0.41	1			

Class Levels Values

MVL 2 1 0

Number of observations used = 121

Probit Procedure

Data Set =WORK.INDATA
 Dependent Variable=MVL

Weighted Frequency Counts for the Ordered Response Categories

Level	Count
1	56
0	65

Log Likelihood for NORMAL -49.9171578

Goodness-of-Fit Tests

Statistic	Value	DF	Prob>Chi-Sq
Pearson Chi-Square	81.7423	83	0.5185
L.R. Chi-Square	77.6536	83	0.6451

Response Levels: 2 Number of Covariate Values: 85

NOTE: Since the chi-square is small ($p > 0.1000$), fiducial limits will be calculated using a t value of 1.96.

Variable	DF	Estimate	Std Err	ChiSquare	Pr>Chi	Label/Value
INTERCPT	1	0.46129666	0.167927	7.546072	0.0060	Intercept
Log10(ENE)	1	2.07415829	0.342131	36.7535	0.0001	

Estimated Covariance Matrix

	INTERCPT	Log10(ENERG)
INTERCPT	0.028199	0.029872
Log10(ENERG)	0.029872	0.117054

Estimated Correlation Matrix

	INTERCPT	Log10(ENERG)
INTERCPT	1.000000	0.519931
Log10(ENERG)	0.519931	1.000000

Probit Model in Terms of Tolerance Distribution

	MU	SIGMA
	-0.2224	0.482123

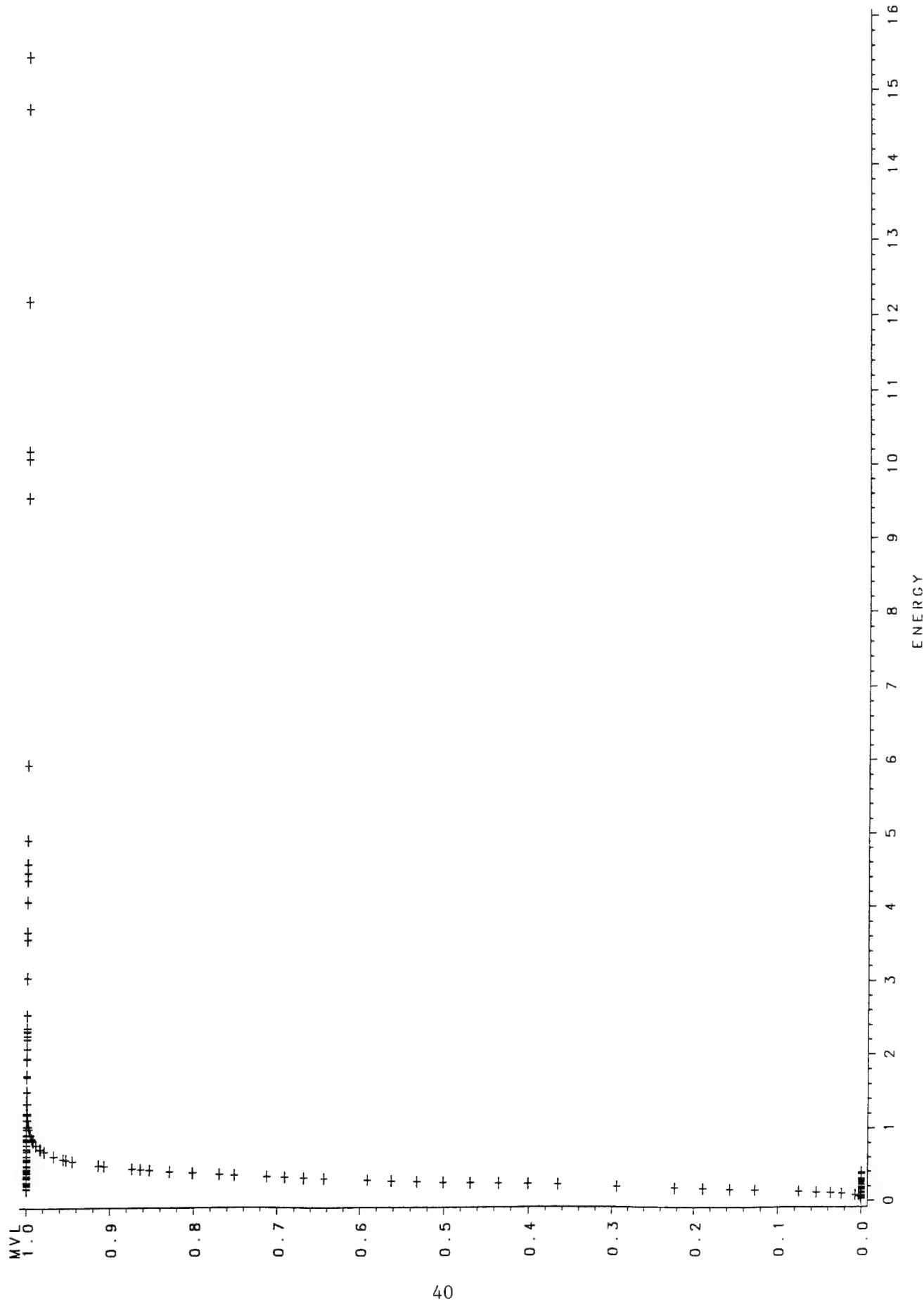
Estimated Covariance Matrix for Tolerance Parameters

	MU	SIGMA
MU	0.004812	0.000430
SIGMA	0.000430	0.006324

Probit Procedure
 Probit Analysis on ENERGY

Probability	ENERGY	95 Percent Fiducial Limits	
		Lower	Upper
0.01	0.04529	0.01290	0.08857
0.02	0.06130	0.02002	0.11216
0.03	0.07427	0.02644	0.13042
0.04	0.08581	0.03257	0.14619
0.05	0.09651	0.03857	0.16049
0.06	0.10666	0.04452	0.17383
0.07	0.11644	0.05047	0.18651
0.08	0.12594	0.05645	0.19871
0.09	0.13527	0.06248	0.21056
0.10	0.14445	0.06858	0.22216
0.15	0.18963	0.10051	0.27837
0.20	0.23541	0.13543	0.33489
0.25	0.28341	0.17392	0.39466
0.30	0.33479	0.21642	0.46013
0.35	0.39068	0.26330	0.53394
0.40	0.45233	0.31492	0.61923
0.45	0.52121	0.37169	0.72005
0.50	0.59924	0.43421	0.84170
0.55	0.68894	0.50341	0.99137
0.60	0.79386	0.58083	1.17925
0.65	0.91912	0.66887	1.42043
0.70	1.07257	0.77137	1.73885
0.75	1.26703	0.89462	2.17521
0.80	1.52533	1.04964	2.80588
0.85	1.89359	1.25805	3.79475
0.90	2.48579	1.57134	5.57894
0.91	2.65465	1.65690	6.12740
0.92	2.85112	1.75470	6.78617
0.93	3.08398	1.86841	7.59462
0.94	3.36659	2.00355	8.61446
0.95	3.72066	2.16889	9.94919
0.96	4.18451	2.37970	11.78865
0.97	4.83473	2.66575	14.52999
0.98	5.85812	3.09764	19.19957
0.99	7.92838	3.91945	29.82851

m600f2h.dat



OBS	ENERGY	MVL	OBS	ENERGY	MVL
1	0.02	0	62	0.43	1
2	0.03	0	63	0.44	1
3	0.03	0	64	0.44	1
4	0.03	0	65	0.45	1
5	0.03	0	66	0.49	1
6	0.03	0	67	0.50	1
7	0.04	0	68	0.56	1
8	0.04	0	69	0.58	1
9	0.05	0	70	0.59	1
10	0.05	0	71	0.63	1
11	0.05	0	72	0.69	1
12	0.06	0	73	0.72	1
13	0.07	0	74	0.73	1
14	0.08	0	75	0.78	1
15	0.08	0	76	0.83	1
16	0.10	0	77	0.83	1
17	0.11	0	78	0.85	1
18	0.11	0	79	0.86	1
19	0.11	0	80	0.87	1
20	0.12	0	81	0.91	1
21	0.13	0	82	0.92	1
22	0.13	0	83	1.00	1
23	0.15	0	84	1.00	1
24	0.16	0	85	1.03	1
25	0.17	1	86	1.03	1
26	0.17	1	87	1.12	1
27	0.17	0	88	1.19	1
28	0.17	0	89	1.20	1
29	0.18	1	90	1.21	1
30	0.18	0	91	1.34	1
31	0.20	0	92	1.50	1
32	0.22	1	93	1.70	1
33	0.22	1	94	1.72	1
34	0.22	0	95	1.94	1
35	0.23	0	96	1.95	1
36	0.24	1	97	1.95	1
37	0.25	0	98	2.08	1
38	0.25	0	99	2.21	1
39	0.25	0	100	2.26	1
40	0.25	1	101	2.31	1
41	0.26	0	102	2.32	1
42	0.26	1	103	2.36	1
43	0.26	0	104	2.54	1
44	0.27	1	105	3.04	1
45	0.28	0	106	3.56	1
46	0.29	0	107	3.66	1
47	0.31	0	108	4.07	1
48	0.32	1	109	4.36	1
49	0.32	1	110	4.46	1
50	0.32	1	111	4.58	1
51	0.32	1	112	4.91	1
52	0.33	1	113	4.91	1
53	0.34	1	114	5.94	1
54	0.36	1	115	9.57	1
55	0.37	0	116	10.10	1
56	0.37	0	117	10.10	1
57	0.37	0	118	10.20	1
58	0.39	1	119	12.20	1
59	0.39	0	120	14.80	1
60	0.41	1	121	15.50	1
61	0.41	1			

Class Levels Values

MVL 2 1 0

Number of observations used = 121

Probit Procedure

Data Set =WORK.INDATA
 Dependent Variable=MVL

Weighted Frequency Counts for the Ordered Response Categories

Level	Count
1	79
0	42

Log Likelihood for NORMAL -28.75843126

Goodness-of-Fit Tests

Statistic	Value	DF	Prob>Chi-Sq
Pearson Chi-Square	30.0650	83	1.0000
L.R. Chi-Square	34.2897	83	1.0000

Response Levels: 2 Number of Covariate Values: 85

NOTE: Since the chi-square is small ($p > 0.1000$), fiducial limits will be calculated using a t value of 1.96.

Variable	DF	Estimate	Std Err	ChiSquare	Pr>Chi	Label/Value
INTERCPT	1	2.80507213	0.613371	20.91425	0.0001	Intercept
Log10(ENE)	1	4.78979054	1.042264	21.11919	0.0001	

Estimated Covariance Matrix

	INTERCPT	Log10(ENERG)
INTERCPT	0.376223	0.607977
Log10(ENERG)	0.607977	1.086315

Estimated Correlation Matrix

	INTERCPT	Log10(ENERG)
INTERCPT	1.000000	0.951013
Log10(ENERG)	0.951013	1.000000

Probit Model in Terms of Tolerance Distribution

MU	SIGMA
-0.58564	0.208777

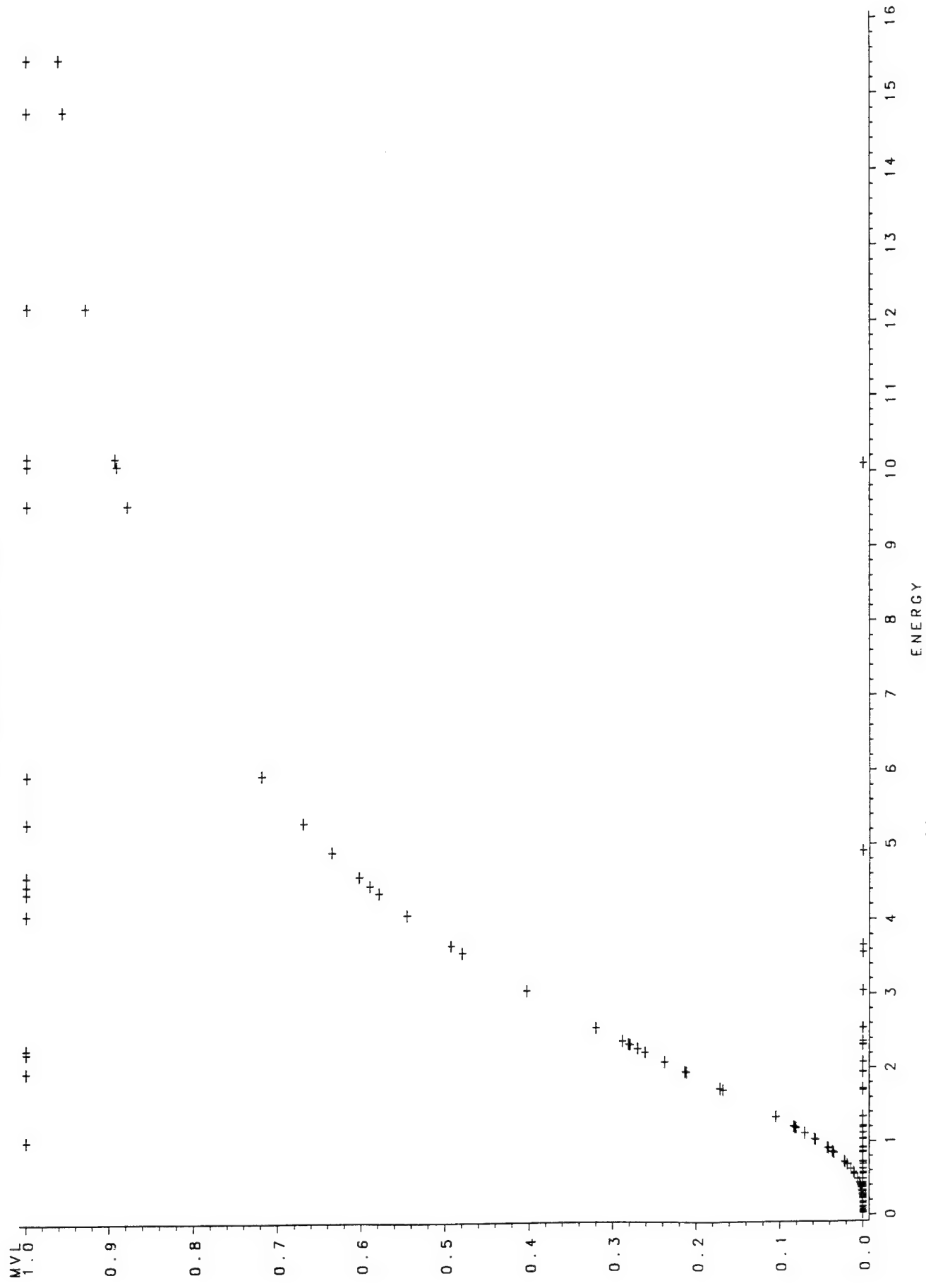
Estimated Covariance Matrix for Tolerance Parameters

MU	SIGMA
0.001599	-0.000257
-0.000257	0.002064

Probit Procedure
 Probit Analysis on ENERGY

Probability	ENERGY	95 Percent Fiducial Limits
		Lower Upper
0.01	0.08485	0.03425 0.12448
0.02	0.09674	0.04289 0.13696
0.03	0.10512	0.04944 0.14559
0.04	0.11191	0.05501 0.15248
0.05	0.11775	0.05998 0.15836
0.06	0.12296	0.06455 0.16357
0.07	0.12772	0.06884 0.16831
0.08	0.13213	0.07290 0.17270
0.09	0.13628	0.07680 0.17681
0.10	0.14022	0.08056 0.18071
0.15	0.15775	0.09803 0.19807
0.20	0.17324	0.11432 0.21355
0.25	0.18774	0.13011 0.22835
0.30	0.20178	0.14576 0.24315
0.35	0.21573	0.16147 0.25848
0.40	0.22986	0.17734 0.27483
0.45	0.24442	0.19343 0.29277
0.50	0.25964	0.20977 0.31293
0.55	0.27580	0.22640 0.33608
0.60	0.29326	0.24340 0.36322
0.65	0.31247	0.26095 0.39563
0.70	0.33408	0.27939 0.43513
0.75	0.35907	0.29930 0.48455
0.80	0.38911	0.32165 0.54873
0.85	0.42732	0.34824 0.63722
0.90	0.48075	0.38305 0.77274
0.91	0.49463	0.39173 0.81004
0.92	0.51017	0.40132 0.85279
0.93	0.52781	0.41203 0.90259
0.94	0.54823	0.42424 0.96189
0.95	0.57250	0.43848 1.03457
0.96	0.60238	0.45568 1.12737
0.97	0.64126	0.47756 1.25344
0.98	0.69685	0.50800 1.44394
0.99	0.79443	0.55939 1.80646

m600nf.dat



OBS	ENERGY	MVL	OBS	ENERGY	MVL
1	0.02	0	62	1.04	0
2	0.03	0	63	1.12	0
3	0.03	0	64	1.19	0
4	0.03	0	65	1.20	0
5	0.04	0	66	1.21	0
6	0.04	0	67	1.34	0
7	0.05	0	68	1.70	0
8	0.05	0	69	1.72	0
9	0.05	0	70	1.94	0
10	0.06	0	71	1.95	1
11	0.08	0	72	1.95	0
12	0.10	0	73	2.08	0
13	0.11	0	74	2.21	1
14	0.11	0	75	2.26	1
15	0.11	0	76	2.31	0
16	0.12	0	77	2.32	0
17	0.15	0	78	2.36	0
18	0.16	0	79	2.54	0
19	0.17	0	80	3.04	0
20	0.17	0	81	3.56	0
21	0.18	0	82	3.66	0
22	0.22	0	83	4.07	1
23	0.22	0	84	4.36	1
24	0.23	0	85	4.46	1
25	0.24	0	86	4.58	1
26	0.24	0	87	4.91	0
27	0.25	0	88	5.30	1
28	0.25	0	89	5.94	1
29	0.25	0	90	9.57	1
30	0.26	0	91	10.10	0
31	0.26	0	92	10.10	1
32	0.27	0	93	10.20	1
33	0.28	0	94	12.20	1
34	0.29	0	95	14.80	1
35	0.31	0	96	15.50	1
36	0.32	0			
37	0.32	0			
38	0.32	0			
39	0.32	0			
40	0.33	0			
41	0.34	0			
42	0.37	0			
43	0.37	0			
44	0.39	0			
45	0.41	0			
46	0.43	0			
47	0.44	0			
48	0.49	0			
49	0.56	0			
50	0.58	0			
51	0.63	0			
52	0.69	0			
53	0.72	0			
54	0.73	0			
55	0.85	0			
56	0.86	0			
57	0.87	0			
58	0.91	0			
59	0.92	0			
60	1.03	1			
61	1.03	0			

Class Levels Values

MVL 2 1 0

Number of observations used = 96

Probit Procedure

Data Set =WORK.INDATA
 Dependent Variable=MVL

Weighted Frequency Counts for the Ordered Response Categories

Level	Count
1	16
0	80

Log Likelihood for NORMAL -18.96758625

Goodness-of-Fit Tests

Statistic	Value	DF	Prob>Chi-Sq
Pearson Chi-Square	29.0354	74	1.0000
L.R. Chi-Square	29.6174	74	1.0000

Response Levels: 2 Number of Covariate Values: 76

NOTE: Since the chi-square is small ($p > 0.1000$), fiducial limits will be calculated using a t value of 1.96.

Variable	DF	Estimate	Std Err	ChiSquare	Pr>Chi	Label/Value
INTERCPT	1	-1.618235	0.364521	19.70776	0.0001	Intercept
Log10(ENE)	1	2.84105928	0.663249	18.3488	0.0001	

Estimated Covariance Matrix

	INTERCPT	Log10(ENERG)
INTERCPT	0.132876	-0.187481
Log10(ENERG)	-0.187481	0.439899

Estimated Correlation Matrix

	INTERCPT	Log10(ENERG)
INTERCPT	1.000000	-0.775459
Log10(ENERG)	-0.775459	1.000000

Probit Model in Terms of Tolerance Distribution

	MU	SIGMA
	0.569589	0.351981

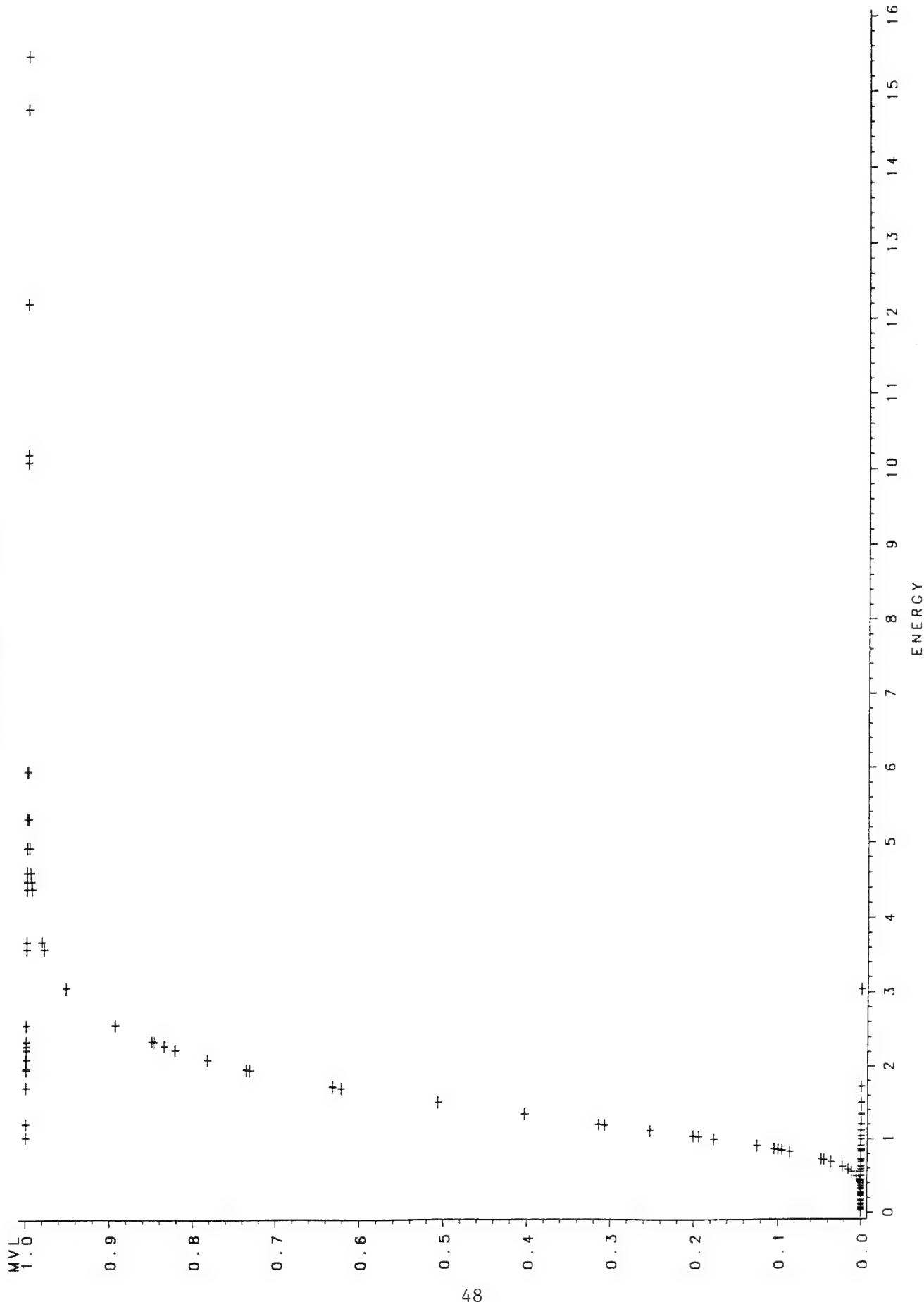
Estimated Covariance Matrix for Tolerance Parameters

	MU	SIGMA
MU	0.007683	0.002751
SIGMA	0.002751	0.006752

Probit Procedure
Probit Analysis on ENERGY

Probability	ENERGY 95 Percent Fiducial Limits		
	Lower	Upper	
0.01	0.56332	0.13872	1.00381
0.02	0.70260	0.20574	1.18359
0.03	0.80832	0.26364	1.31672
0.04	0.89821	0.31727	1.42863
0.05	0.97866	0.36845	1.52829
0.06	1.05278	0.41808	1.62005
0.07	1.12237	0.46670	1.70637
0.08	1.18858	0.51464	1.78886
0.09	1.25218	0.56213	1.86857
0.10	1.31373	0.60932	1.94631
0.15	1.60245	0.84404	2.32242
0.20	1.87652	1.08045	2.70495
0.25	2.14872	1.32011	3.11862
0.30	2.42666	1.56296	3.58311
0.35	2.71621	1.80881	4.11765
0.40	3.02284	2.05809	4.74332
0.45	3.35242	2.31233	5.48512
0.50	3.71183	2.57423	6.37492
0.55	4.10978	2.84780	7.45588
0.60	4.55787	3.13857	8.78949
0.65	5.07241	3.45418	10.46784
0.70	5.67764	3.80550	12.63643
0.75	6.41204	4.20908	15.54122
0.80	7.34216	4.69246	19.63728
0.85	8.59793	5.30751	25.88495
0.90	10.48747	6.17258	36.78905
0.91	11.00296	6.39854	40.06987
0.92	11.59171	6.65213	43.97485
0.93	12.27551	6.94111	48.71950
0.94	13.08700	7.27700	54.63911
0.95	14.07818	7.67786	62.29043
0.96	15.33902	8.17437	72.68380
0.97	17.04484	8.82516	87.90515
0.98	19.60966	9.76498	113.25592
0.99	24.45793	11.43990	169.05401

m600of2hf.dat



OBS	ENERGY	MVL	OBS	ENERGY	MVL
1	0.02	0	62	0.44	0
2	0.03	0	63	0.44	0
3	0.03	0	64	0.45	0
4	0.03	0	65	0.50	0
5	0.03	0	66	0.56	0
6	0.03	0	67	0.59	0
7	0.04	0	68	0.63	0
8	0.04	0	69	0.69	0
9	0.05	0	70	0.72	0
10	0.05	0	71	0.73	0
11	0.05	0	72	0.83	0
12	0.06	0	73	0.83	0
13	0.07	0	74	0.85	0
14	0.08	0	75	0.86	0
15	0.08	0	76	0.87	0
16	0.10	0	77	0.91	0
17	0.11	0	78	1.00	0
18	0.11	0	79	1.03	1
19	0.11	0	80	1.03	1
20	0.12	0	81	1.04	0
21	0.13	0	82	1.12	0
22	0.15	0	83	1.20	0
23	0.16	0	84	1.21	1
24	0.17	0	85	1.34	0
25	0.17	0	86	1.50	0
26	0.17	0	87	1.70	1
27	0.17	0	88	1.72	0
28	0.18	0	89	1.94	1
29	0.18	0	90	1.95	1
30	0.22	0	91	1.95	1
31	0.22	0	92	2.08	1
32	0.22	0	93	2.21	1
33	0.23	0	94	2.26	1
34	0.24	0	95	2.31	1
35	0.24	0	96	2.32	1
36	0.25	0	97	2.54	1
37	0.25	0	98	3.04	0
38	0.25	0	99	3.56	1
39	0.25	0	100	3.66	1
40	0.26	0	101	4.36	1
41	0.26	0	102	4.46	1
42	0.26	0	103	4.58	1
43	0.27	0	104	4.91	1
44	0.28	0	105	5.30	1
45	0.29	0	106	5.94	1
46	0.31	0	107	10.10	1
47	0.32	0	108	10.10	1
48	0.32	0	109	10.20	1
49	0.32	0	110	12.20	1
50	0.32	0	111	14.80	1
51	0.33	0	112	15.50	1
52	0.34	0			
53	0.36	0			
54	0.37	0			
55	0.37	0			
56	0.37	0			
57	0.39	0			
58	0.39	0			
59	0.41	0			
60	0.41	0			
61	0.43	0			

Class	Levels	Values
-------	--------	--------

MVL	2	1 0
-----	---	-----

Number of observations used = 112

Probit Procedure

Data Set =WORK.INDATA
 Dependent Variable=MVL

Weighted Frequency Counts for the Ordered Response Categories

Level	Count
1	27
0	85

Log Likelihood for NORMAL -14.12820084

Goodness-of-Fit Tests

Statistic	Value	DF	Prob>Chi-Sq
Pearson Chi-Square	38.9485	76	0.9999
L.R. Chi-Square	28.2564	76	1.0000

Response Levels: 2 Number of Covariate Values: 78

NOTE: Since the chi-square is small ($p > 0.1000$), fiducial limits will be calculated using a t value of 1.96.

Variable	DF	Estimate	Std Err	ChiSquare	Pr>Chi	Label/Value
INTERCPT	1	-0.9300568	0.331547	7.869169	0.0050	Intercept
Log10(ENE)	1	5.3827644	1.308593	16.92005	0.0001	

Estimated Covariance Matrix

	INTERCPT	Log10(ENERG)
INTERCPT	0.109923	-0.259593
Log10(ENERG)	-0.259593	1.712415

Estimated Correlation Matrix

	INTERCPT	Log10(ENERG)
INTERCPT	1.000000	-0.598334
Log10(ENERG)	-0.598334	1.000000

Probit Model in Terms of Tolerance Distribution

MU	SIGMA
0.172784	0.185778

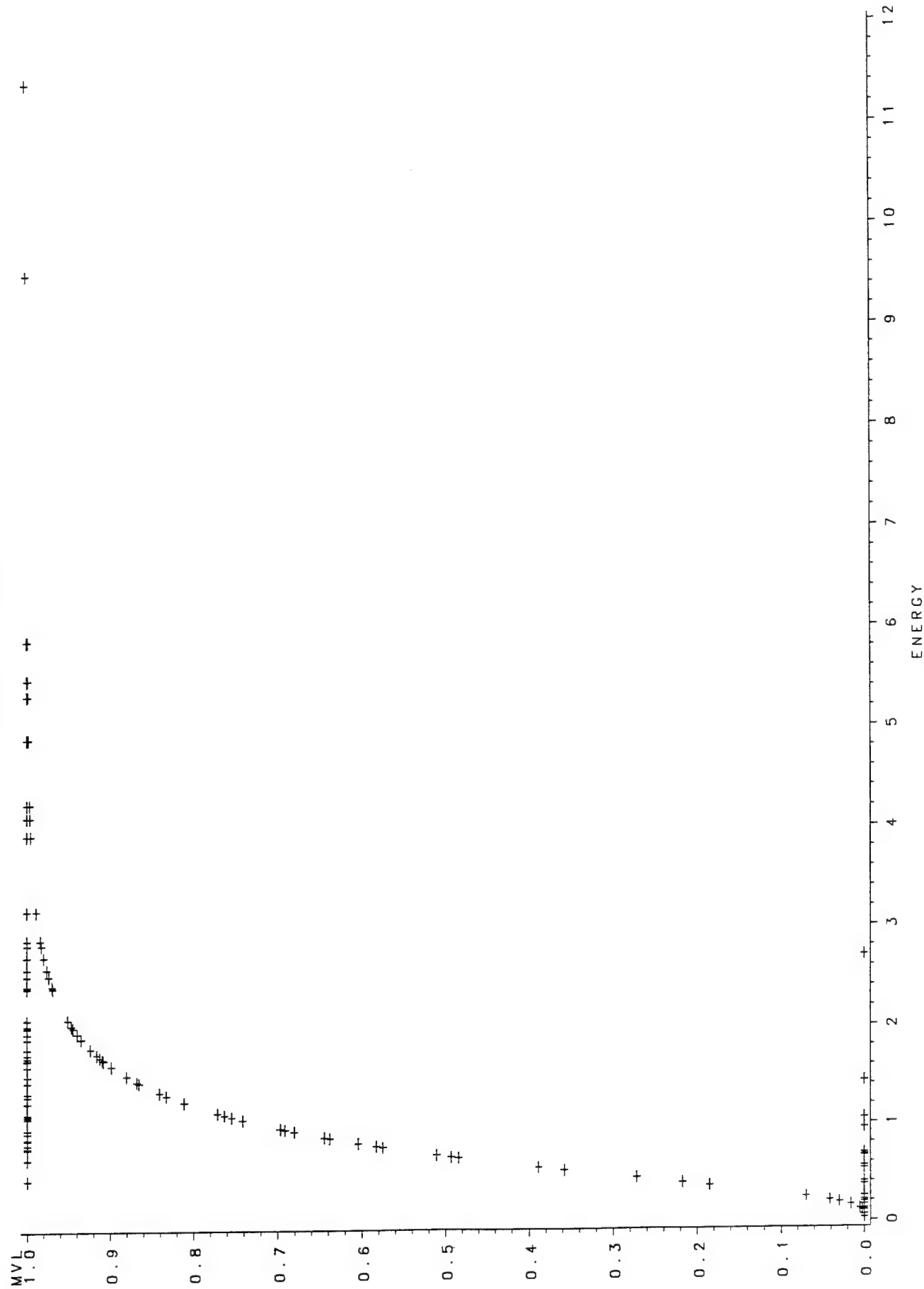
Estimated Covariance Matrix for Tolerance Parameters

MU	SIGMA
0.002462	0.000233
0.000233	0.002040

Probit Procedure
Probit Analysis on ENERGY

Probability	ENERGY 95 Percent Fiducial Limits		
	Lower	Upper	
0.01	0.55030	0.22063	0.78722
0.02	0.61836	0.27384	0.85761
0.03	0.66585	0.31380	0.90631
0.04	0.70396	0.34745	0.94531
0.05	0.73656	0.37731	0.97870
0.06	0.76549	0.40458	1.00841
0.07	0.79180	0.42998	1.03553
0.08	0.81612	0.45395	1.06072
0.09	0.83888	0.47678	1.08443
0.10	0.86040	0.49870	1.10699
0.15	0.95552	0.59894	1.20901
0.20	1.03855	0.68978	1.30239
0.25	1.11552	0.77539	1.39403
0.30	1.18949	0.85769	1.48802
0.35	1.26241	0.93772	1.58753
0.40	1.33573	1.01612	1.69547
0.45	1.41071	1.09339	1.81484
0.50	1.48862	1.17007	1.94897
0.55	1.57083	1.24685	2.10188
0.60	1.65902	1.32466	2.27874
0.65	1.75537	1.40482	2.48667
0.70	1.86297	1.48917	2.73622
0.75	1.98651	1.58045	3.04411
0.80	2.13373	1.68306	3.43938
0.85	2.31916	1.80492	3.97894
0.90	2.57554	1.96331	4.79805
0.91	2.64160	2.00261	5.02245
0.92	2.71529	2.04582	5.27911
0.93	2.79868	2.09399	5.57760
0.94	2.89486	2.14866	5.93228
0.95	3.00858	2.21218	6.36606
0.96	3.14792	2.28849	6.91854
0.97	3.32809	2.38497	7.66696
0.98	3.58365	2.51808	8.79376
0.99	4.02688	2.74019	10.92701

m3ps1h.dat



OBS	ENERGY	MVL	OBS	ENERGY	MVL
1	0.03	0	62	4.23	1
2	0.03	0	63	4.88	1
3	0.03	0	64	5.31	1
4	0.06	0	65	5.47	1
5	0.10	0	66	5.86	1
6	0.10	0	67	9.50	1
7	0.12	0	68	11.40	1
8	0.16	0			
9	0.19	0			
10	0.21	0			
11	0.25	0			
12	0.37	0			
13	0.40	0			
14	0.45	1			
15	0.53	0			
16	0.56	0			
17	0.66	0			
18	0.66	1			
19	0.67	0			
20	0.69	0			
21	0.77	1			
22	0.78	1			
23	0.81	1			
24	0.86	1			
25	0.87	1			
26	0.93	1			
27	0.95	0			
28	0.96	1			
29	1.05	0			
30	1.08	1			
31	1.10	1			
32	1.12	1			
33	1.23	1			
34	1.30	1			
35	1.33	1			
36	1.43	0			
37	1.44	1			
38	1.50	1			
39	1.60	1			
40	1.66	1			
41	1.67	1			
42	1.69	1			
43	1.72	1			
44	1.78	1			
45	1.88	1			
46	1.93	1			
47	1.99	1			
48	2.01	1			
49	2.01	1			
50	2.07	1			
51	2.39	1			
52	2.41	1			
53	2.51	1			
54	2.58	1			
55	2.70	0			
56	2.70	1			
57	2.82	1			
58	2.87	1			
59	3.16	1			
60	3.92	1			
61	4.10	1			

Class	Levels	Values
-------	--------	--------

MVL	2	1 0
-----	---	-----

Number of observations used = 68

Probit Procedure

Data Set =WORK.INDATA
 Dependent Variable=MVL

Weighted Frequency Counts for the Ordered Response Categories

Level	Count
1	46
0	22

Log Likelihood for NORMAL -20.05167322

Goodness-of-Fit Tests

Statistic	Value	DF	Prob>Chi-Sq
Pearson Chi-Square	48.3257	60	0.8604
L.R. Chi-Square	34.5582	60	0.9966

Response Levels: 2 Number of Covariate Values: 62

NOTE: Since the chi-square is small ($p > 0.1000$), fiducial limits will be calculated using a t value of 1.96.

Variable	DF	Estimate	Std Err	ChiSquare	Pr>Chi	Label/Value
INTERCPT	1	0.57647516	0.223289	6.665385	0.0098	Intercept
Log10(ENE)	1	3.40901749	0.843318	16.34087	0.0001	

Estimated Covariance Matrix

	INTERCPT	Log10(ENERG)
INTERCPT	0.049858	0.004998
Log10(ENERG)	0.004998	0.711186

Estimated Correlation Matrix

	INTERCPT	Log10(ENERG)
INTERCPT	1.000000	0.026542
Log10(ENERG)	0.026542	1.000000

Probit Model in Terms of Tolerance Distribution

	MU	SIGMA
	-0.1691	0.29334

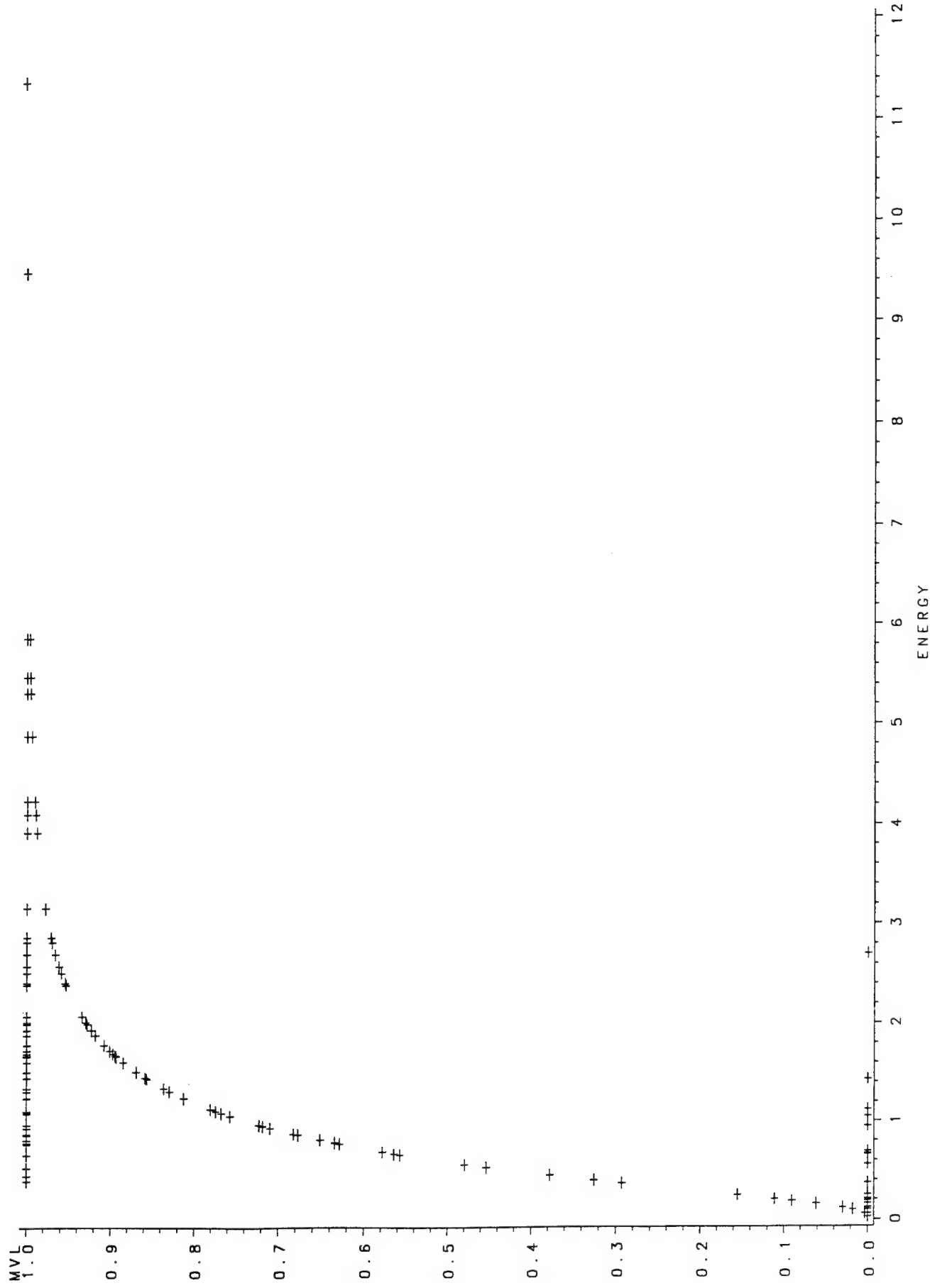
Estimated Covariance Matrix for Tolerance Parameters

	MU	SIGMA
MU	0.005895	-0.002909
SIGMA	-0.002909	0.005266

Probit Procedure
Probit Analysis on ENERGY

Probability	ENERGY 95 Percent Fiducial Limits		
	Lower	Upper	
0.01	0.14076	0.02157	0.27796
0.02	0.16922	0.03070	0.31610
0.03	0.19019	0.03838	0.34313
0.04	0.20766	0.04539	0.36510
0.05	0.22305	0.05202	0.38408
0.06	0.23704	0.05840	0.40109
0.07	0.25003	0.06463	0.41669
0.08	0.26226	0.07076	0.43123
0.09	0.27391	0.07683	0.44495
0.10	0.28508	0.08286	0.45801
0.15	0.33641	0.11317	0.51701
0.20	0.38372	0.14469	0.57043
0.25	0.42958	0.17830	0.62185
0.30	0.47541	0.21465	0.67334
0.35	0.52224	0.25434	0.72648
0.40	0.57093	0.29799	0.78280
0.45	0.62235	0.34627	0.84405
0.50	0.67748	0.39991	0.91245
0.55	0.73749	0.45967	0.99106
0.60	0.80392	0.52640	1.08435
0.65	0.87887	0.60098	1.19907
0.70	0.96544	0.68448	1.34592
0.75	1.06844	0.77852	1.54251
0.80	1.19613	0.88628	1.82019
0.85	1.36434	1.01490	2.24223
0.90	1.61000	1.18246	2.96704
0.91	1.67569	1.22423	3.18167
0.92	1.75009	1.27031	3.43509
0.93	1.83571	1.32191	3.74012
0.94	1.93630	1.38082	4.11653
0.95	2.05777	1.44980	4.59675
0.96	2.21026	1.53353	5.23887
0.97	2.41328	1.64088	6.16092
0.98	2.71233	1.79196	7.65685
0.99	3.26067	2.05225	10.82003

m3ps24h.dat



OBS	ENERGY	MVL	OBS	ENERGY	MVL
1	0.03	0	62	4.23	1
2	0.03	0	63	4.88	1
3	0.03	0	64	5.31	1
4	0.06	0	65	5.47	1
5	0.10	0	66	5.86	1
6	0.10	0	67	9.50	1
7	0.12	0	68	11.40	1
8	0.16	0			
9	0.19	0			
10	0.21	0			
11	0.25	0			
12	0.37	0			
13	0.40	1			
14	0.45	1			
15	0.53	1			
16	0.56	0			
17	0.66	0			
18	0.66	1			
19	0.67	0			
20	0.69	0			
21	0.77	1			
22	0.78	1			
23	0.81	1			
24	0.86	1			
25	0.87	1			
26	0.93	1			
27	0.95	0			
28	0.96	1			
29	1.05	0			
30	1.08	1			
31	1.10	1			
32	1.12	0			
33	1.23	1			
34	1.30	1			
35	1.33	1			
36	1.43	0			
37	1.44	1			
38	1.50	1			
39	1.60	1			
40	1.66	1			
41	1.67	1			
42	1.69	1			
43	1.72	1			
44	1.78	1			
45	1.88	1			
46	1.93	1			
47	1.99	1			
48	2.01	1			
49	2.01	1			
50	2.07	1			
51	2.39	1			
52	2.41	1			
53	2.51	1			
54	2.58	1			
55	2.70	0			
56	2.70	1			
57	2.82	1			
58	2.87	1			
59	3.16	1			
60	3.92	1			
61	4.10	1			

Class	Levels	Values
MVL	2	1 0

Number of observations used = 68

Probit Procedure

Data Set =WORK.INDATA
 Dependent Variable=MVL

Weighted Frequency Counts for the Ordered Response Categories

Level	Count
1	47
0	21

Log Likelihood for NORMAL -22.6459858

Goodness-of-Fit Tests

Statistic	Value	DF	Prob>Chi-Sq
Pearson Chi-Square	44.3226	60	0.9353
L.R. Chi-Square	39.7468	60	0.9797

Response Levels: 2 Number of Covariate Values: 62

NOTE: Since the chi-square is small ($p > 0.1000$), fiducial limits will be calculated using a t value of 1.96.

Variable	DF	Estimate	Std Err	ChiSquare	Pr>Chi	Label/Value
INTERCPT	1	0.6391902	0.211532	9.130757	0.0025	Intercept
Log10(ENE)	1	2.7440567	0.67582	16.48634	0.0001	

Estimated Covariance Matrix

	INTERCPT	Log10(ENERG)
INTERCPT	0.044746	0.011864
Log10(ENERG)	0.011864	0.456732

Estimated Correlation Matrix

	INTERCPT	Log10(ENERG)
INTERCPT	1.000000	0.082991
Log10(ENERG)	0.082991	1.000000

Probit Model in Terms of Tolerance Distribution

MU	SIGMA
-0.23294	0.364424

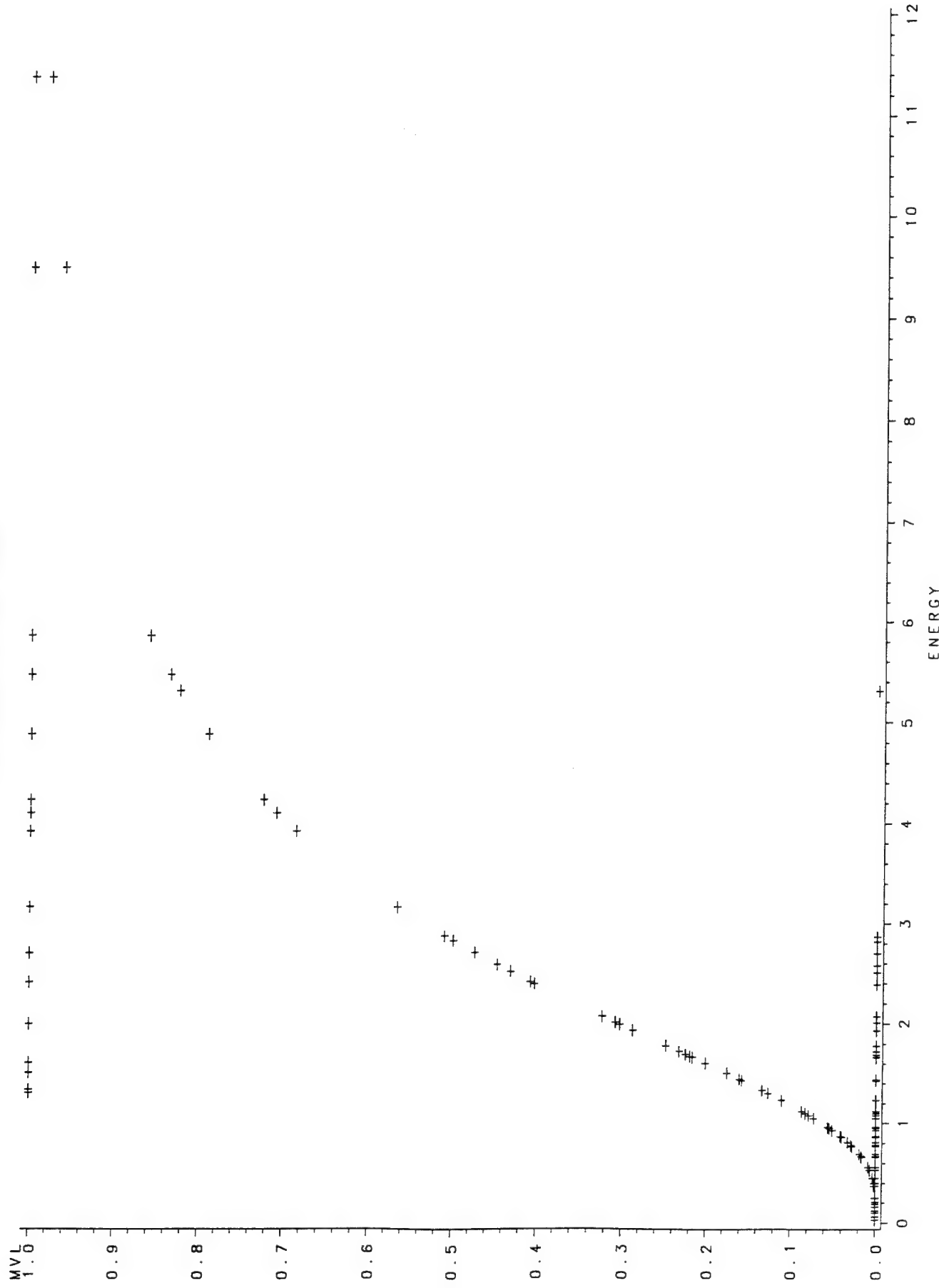
Estimated Covariance Matrix for Tolerance Parameters

MU	MU	SIGMA
0.008500	-0.004575	
-0.004575	0.008055	

Probit Procedure
Probit Analysis on ENERGY

Probability	ENERGY 95 Percent Fiducial Limits		
	Lower	Upper	
0.01	0.08304	0.00819	0.19256
0.02	0.10438	0.01268	0.22582
0.03	0.12069	0.01672	0.24998
0.04	0.13461	0.02058	0.26993
0.05	0.14711	0.02437	0.28741
0.06	0.15866	0.02813	0.30323
0.07	0.16953	0.03189	0.31788
0.08	0.17990	0.03569	0.33164
0.09	0.18987	0.03952	0.34472
0.10	0.19954	0.04341	0.35726
0.15	0.24511	0.06391	0.41485
0.20	0.28864	0.08672	0.46823
0.25	0.33210	0.11244	0.52061
0.30	0.37667	0.14164	0.57395
0.35	0.42330	0.17497	0.62986
0.40	0.47287	0.21320	0.68999
0.45	0.52634	0.25719	0.75633
0.50	0.58488	0.30796	0.83154
0.55	0.64992	0.36667	0.91942
0.60	0.72342	0.43462	1.02569
0.65	0.80813	0.51323	1.15937
0.70	0.90817	0.60413	1.33527
0.75	1.03006	0.70959	1.57878
0.80	1.18514	0.83377	1.93689
0.85	1.39561	0.98603	2.50834
0.90	1.71432	1.19048	3.55210
0.91	1.80164	1.24249	3.87413
0.92	1.90154	1.30034	4.26115
0.93	2.01780	1.36571	4.73619
0.94	2.15606	1.44106	5.33532
0.95	2.32535	1.53028	6.11890
0.96	2.54130	1.63997	7.19748
0.97	2.83446	1.78271	8.80184
0.98	3.27717	1.98748	11.52677
0.99	4.11946	2.35016	17.69933

m3ps1hfa.dat



OBS	ENERGY	MVL	OBS	ENERGY	MVL
1	0.03	0	62	4.88	1
2	0.03	0	63	5.31	0
3	0.03	0	64	5.47	1
4	0.06	0	65	5.86	1
5	0.10	0	66	9.50	1
6	0.10	0	67	11.40	1
7	0.12	0			
8	0.16	0			
9	0.19	0			
10	0.21	0			
11	0.25	0			
12	0.37	0			
13	0.40	0			
14	0.45	0			
15	0.53	0			
16	0.56	0			
17	0.66	0			
18	0.66	0			
19	0.67	0			
20	0.69	0			
21	0.77	0			
22	0.78	0			
23	0.81	0			
24	0.86	0			
25	0.87	0			
26	0.93	0			
27	0.95	0			
28	0.96	0			
29	1.05	0			
30	1.08	0			
31	1.10	0			
32	1.12	0			
33	1.23	0			
34	1.30	1			
35	1.33	1			
36	1.43	0			
37	1.44	0			
38	1.50	1			
39	1.60	1			
40	1.66	0			
41	1.67	0			
42	1.69	0			
43	1.72	0			
44	1.78	0			
45	1.93	0			
46	1.99	1			
47	2.01	0			
48	2.01	0			
49	2.07	0			
50	2.39	0			
51	2.41	1			
52	2.51	0			
53	2.58	0			
54	2.70	1			
55	2.70	0			
56	2.82	0			
57	2.87	0			
58	3.16	1			
59	3.92	1			
60	4.10	1			
61	4.23	1			

Class	Levels	Values
-------	--------	--------

MVL	2	1 0
-----	---	-----

Number of observations used = 67

Probit Procedure

Data Set =WORK.INDATA
 Dependent Variable=MVL

Weighted Frequency Counts for the Ordered Response Categories

Level	Count
1	16
0	51

Log Likelihood for NORMAL -21.94752531

Goodness-of-Fit Tests

Statistic	Value	DF	Prob>Chi-Sq
Pearson Chi-Square	42.0173	59	0.9537
L.R. Chi-Square	41.1225	59	0.9630

Response Levels: 2 Number of Covariate Values: 61

NOTE: Since the chi-square is small ($p > 0.1000$), fiducial limits will be calculated using a t value of 1.96.

Variable	DF	Estimate	Std Err	ChiSquare	Pr>Chi	Label/Value
INTERCPT	1	-1.5297519	0.358923	18.16515	0.0001	Intercept
Log10(ENE)	1	3.39259641	0.902304	14.13706	0.0002	

Estimated Covariance Matrix

	INTERCPT	Log10(ENERG)
INTERCPT	0.128826	-0.258805
Log10(ENERG)	-0.258805	0.814152

Estimated Correlation Matrix

	INTERCPT	Log10(ENERG)
INTERCPT	1.000000	-0.799131
Log10(ENERG)	-0.799131	1.000000

Probit Model in Terms of Tolerance Distribution

	MU	SIGMA
	0.450909	0.294759

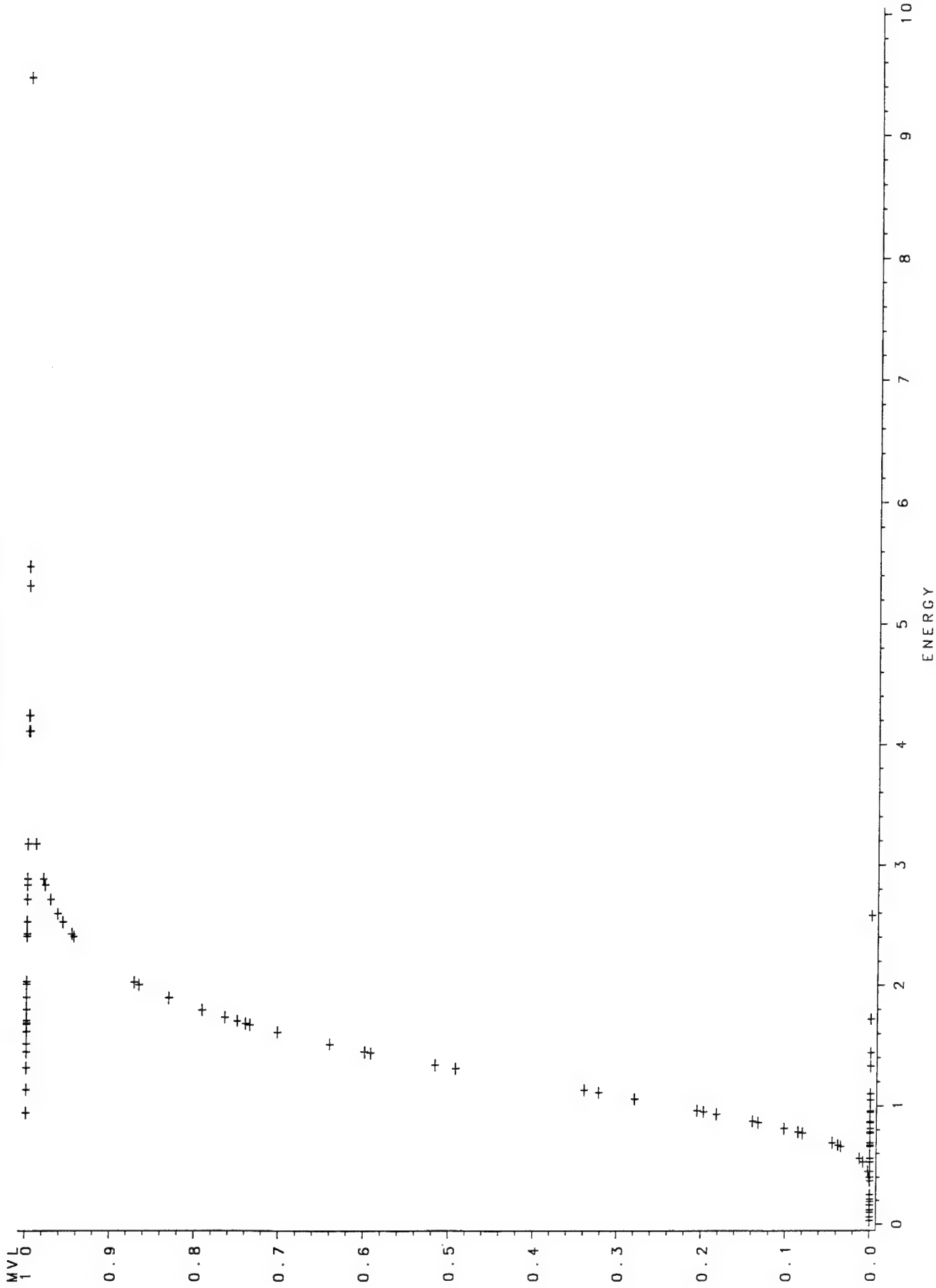
Estimated Covariance Matrix for Tolerance Parameters

	MU	SIGMA
MU	0.005297	0.002774
SIGMA	0.002774	0.006146

Probit Procedure
 Probit Analysis on ENERGY

Probability	ENERGY 95 Percent Fiducial Limits		
	Lower	Upper	
0.01	0.58237	0.13717	0.95650
0.02	0.70072	0.19999	1.09045
0.03	0.78800	0.25362	1.18692
0.04	0.86075	0.30292	1.26650
0.05	0.92485	0.34968	1.33636
0.06	0.98316	0.39483	1.39994
0.07	1.03730	0.43888	1.45918
0.08	1.08831	0.48216	1.51534
0.09	1.13686	0.52489	1.56926
0.10	1.18348	0.56723	1.62155
0.15	1.39769	0.77589	1.87202
0.20	1.59527	0.98224	2.12614
0.25	1.78689	1.18597	2.40450
0.30	1.97850	1.38488	2.72384
0.35	2.17436	1.57708	3.09973
0.40	2.37811	1.76229	3.54758
0.45	2.59340	1.94205	4.08423
0.50	2.82429	2.11923	4.73057
0.55	3.07573	2.29752	5.51511
0.60	3.35417	2.48120	6.47906
0.65	3.66848	2.67536	7.68461
0.70	4.03163	2.88651	9.23029
0.75	4.46397	3.12386	11.28216
0.80	5.00017	3.40211	14.14578
0.85	5.70699	3.74816	18.46100
0.90	6.73998	4.22216	25.87970
0.91	7.01632	4.34381	28.08974
0.92	7.32938	4.47936	30.70905
0.93	7.68975	4.63263	33.87673
0.94	8.11322	4.80924	37.80835
0.95	8.62472	5.01798	42.86022
0.96	9.26702	5.27364	49.67555
0.97	10.12257	5.60425	59.57394
0.98	11.38337	6.07351	75.88220
0.99	13.69689	6.88876	111.19984

m3ps2hf.dat



OBS	ENERGY	MVL
1	0.03	0
2	0.03	0
3	0.03	0
4	0.06	0
5	0.10	0
6	0.10	0
7	0.12	0
8	0.16	0
9	0.19	0
10	0.21	0
11	0.25	0
12	0.37	0
13	0.40	0
14	0.45	0
15	0.53	0
16	0.56	0
17	0.66	0
18	0.67	0
19	0.69	0
20	0.77	0
21	0.78	0
22	0.81	0
23	0.86	0
24	0.87	0
25	0.93	1
26	0.95	0
27	0.96	0
28	1.05	0
29	1.10	0
30	1.12	1
31	1.30	1
32	1.33	0
33	1.43	1
34	1.44	0
35	1.50	1
36	1.60	1
37	1.66	1
38	1.67	1
39	1.69	1
40	1.72	0
41	1.78	1
42	1.88	1
43	1.99	1
44	2.01	1
45	2.01	1
46	2.39	1
47	2.41	1
48	2.51	1
49	2.58	0
50	2.70	1
51	2.70	1
52	2.82	1
53	2.87	1
54	3.16	1
55	4.10	1
56	4.23	1
57	5.31	1
58	5.47	1
59	9.50	1

Class	Levels	Values
MVL	2	1 0

Number of observations used = 59

Probit Procedure

Data Set =WORK.INDATA
 Dependent Variable=MVL

Weighted Frequency Counts for the Ordered Response Categories

Level	Count
1	27
0	32

Log Likelihood for NORMAL -15.09910172

Goodness-of-Fit Tests

Statistic	Value	DF	Prob>Chi-Sq
Pearson Chi-Square	46.0333	52	0.7064
L.R. Chi-Square	30.1982	52	0.9933

Response Levels: 2 Number of Covariate Values: 54

NOTE: Since the chi-square is small ($p > 0.1000$), fiducial limits will be calculated using a t value of 1.96.

Variable	DF	Estimate	Std Err	ChiSquare	Pr>Chi	Label/Value
INTERCPT	1	-0.7143053	0.3377	4.474109	0.0344	Intercept
Log10(ENE)	1	6.10424247	1.52533	16.01534	0.0001	

Estimated Covariance Matrix

	INTERCPT	Log10(ENERG)
INTERCPT	0.114041	-0.333413
Log10(ENERG)	-0.333413	2.326630

Estimated Correlation Matrix

	INTERCPT	Log10(ENERG)
INTERCPT	1.000000	-0.647274
Log10(ENERG)	-0.647274	1.000000

Probit Model in Terms of Tolerance Distribution

	MU	SIGMA
	0.117018	0.16382

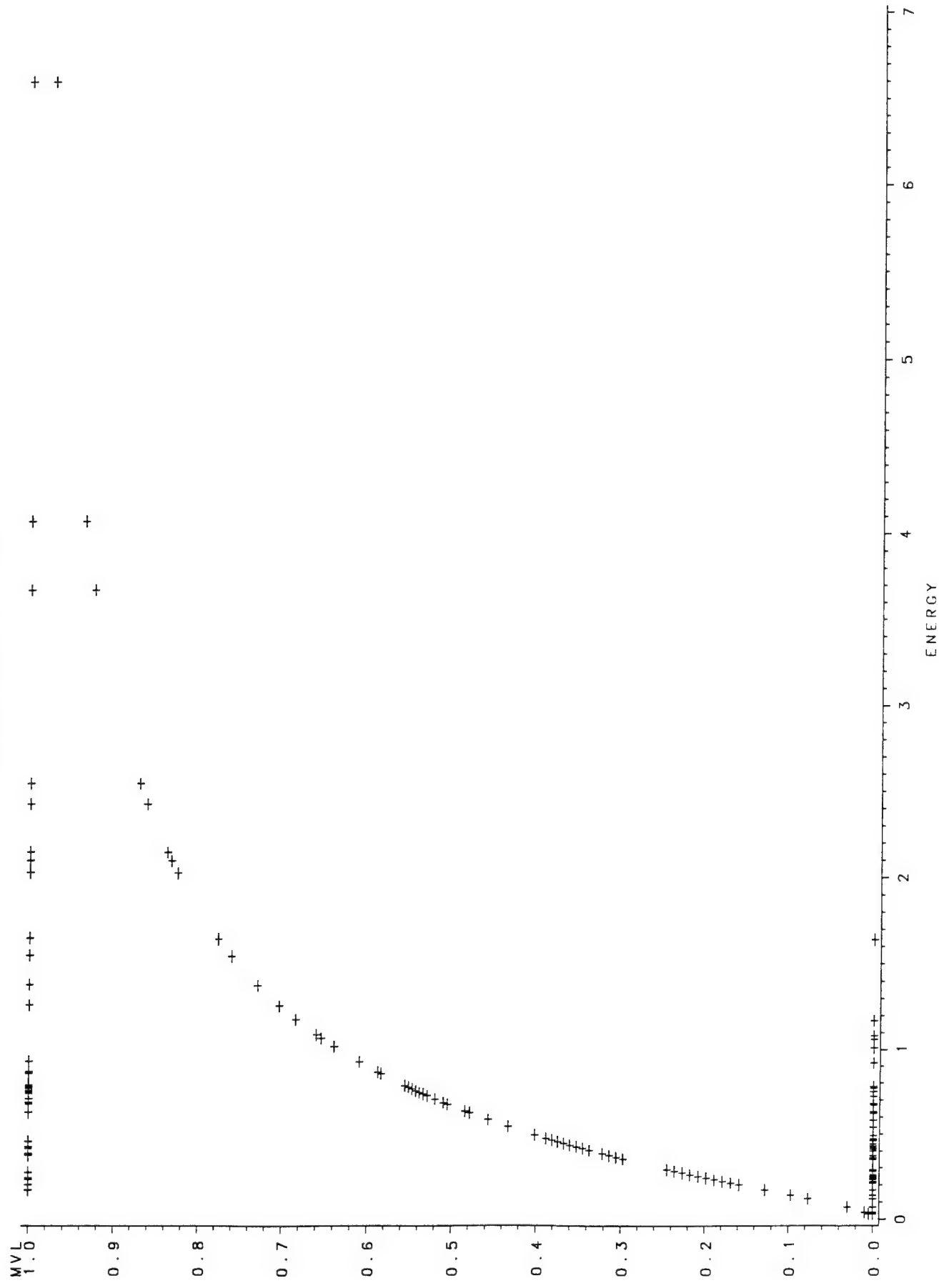
Estimated Covariance Matrix for Tolerance Parameters

	MU	SIGMA
MU	0.001821	-0.000269
SIGMA	-0.000269	0.001676

Probit Procedure
 Probit Analysis on ENERGY

Probability	ENERGY 95 Percent Fiducial Limits		
	Lower	Upper	
0.01	0.54440	0.21295	0.76991
0.02	0.60335	0.25936	0.82854
0.03	0.64403	0.29376	0.86851
0.04	0.67642	0.32250	0.90014
0.05	0.70397	0.34785	0.92697
0.06	0.72831	0.37092	0.95062
0.07	0.75033	0.39233	0.97204
0.08	0.77062	0.41248	0.99178
0.09	0.78954	0.43164	1.01023
0.10	0.80737	0.45000	1.02765
0.15	0.88558	0.53383	1.10485
0.20	0.95311	0.60996	1.17322
0.25	1.01513	0.68222	1.23822
0.30	1.07426	0.75247	1.30294
0.35	1.13213	0.82177	1.36966
0.40	1.18991	0.89073	1.44046
0.45	1.24862	0.95972	1.51753
0.50	1.30924	1.02901	1.60334
0.55	1.37279	1.09884	1.70089
0.60	1.44053	1.16955	1.81397
0.65	1.51405	1.24176	1.94757
0.70	1.59561	1.31659	2.10877
0.75	1.68855	1.39591	2.30843
0.80	1.79843	1.48294	2.56501
0.85	1.93556	1.58368	2.91418
0.90	2.12306	1.71117	3.43989
0.91	2.17101	1.74231	3.58286
0.92	2.22432	1.77637	3.74581
0.93	2.28446	1.81411	3.93456
0.94	2.35354	1.85669	4.15783
0.95	2.43489	1.90584	4.42941
0.96	2.53406	1.96449	4.77308
0.97	2.66152	2.03808	5.23490
0.98	2.84095	2.13871	5.92281
0.99	3.14863	2.30461	7.20413

m60ps1h.dat



14:28 Thursday, September 1, 1994

OBS	ENERGY	MVL	OBS	ENERGY	MVL
1	0.03	0	62	0.76	1
2	0.04	0	63	0.77	0
3	0.07	0	64	0.77	1
4	0.12	0	65	0.78	1
5	0.14	0	66	0.78	0
6	0.17	0	67	0.85	1
7	0.17	0	68	0.86	1
8	0.17	1	69	0.86	1
9	0.17	0	70	0.92	0
10	0.20	1	71	0.92	1
11	0.21	0	72	1.01	0
12	0.21	0	73	1.06	0
13	0.21	0	74	1.08	0
14	0.21	0	75	1.17	0
15	0.22	0	76	1.25	1
16	0.23	1	77	1.37	1
17	0.23	0	78	1.54	1
18	0.24	1	79	1.64	0
19	0.24	0	80	1.64	1
20	0.25	0	81	2.02	1
21	0.26	0	82	2.09	1
22	0.26	0	83	2.14	1
23	0.26	0	84	2.42	1
24	0.27	1	85	2.54	1
25	0.28	0	86	3.67	1
26	0.29	0	87	4.07	1
27	0.29	0	88	6.60	1
28	0.35	0			
29	0.36	0			
30	0.37	0			
31	0.37	1			
32	0.38	1			
33	0.40	0			
34	0.41	1			
35	0.41	0			
36	0.42	0			
37	0.42	1			
38	0.43	0			
39	0.44	0			
40	0.45	1			
41	0.46	0			
42	0.47	0			
43	0.49	0			
44	0.54	0			
45	0.58	0			
46	0.62	1			
47	0.62	0			
48	0.63	0			
49	0.67	0			
50	0.67	1			
51	0.68	0			
52	0.68	1			
53	0.68	0			
54	0.70	1			
55	0.70	1			
56	0.72	0			
57	0.73	1			
58	0.73	1			
59	0.74	1			
60	0.75	1			
61	0.75	0			

Class Levels Values

MVL 2 1 0

Number of observations used = 88

Probit Procedure

Data Set =WORK.INDATA
 Dependent Variable=MVL

Weighted Frequency Counts for the Ordered Response Categories

Level	Count
1	38
0	50

Log Likelihood for NORMAL -49.10440091

Goodness-of-Fit Tests

Statistic	Value	DF	Prob>Chi-Sq
Pearson Chi-Square	46.3840	60	0.9014
L.R. Chi-Square	56.6200	60	0.6000

Response Levels: 2 Number of Covariate Values: 62

NOTE: Since the chi-square is small ($p > 0.1000$), fiducial limits will be calculated using a t value of 1.96.

Variable	DF	Estimate	Std Err	ChiSquare	Pr>Chi	Label/Value
INTERCPT	1	0.34731348	0.192389	3.25899	0.0710	Intercept
Log10(ENE)	1	1.92828983	0.472565	16.65029	0.0001	

Estimated Covariance Matrix

	INTERCPT	Log10(ENERG)
INTERCPT	0.037014	0.058895
Log10(ENERG)	0.058895	0.223317

Estimated Correlation Matrix

	INTERCPT	Log10(ENERG)
INTERCPT	1.000000	0.647794
Log10(ENERG)	0.647794	1.000000

Probit Model in Terms of Tolerance Distribution

	MU	SIGMA
	-0.18011	0.518594

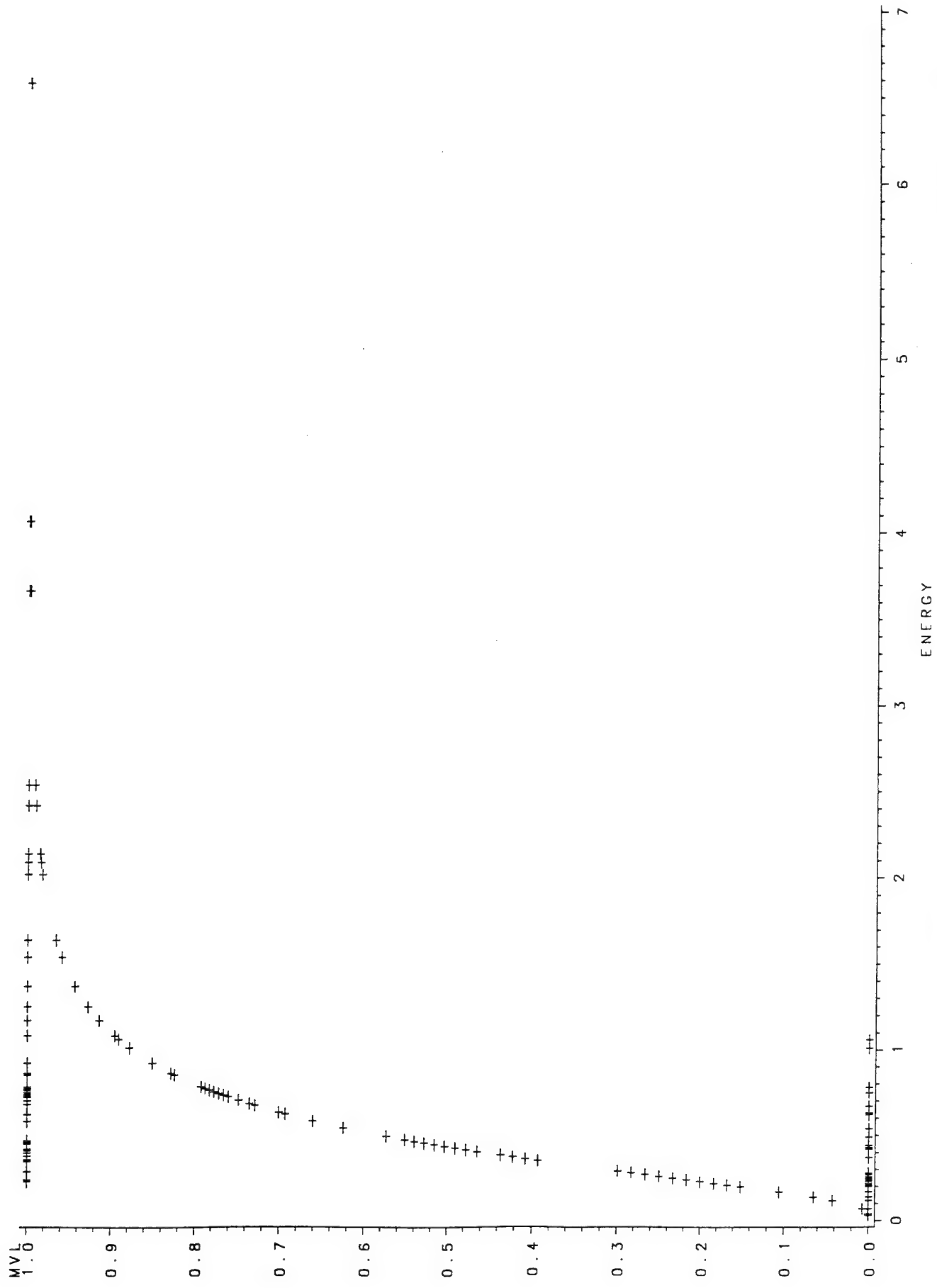
Estimated Covariance Matrix for Tolerance Parameters

	MU	SIGMA
MU	0.006197	0.002604
SIGMA	0.002604	0.016152

Probit Procedure
Probit Analysis on ENERGY

Probability	ENERGY 95 Percent Fiducial Limits		
	Lower	Upper	
0.01	0.04106	0.00359	0.09956
0.02	0.05686	0.00668	0.12485
0.03	0.06991	0.00988	0.14428
0.04	0.08166	0.01327	0.16097
0.05	0.09266	0.01685	0.17606
0.06	0.10318	0.02064	0.19010
0.07	0.11338	0.02465	0.20342
0.08	0.12337	0.02888	0.21621
0.09	0.13322	0.03335	0.22862
0.10	0.14298	0.03806	0.24077
0.15	0.19160	0.06544	0.29969
0.20	0.24178	0.09986	0.35957
0.25	0.29519	0.14211	0.42453
0.30	0.35313	0.19269	0.49893
0.35	0.41693	0.25148	0.58872
0.40	0.48809	0.31748	0.70247
0.45	0.56848	0.38905	0.85210
0.50	0.66052	0.46480	1.05356
0.55	0.76745	0.54460	1.32823
0.60	0.89386	0.62987	1.70706
0.65	1.04643	0.72347	2.23881
0.70	1.23548	0.82974	3.00617
0.75	1.47799	0.95533	4.16064
0.80	1.80445	1.11136	6.00894
0.85	2.27706	1.31909	9.26904
0.90	3.05134	1.62852	16.06949
0.91	3.27486	1.71256	18.36418
0.92	3.53628	1.80841	21.23417
0.93	3.84788	1.91959	24.91560
0.94	4.22846	2.05138	29.79366
0.95	4.70865	2.21216	36.54299
0.96	5.34295	2.41647	46.46543
0.97	6.24100	2.69260	62.45386
0.98	7.67269	3.10735	92.58257
0.99	10.62468	3.89056	172.36246

m60ps2h.dat



OBS	ENERGY	MVL	OBS	ENERGY	MVL
1	0.03	0	62	0.76	1
2	0.04	0	63	0.77	1
3	0.07	0	64	0.77	1
4	0.12	0	65	0.78	1
5	0.14	0	66	0.78	0
6	0.17	0	67	0.85	1
7	0.17	0	68	0.86	1
8	0.17	0	69	0.86	1
9	0.17	0	70	0.92	1
10	0.20	0	71	0.92	1
11	0.21	0	72	1.01	0
12	0.21	0	73	1.06	0
13	0.21	0	74	1.08	1
14	0.21	0	75	1.17	1
15	0.22	0	76	1.25	1
16	0.23	1	77	1.37	1
17	0.23	0	78	1.54	1
18	0.24	1	79	1.64	1
19	0.24	0	80	1.64	1
20	0.25	0	81	2.02	1
21	0.26	0	82	2.09	1
22	0.26	0	83	2.14	1
23	0.26	0	84	2.42	1
24	0.27	0	85	2.54	1
25	0.28	0	86	3.67	1
26	0.29	1	87	4.07	1
27	0.29	1	88	6.60	1
28	0.35	1			
29	0.36	1			
30	0.37	0			
31	0.37	0			
32	0.38	1			
33	0.40	1			
34	0.41	1			
35	0.41	1			
36	0.42	0			
37	0.42	1			
38	0.43	0			
39	0.44	0			
40	0.45	1			
41	0.46	1			
42	0.47	1			
43	0.49	0			
44	0.54	0			
45	0.58	1			
46	0.62	1			
47	0.62	0			
48	0.63	0			
49	0.67	0			
50	0.67	0			
51	0.68	1			
52	0.68	1			
53	0.68	1			
54	0.70	1			
55	0.70	1			
56	0.72	1			
57	0.73	1			
58	0.73	1			
59	0.74	1			
60	0.75	1			
61	0.75	0			

Class	Levels	Values
MVL	2	1 0

Number of observations used = 88

Probit Procedure

Data Set =WORK.INDATA
 Dependent Variable=MVL

Weighted Frequency Counts for the Ordered Response Categories

Level	Count
1	50
0	38

Log Likelihood for NORMAL -40.30846562

Goodness-of-Fit Tests

Statistic	Value	DF	Prob>Chi-Sq
Pearson Chi-Square	58.5556	60	0.5287
L.R. Chi-Square	63.9814	60	0.3386

Response Levels: 2 Number of Covariate Values: 62

NOTE: Since the chi-square is small ($p > 0.1000$), fiducial limits will be calculated using a t value of 1.96.

Variable	DF	Estimate	Std Err	ChiSquare	Pr>Chi	Label/Value
INTERCPT	1	1.15269993	0.26359	19.12384	0.0001	Intercept
Log10(ENE)	1	3.12472526	0.647079	23.31898	0.0001	

Estimated Covariance Matrix

	INTERCPT	Log10(ENERG)
INTERCPT	0.069480	0.135351
Log10(ENERG)	0.135351	0.418711

Estimated Correlation Matrix

	INTERCPT	Log10(ENERG)
INTERCPT	1.000000	0.793554
Log10(ENERG)	0.793554	1.000000

Probit Model in Terms of Tolerance Distribution

MU	SIGMA
-0.3689	0.320028

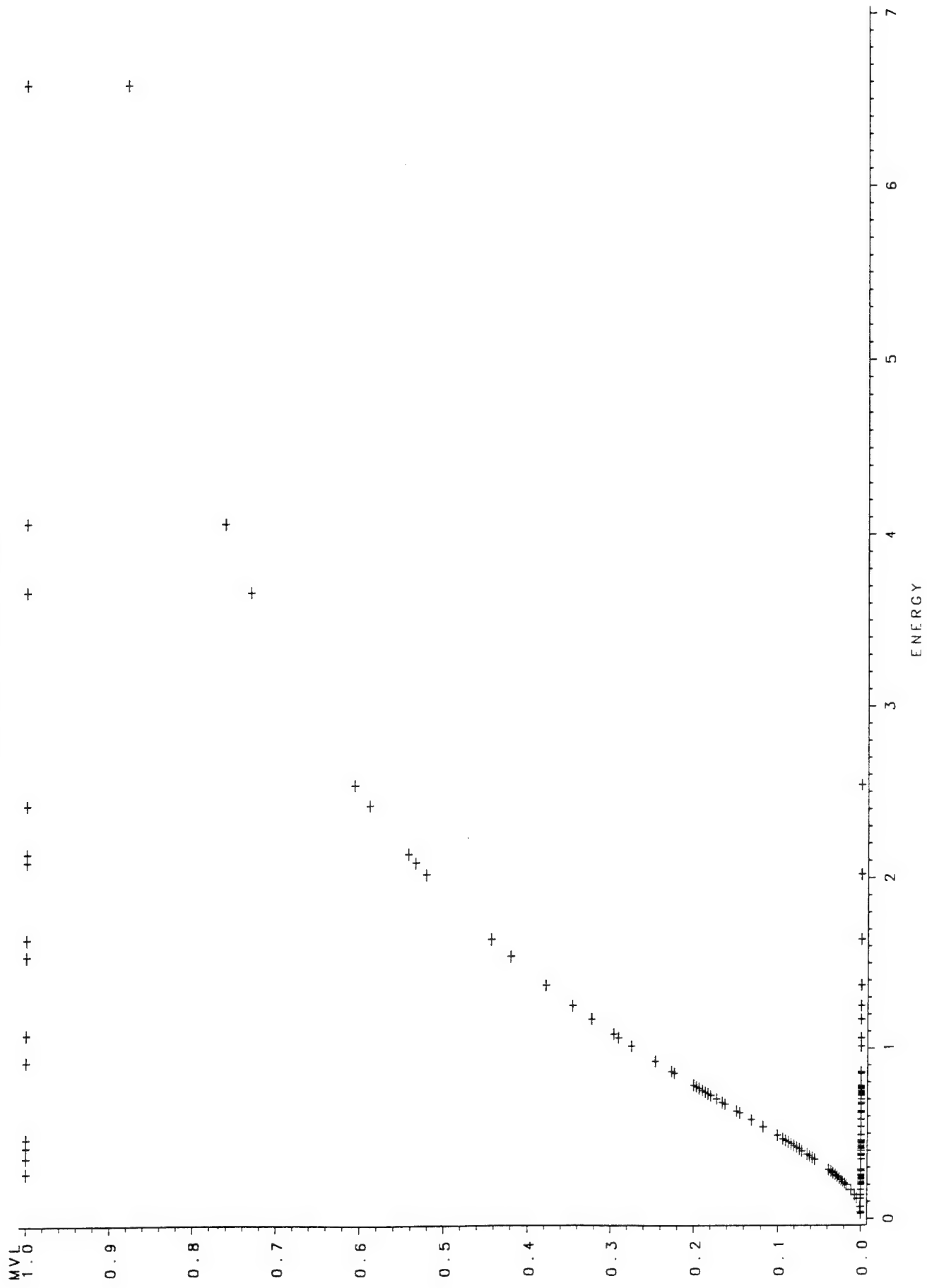
Estimated Covariance Matrix for Tolerance Parameters

MU	MU	SIGMA
0.002724	-0.000626	
-0.000626	0.004392	

Probit Procedure
 Probit Analysis on ENERGY

Probability	ENERGY	95 Percent Fiducial Limits	
		Lower	Upper
0.01	0.07702	0.02145	0.13496
0.02	0.09416	0.02995	0.15634
0.03	0.10695	0.03699	0.17173
0.04	0.11772	0.04335	0.18436
0.05	0.12726	0.04931	0.19537
0.06	0.13600	0.05500	0.20530
0.07	0.14415	0.06053	0.21447
0.08	0.15186	0.06593	0.22306
0.09	0.15923	0.07125	0.23121
0.10	0.16633	0.07652	0.23900
0.15	0.19926	0.10260	0.27470
0.20	0.23002	0.12915	0.30773
0.25	0.26016	0.15687	0.34025
0.30	0.29059	0.18618	0.37362
0.35	0.32195	0.21734	0.40907
0.40	0.35483	0.25055	0.44789
0.45	0.38984	0.28591	0.49168
0.50	0.42766	0.32345	0.54250
0.55	0.46916	0.36319	0.60306
0.60	0.51544	0.40527	0.67701
0.65	0.56809	0.45016	0.76933
0.70	0.62940	0.49883	0.88736
0.75	0.70301	0.55314	1.04286
0.80	0.79514	0.61639	1.25684
0.85	0.91789	0.69486	1.57225
0.90	1.09960	0.80276	2.09734
0.91	1.14864	0.83060	2.25023
0.92	1.20439	0.86172	2.42963
0.93	1.26881	0.89703	2.64417
0.94	1.34485	0.93790	2.90715
0.95	1.43715	0.98644	3.24027
0.96	1.55372	1.04626	3.68222
0.97	1.71006	1.12424	4.31115
0.98	1.94250	1.23610	5.32026
0.99	2.37465	1.43364	7.42056

m60p1hfa.dat



14:28 Thursday, September 1, 1994

OBS	ENERGY	MVL	OBS	ENERGY	MVL
1	0.03	0	62	0.76	0
2	0.04	0	63	0.77	0
3	0.07	0	64	0.77	0
4	0.12	0	65	0.78	0
5	0.14	0	66	0.78	0
6	0.17	0	67	0.85	0
7	0.17	0	68	0.86	0
8	0.17	0	69	0.86	0
9	0.17	0	70	0.92	1
10	0.20	0	71	0.92	1
11	0.21	0	72	1.01	0
12	0.21	0	73	1.06	0
13	0.21	0	74	1.08	1
14	0.21	0	75	1.17	0
15	0.22	0	76	1.25	0
16	0.23	0	77	1.37	0
17	0.23	0	78	1.54	1
18	0.24	0	79	1.64	0
19	0.24	0	80	1.64	1
20	0.25	0	81	2.02	0
21	0.26	0	82	2.09	1
22	0.26	0	83	2.14	1
23	0.26	0	84	2.42	1
24	0.27	1	85	2.54	0
25	0.28	0	86	3.67	1
26	0.29	0	87	4.07	1
27	0.29	0	88	6.60	1
28	0.35	0			
29	0.36	1			
30	0.37	0			
31	0.37	0			
32	0.38	0			
33	0.40	0			
34	0.41	0			
35	0.41	0			
36	0.42	0			
37	0.42	1			
38	0.43	0			
39	0.44	0			
40	0.45	0			
41	0.46	0			
42	0.47	1			
43	0.49	0			
44	0.54	0			
45	0.58	0			
46	0.62	0			
47	0.62	0			
48	0.63	0			
49	0.67	0			
50	0.67	0			
51	0.68	0			
52	0.68	0			
53	0.68	0			
54	0.70	0			
55	0.70	0			
56	0.72	0			
57	0.73	0			
58	0.73	0			
59	0.74	0			
60	0.75	0			
61	0.75	0			

Class Levels Values

MVL 2 1 0

Number of observations used = 88

Probit Procedure

Data Set =WORK.INDATA
 Dependent Variable=MVL

Weighted Frequency Counts for the Ordered Response Categories

Level	Count
1	15
0	73

Log Likelihood for NORMAL -30.21481609

Goodness-of-Fit Tests

Statistic	Value	DF	Prob>Chi-Sq
Pearson Chi-Square	85.2157	60	0.0179
L.R. Chi-Square	54.8845	60	0.6626

Response Levels: 2 Number of Covariate Values: 62

WARNING: All variances and covariances have been multiplied by the heterogeneity factor H= 1.4203. Please check to be sure that the large chi-square (p < 0.0179) is not caused by systematic departure from the model. A t value of 2.0003 will be used in computing fiducial limits.

Variable	DF	Estimate	Std Err	ChiSquare	Pr>Chi	Label/Value
INTERCPT	1	-0.6061335	0.227784	7.080923	0.0078	Intercept
Log10(ENE)	1	2.16463176	0.678151	10.18861	0.0014	

Estimated Covariance Matrix

	INTERCPT	Log10(ENERG)
INTERCPT	0.051886	0.049418
Log10(ENERG)	0.049418	0.459889

Estimated Correlation Matrix

	INTERCPT	Log10(ENERG)
INTERCPT	1.000000	0.319916
Log10(ENERG)	0.319916	1.000000

Probit Model in Terms of Tolerance Distribution

MU	SIGMA
0.280017	0.461972

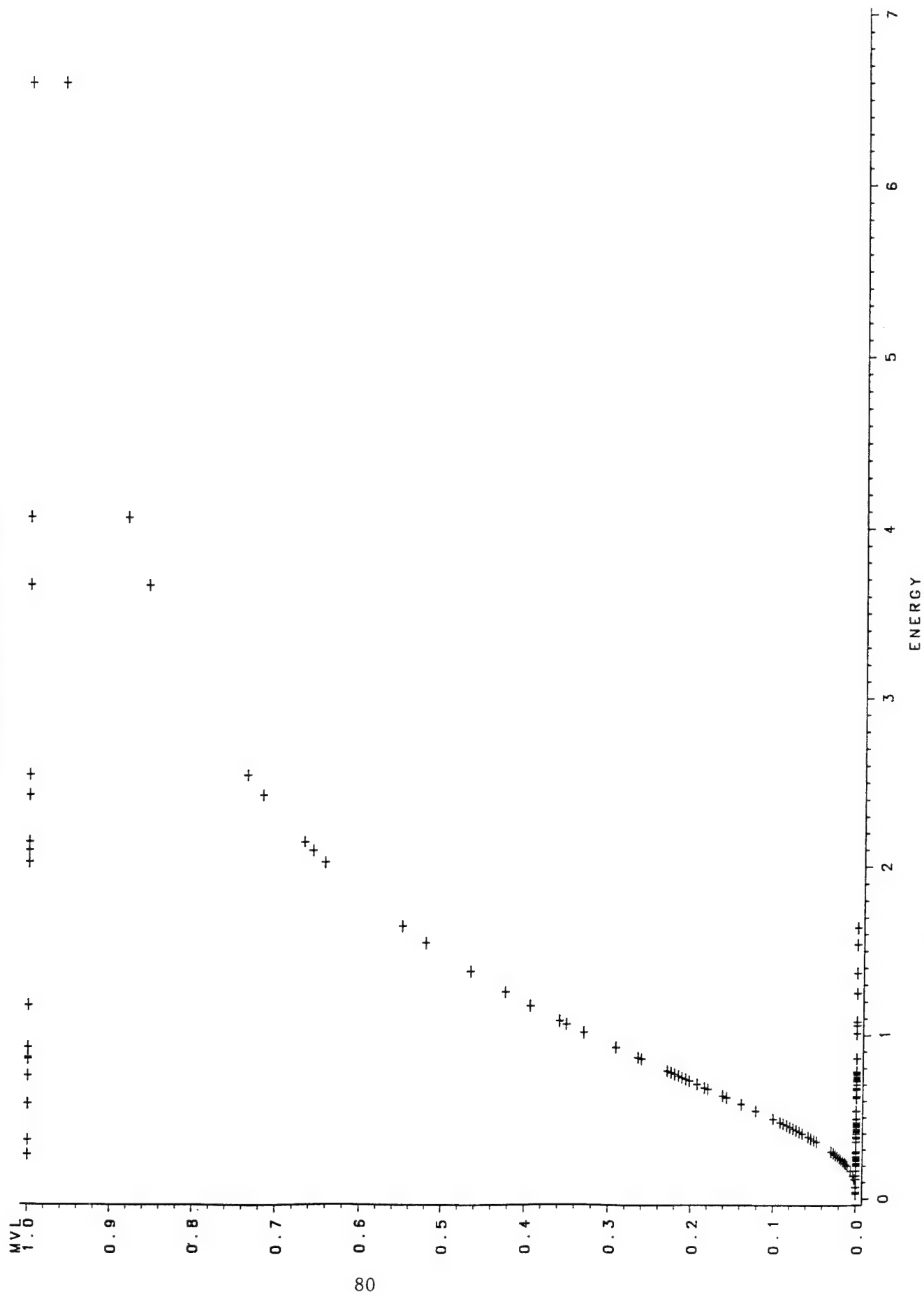
Estimated Covariance Matrix for Tolerance Parameters

MU	MU	SIGMA
0.024676	0.017569	
0.017569	0.020947	

Probit Procedure
 Probit Analysis on ENERGY

Probability	ENERGY 95 Percent Fiducial Limits		
	Lower	Upper	
0.01	0.16044	0.01016	0.32721
0.02	0.21441	0.02163	0.39948
0.03	0.25772	0.03476	0.45566
0.04	0.29597	0.04947	0.50499
0.05	0.33124	0.06571	0.55083
0.06	0.36455	0.08341	0.59493
0.07	0.39650	0.10251	0.63836
0.08	0.42748	0.12295	0.68190
0.09	0.45775	0.14463	0.72616
0.10	0.48750	0.16747	0.77167
0.15	0.63272	0.29474	1.03483
0.20	0.77841	0.43096	1.40044
0.25	0.92987	0.56217	1.92802
0.30	1.09083	0.68408	2.68053
0.35	1.26476	0.79888	3.73633
0.40	1.45538	0.91037	5.20592
0.45	1.66711	1.02210	7.25246
0.50	1.90553	1.13726	10.12292
0.55	2.17806	1.25894	14.20185
0.60	2.49492	1.39058	20.11029
0.65	2.87094	1.53647	28.89869
0.70	3.32871	1.70254	42.45268
0.75	3.90492	1.89780	64.43214
0.80	4.66469	2.13737	102.74315
0.85	5.73879	2.45008	177.35519
0.90	7.44832	2.90276	353.29990
0.91	7.93247	3.02319	417.40988
0.92	8.49417	3.15934	500.36225
0.93	9.15781	3.31573	610.79672
0.94	9.96046	3.49907	763.28956
0.95	10.96210	3.71997	984.35660
0.96	12.26833	3.99659	1327
0.97	14.08937	4.36387	1918
0.98	16.93527	4.90299	3129
0.99	22.63212	5.88676	6771

m6op2hfa.dat



m60p2hfa.dat

10:49 Monday, September 19, 1994

1

OBS	ENERGY	MVL	OBS	ENERGY	MVL
1	0.03	0	62	0.76	0
2	0.04	0	63	0.77	0
3	0.07	0	64	0.77	0
4	0.12	0	65	0.78	0
5	0.14	0	66	0.78	0
6	0.17	0	67	0.85	1
7	0.17	0	68	0.86	1
8	0.17	0	69	0.86	0
9	0.17	0	70	0.92	1
10	0.20	0	71	0.92	1
11	0.21	0	72	1.01	0
12	0.21	0	73	1.06	0
13	0.21	0	74	1.08	0
14	0.21	0	75	1.17	1
15	0.22	0	76	1.25	0
16	0.23	0	77	1.37	0
17	0.23	0	78	1.54	0
18	0.24	0	79	1.64	0
19	0.24	0	80	1.64	0
20	0.25	0	81	2.02	1
21	0.26	0	82	2.09	1
22	0.26	0	83	2.14	1
23	0.26	0	84	2.42	1
24	0.27	1	85	2.54	1
25	0.28	0	86	3.67	1
26	0.29	0	87	4.07	1
27	0.29	0	88	6.60	1
28	0.35	0			
29	0.36	1			
30	0.37	0			
31	0.37	0			
32	0.38	0			
33	0.40	0			
34	0.41	0			
35	0.41	0			
36	0.42	0			
37	0.42	0			
38	0.43	0			
39	0.44	0			
40	0.45	0			
41	0.46	0			
42	0.47	0			
43	0.49	0			
44	0.54	0			
45	0.58	1			
46	0.62	0			
47	0.62	0			
48	0.63	0			
49	0.67	0			
50	0.67	0			
51	0.68	0			
52	0.68	0			
53	0.68	0			
54	0.70	0			
55	0.70	0			
56	0.72	0			
57	0.73	0			
58	0.73	0			
59	0.74	0			
60	0.75	0			
61	0.75	1			

Class	Levels	Values
MVL	2	1 0

Number of observations used = 88

Probit Procedure

Data Set =WORK.INDATA
 Dependent Variable=MVL

Weighted Frequency Counts for the Ordered Response Categories

Level	Count
1	17
0	71

Log Likelihood for NORMAL -29.58785691

Goodness-of-Fit Tests

Statistic	Value	DF	Prob>Chi-Sq
Pearson Chi-Square	91.7675	60	0.0052
L.R. Chi-Square	53.6305	60	0.7061

Response Levels: 2 Number of Covariate Values: 62

WARNING: All variances and covariances have been multiplied by the heterogeneity factor H= 1.5295. Please check to be sure that the large chi-square ($p < 0.0052$) is not caused by systematic departure from the model. A t value of 2.0003 will be used in computing fiducial limits.

Variable	DF	Estimate	Std Err	ChiSquare	Pr>Chi	Label/Value
INTERCPT	1	-0.4513701	0.241771	3.485425	0.0619	Intercept
Log10(ENE)	1	2.67787959	0.794166	11.36998	0.0007	

Estimated Covariance Matrix

	INTERCPT	Log10(ENERG)
INTERCPT	0.058453	0.066039
Log10(ENERG)	0.066039	0.630699

Estimated Correlation Matrix

	INTERCPT	Log10(ENERG)
INTERCPT	1.000000	0.343942
Log10(ENERG)	0.343942	1.000000

Probit Model in Terms of Tolerance Distribution

MU	SIGMA
0.168555	0.37343

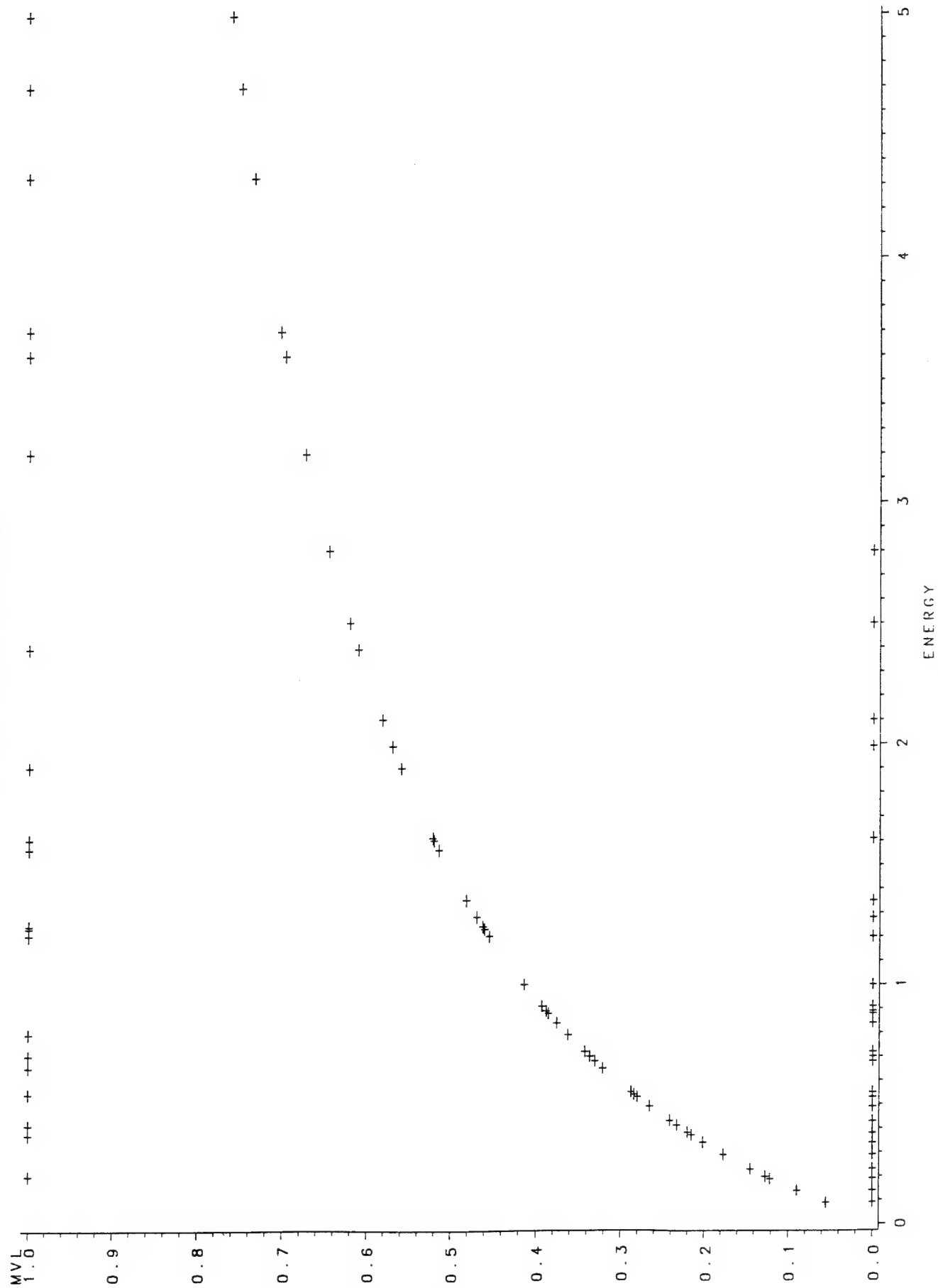
Estimated Covariance Matrix for Tolerance Parameters

MU	MU	SIGMA
0.013755	0.008975	0.012265
SIGMA	0.008975	0.012265

Probit Procedure
 Probit Analysis on ENERGY

Probability	ENERGY 95 Percent Fiducial Limits		
	Lower	Upper	
0.01	0.19945	0.02467	0.36377
0.02	0.25213	0.04315	0.42867
0.03	0.29256	0.06131	0.47742
0.04	0.32719	0.07965	0.51906
0.05	0.35836	0.09832	0.55681
0.06	0.38722	0.11739	0.59226
0.07	0.41443	0.13689	0.62634
0.08	0.44041	0.15680	0.65967
0.09	0.46545	0.17711	0.69269
0.10	0.48976	0.19780	0.72576
0.15	0.60467	0.30532	0.90100
0.20	0.71494	0.41498	1.11163
0.25	0.82543	0.52088	1.37990
0.30	0.93914	0.62019	1.72594
0.35	1.05844	0.71329	2.17052
0.40	1.18563	0.80221	2.73922
0.45	1.32321	0.88936	3.46722
0.50	1.47420	0.97707	4.40497
0.55	1.64241	1.06762	5.62685
0.60	1.83300	1.16340	7.24595
0.65	2.05327	1.26728	9.44145
0.70	2.31410	1.38304	12.51277
0.75	2.63287	1.51625	16.99729
0.80	3.03978	1.67607	23.95851
0.85	3.59410	1.87966	35.82400
0.90	4.43736	2.16606	59.57394
0.91	4.66910	2.24083	67.38191
0.92	4.93458	2.32472	77.03722
0.93	5.24396	2.42027	89.26967
0.94	5.61247	2.53127	105.25656
0.95	6.06446	2.66363	127.03432
0.96	6.64222	2.82743	158.47674
0.97	7.42847	3.04183	208.04544
0.98	8.61958	3.35087	298.84671
0.99	10.89639	3.89997	529.28244

mon4ns1h.dat



OBS	ENERGY	MVL
1	0.09	0
2	0.14	0
3	0.19	0
4	0.20	1
5	0.23	0
6	0.29	0
7	0.29	0
8	0.34	0
9	0.37	1
10	0.38	0
11	0.41	1
12	0.43	0
13	0.49	0
14	0.53	0
15	0.54	1
16	0.55	0
17	0.65	1
18	0.68	0
19	0.68	0
20	0.70	1
21	0.70	0
22	0.72	0
23	0.79	1
24	0.84	0
25	0.88	0
26	0.89	0
27	0.91	0
28	1.00	0
29	1.20	1
30	1.20	0
31	1.20	0
32	1.23	1
33	1.24	1
34	1.28	0
35	1.35	0
36	1.56	1
37	1.60	1
38	1.61	0
39	1.90	1
40	1.99	0
41	2.10	0
42	2.39	1
43	2.50	0
44	2.80	0
45	3.20	1
46	3.60	1
47	3.70	1
48	4.33	1
49	4.70	1
50	5.00	1

Class	Levels	Values
MVL	2	1 0

Number of observations used = 50

Probit Procedure

Data Set =WORK.INDATA
 Dependent Variable=MVL

Weighted Frequency Counts for the Ordered Response Categories

Level	Count
1	20
0	30

Log Likelihood for NORMAL -29.89350195

Goodness-of-Fit Tests

Statistic	Value	DF	Prob>Chi-Sq
Pearson Chi-Square	45.3005	43	0.3762
L.R. Chi-Square	53.1953	43	0.1371

Response Levels: 2 Number of Covariate Values: 45

NOTE: Since the chi-square is small ($p > 0.1000$), fiducial limits will be calculated using a t value of 1.96.

Variable	DF	Estimate	Std Err	ChiSquare	Pr>Chi	Label/Value
INTERCPT	1	-0.2174918	0.188589	1.330002	0.2488	Intercept
Log10(ENE)	1	1.32008413	0.511045	6.67244	0.0098	

Estimated Covariance Matrix

	INTERCPT	Log10(ENERG)
INTERCPT	0.035566	0.004526
Log10(ENERG)	0.004526	0.261167

Estimated Correlation Matrix

	INTERCPT	Log10(ENERG)
INTERCPT	1.000000	0.046964
Log10(ENERG)	0.046964	1.000000

Probit Model in Terms of Tolerance Distribution

	MU	SIGMA
	0.164756	0.757527

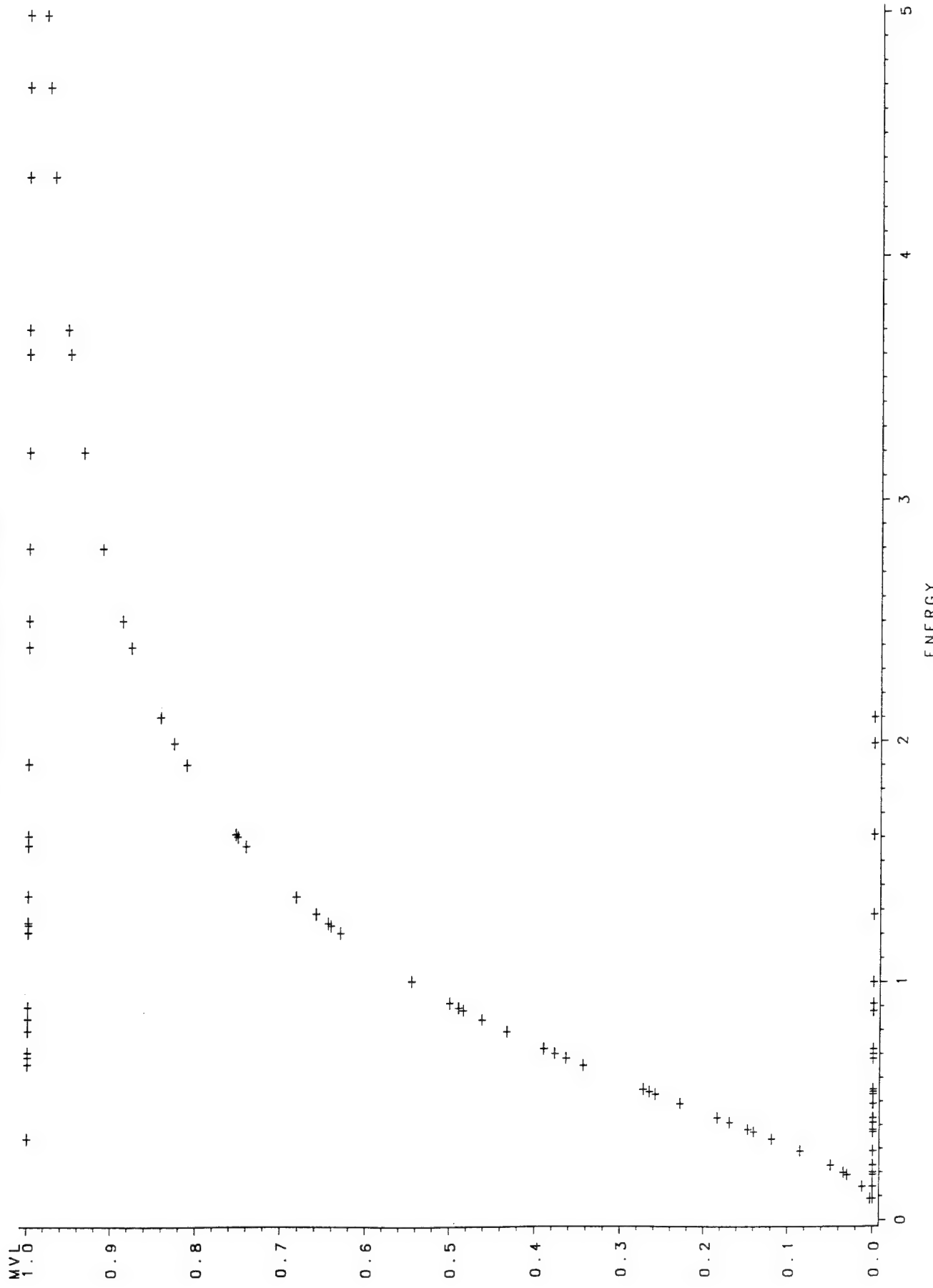
Estimated Covariance Matrix for Tolerance Parameters

	MU	SIGMA
MU	0.025333	0.020672
SIGMA	0.020672	0.086003

Probit Procedure
 Probit Analysis on ENERGY

Probability	ENERGY	95 Percent Fiducial Limits	
		Lower	Upper
0.01	0.02526	2.50915E-7	0.13081
0.02	0.04064	1.78146E-6	0.17333
0.03	0.05495	6.16676E-6	0.20760
0.04	0.06895	0.0000157	0.23808
0.05	0.08293	0.0000334	0.26644
0.06	0.09704	0.0000637	0.29348
0.07	0.11138	0.0001119	0.31972
0.08	0.12600	0.0001852	0.34546
0.09	0.14096	0.0002927	0.37096
0.10	0.15630	0.0004457	0.39640
0.15	0.23968	0.00251	0.52740
0.20	0.33667	0.00973	0.67602
0.25	0.45062	0.03015	0.86251
0.30	0.58547	0.07923	1.12754
0.35	0.74622	0.17851	1.57052
0.40	0.93937	0.33863	2.45060
0.45	1.17372	0.53804	4.40713
0.50	1.46136	0.74632	8.92876
0.55	1.81948	0.95553	19.59826
0.60	2.27339	1.17313	45.61296
0.65	2.86185	1.41125	112.23192
0.70	3.64757	1.68502	294.96937
0.75	4.73915	2.01573	847.08795
0.80	6.34318	2.43835	2768
0.85	8.91010	3.02067	11086
0.90	13.66364	3.92591	64015
0.91	15.15008	4.17892	97853
0.92	16.94870	4.47096	155209
0.93	19.17380	4.81416	257834
0.94	22.00593	5.22688	454642
0.95	25.75004	5.73869	868522
0.96	30.97054	6.40144	1858878
0.97	38.86054	7.31773	4739960
0.98	52.54450	8.73478	16463927
0.99	84.53342	11.52854	117349056

mon4ns2h.dat



14:28 Thursday, September 1, 1994

OBS	ENERGY	MVL
1	0.09	0
2	0.14	0
3	0.19	0
4	0.20	0
5	0.23	0
6	0.29	0
7	0.29	0
8	0.34	1
9	0.37	0
10	0.38	0
11	0.41	0
12	0.43	0
13	0.49	0
14	0.53	0
15	0.54	0
16	0.55	0
17	0.65	1
18	0.68	0
19	0.68	1
20	0.70	1
21	0.70	0
22	0.72	0
23	0.79	1
24	0.84	1
25	0.88	0
26	0.89	1
27	0.91	0
28	1.00	0
29	1.20	1
30	1.20	1
31	1.20	1
32	1.23	1
33	1.24	1
34	1.28	0
35	1.35	1
36	1.56	1
37	1.60	1
38	1.61	0
39	1.90	1
40	1.99	0
41	2.10	0
42	2.39	1
43	2.50	1
44	2.80	1
45	3.20	1
46	3.60	1
47	3.70	1
48	4.33	1
49	4.70	1
50	5.00	1

Class	Levels	Values
-------	--------	--------

MVL	2	1 0
-----	---	-----

Number of observations used = 50

Probit Procedure

Data Set =WORK.INDATA
 Dependent Variable=MVL

Weighted Frequency Counts for the Ordered Response Categories

Level	Count
1	25
0	25

Log Likelihood for NORMAL -23.37262829

Goodness-of-Fit Tests

Statistic	Value	DF	Prob>Chi-Sq
Pearson Chi-Square	39.3919	43	0.6286
L.R. Chi-Square	41.2001	43	0.5496

Response Levels: 2 Number of Covariate Values: 45

NOTE: Since the chi-square is small ($p > 0.1000$), fiducial limits will be calculated using a t value of 1.96.

Variable	DF	Estimate	Std Err	ChiSquare	Pr>Chi	Label/Value
INTERCPT	1	0.11498251	0.212111	0.293858	0.5878	Intercept
Log10(ENE)	1	2.76813575	0.729107	14.41425	0.0001	

Estimated Covariance Matrix

	INTERCPT	Log10(ENERG)
INTERCPT	0.044991	0.018279
Log10(ENERG)	0.018279	0.531597

Estimated Correlation Matrix

	INTERCPT	Log10(ENERG)
INTERCPT	1.000000	0.118194
Log10(ENERG)	0.118194	1.000000

Probit Model in Terms of Tolerance Distribution

MU	SIGMA
-0.04154	0.361254

Estimated Covariance Matrix for Tolerance Parameters

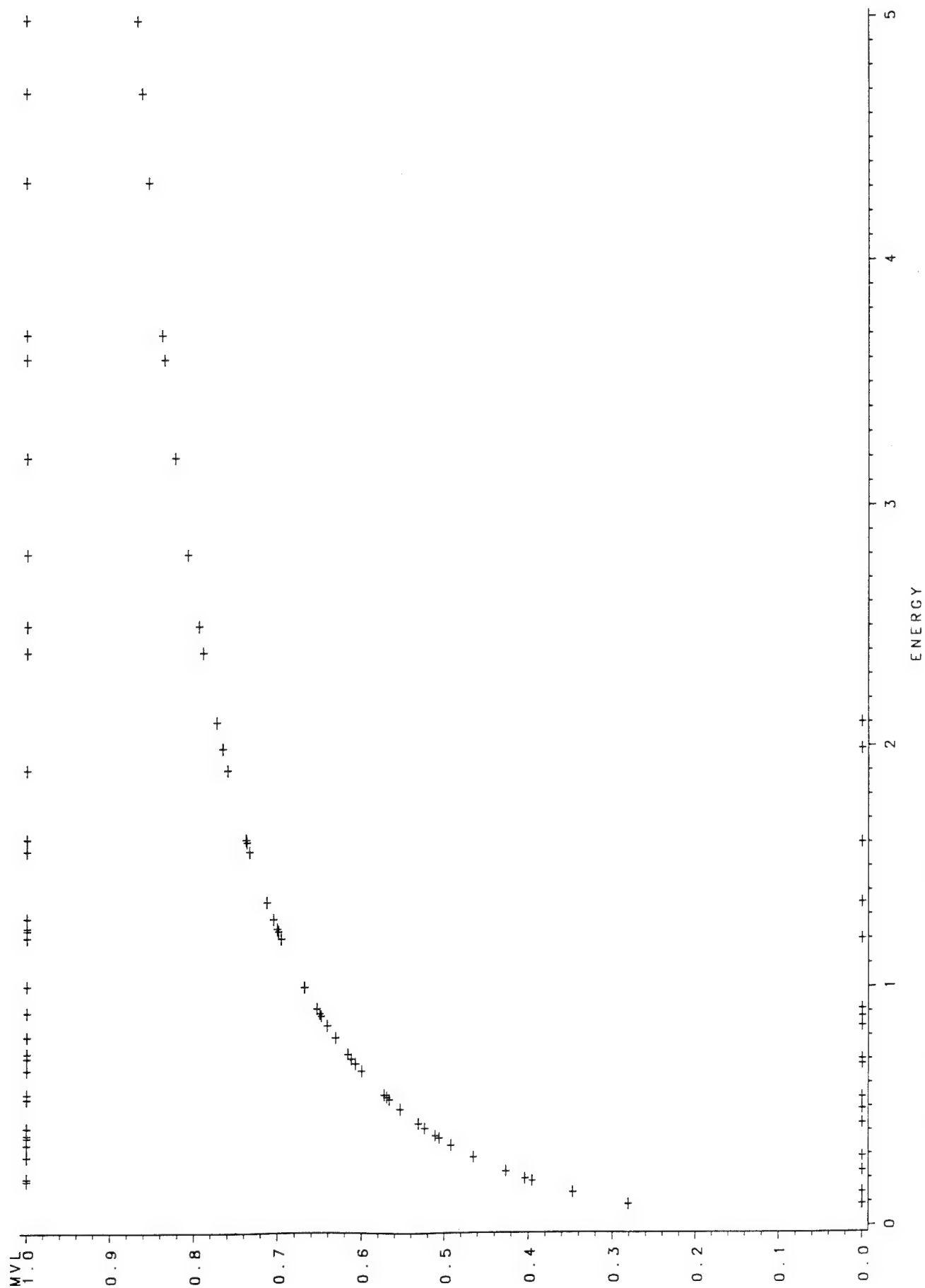
MU	SIGMA	MU	SIGMA
0.005793	-0.000179		
-0.000179	0.009054		

14:28 Thursday, September 1, 1994

Probit Procedure
 Probit Analysis on ENERGY

Probability	ENERGY 95 Percent Fiducial Limits		
	Lower	Upper	
0.01	0.13124	0.01544	0.27010
0.02	0.16464	0.02450	0.31593
0.03	0.19012	0.03280	0.34931
0.04	0.21185	0.04083	0.37696
0.05	0.23134	0.04876	0.40126
0.06	0.24934	0.05669	0.42335
0.07	0.26627	0.06468	0.44387
0.08	0.28241	0.07276	0.46324
0.09	0.29793	0.08095	0.48174
0.10	0.31297	0.08928	0.49956
0.15	0.38375	0.13345	0.58274
0.20	0.45126	0.18262	0.66247
0.25	0.51856	0.23752	0.74410
0.30	0.58752	0.29866	0.83177
0.35	0.65957	0.36624	0.92983
0.40	0.73610	0.44016	1.04366
0.45	0.81859	0.51994	1.18029
0.50	0.90879	0.60486	1.34918
0.55	1.00892	0.69431	1.56298
0.60	1.12198	0.78824	1.83916
0.65	1.25216	0.88768	2.20304
0.70	1.40574	0.99505	2.69422
0.75	1.59266	1.11471	3.38033
0.80	1.83021	1.25422	4.38913
0.85	2.15218	1.42775	5.99786
0.90	2.63893	1.66733	8.95520
0.91	2.77214	1.72935	9.87489
0.92	2.92449	1.79874	10.98498
0.93	3.10168	1.87760	12.35453
0.94	3.31230	1.96900	14.09238
0.95	3.57003	2.07777	16.38188
0.96	3.89856	2.21212	19.56142
0.97	4.34416	2.38771	24.34381
0.98	5.01634	2.64048	32.58767
0.99	6.29310	3.08927	51.68928

m4ns1hfa.dat



14:28 Thursday, September 1, 1994

OBS	ENERGY	MVL
1	0.09	0
2	0.14	0
3	0.19	1
4	0.20	1
5	0.23	0
6	0.29	0
7	0.29	1
8	0.34	1
9	0.37	1
10	0.38	1
11	0.41	1
12	0.43	0
13	0.49	0
14	0.53	1
15	0.54	0
16	0.55	1
17	0.65	1
18	0.68	0
19	0.68	0
20	0.70	1
21	0.70	0
22	0.72	1
23	0.79	1
24	0.84	0
25	0.88	0
26	0.89	1
27	0.91	0
28	1.00	1
29	1.20	1
30	1.20	0
31	1.20	1
32	1.23	1
33	1.24	1
34	1.28	1
35	1.35	0
36	1.56	1
37	1.60	0
38	1.61	1
39	1.90	1
40	1.99	0
41	2.10	0
42	2.39	1
43	2.50	1
44	2.80	1
45	3.20	1
46	3.60	1
47	3.70	1
48	4.33	1
49	4.70	1
50	5.00	1

Class	Levels	Values
MVL	2	1 0

Number of observations used = 50

Probit Procedure

Data Set =WORK.INDATA
 Dependent Variable=MVL

Weighted Frequency Counts for the Ordered Response Categories

Level	Count
1	32
0	18

Log Likelihood for NORMAL -30.57125336

Goodness-of-Fit Tests

Statistic	Value	DF	Prob>Chi-Sq
Pearson Chi-Square	41.5216	43	0.5355
L.R. Chi-Square	51.7782	43	0.1686

Response Levels: 2 Number of Covariate Values: 45

NOTE: Since the chi-square is small ($p > 0.1000$), fiducial limits will be calculated using a t value of 1.96.

Variable	DF	Estimate	Std Err	ChiSquare	Pr>Chi	Label/Value
INTERCPT	1	0.43522957	0.192325	5.121123	0.0236	Intercept
Log10(ENE)	1	0.97061995	0.490926	3.909003	0.0480	

Estimated Covariance Matrix

	INTERCPT	Log10(ENERG)
INTERCPT	0.036989	0.022750
Log10(ENERG)	0.022750	0.241009

Estimated Correlation Matrix

	INTERCPT	Log10(ENERG)
INTERCPT	1.000000	0.240953
Log10(ENERG)	0.240953	1.000000

Probit Model in Terms of Tolerance Distribution

	MU	SIGMA
	-0.4484	1.030269

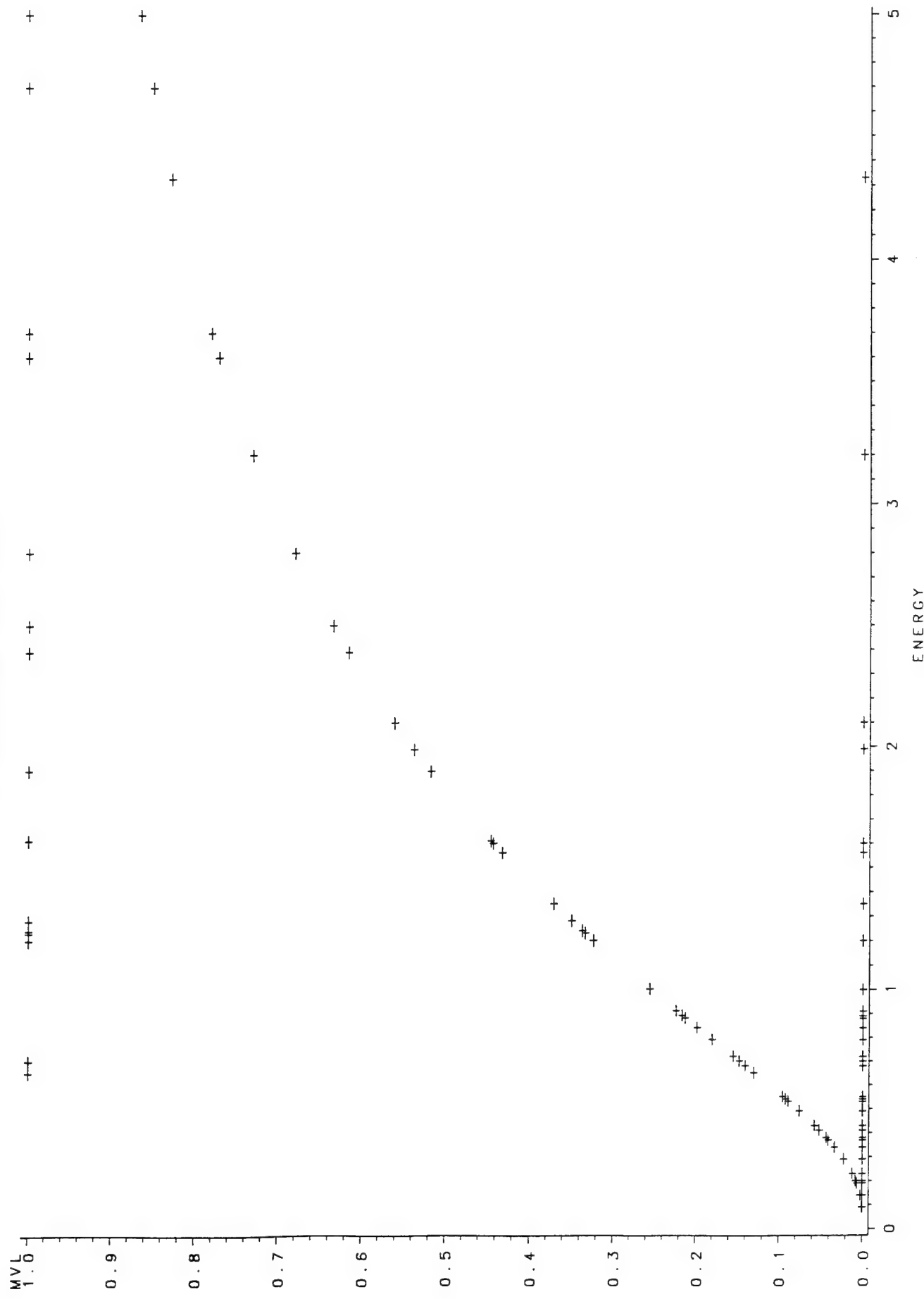
Estimated Covariance Matrix for Tolerance Parameters

	MU	SIGMA
MU	0.069042	-0.093304
SIGMA	-0.093304	0.271541

Probit Procedure
 Probit Analysis on ENERGY

Probability	ENERGY	95 Percent Fiducial Limits	
		Lower	Upper
0.01	0.00143	0	0.03550
0.02	0.00273	4.311E-286	0.04946
0.03	0.00411	1.625E-265	0.06110
0.04	0.00560	4.891E-250	0.07166
0.05	0.00719	1.904E-237	0.08162
0.06	0.00891	9.908E-227	0.09121
0.07	0.01074	2.466E-217	0.10058
0.08	0.01271	6.378E-209	0.10981
0.09	0.01480	2.856E-201	0.11897
0.10	0.01703	3.15E-194	0.12811
0.15	0.03046	4.522E-165	0.17458
0.20	0.04836	6.702E-142	0.22442
0.25	0.07189	5.037E-122	0.27999
0.30	0.10264	3.534E-104	0.34402
0.35	0.14276	1.2052E-87	0.42052
0.40	0.19525	5.7877E-72	0.51650
0.45	0.26432	8.3811E-57	0.64660
0.50	0.35612	6.6241E-42	0.84967
0.55	0.47980	4.5572E-27	1.28268
0.60	0.64955	2.7825E-12	3.80839
0.65	0.88834	0.04079	1532132
0.70	1.23558	0.41794	6.23365E21
0.75	1.76402	0.73741	3.04579E39
0.80	2.62236	1.05666	1.99327E59
0.85	4.16296	1.45811	2.75183E82
0.90	7.44628	2.07381	3.7852E111
0.91	8.56910	2.24799	4.1479E118
0.92	9.98156	2.45070	1.8455E126
0.93	11.80480	2.69132	4.7464E134
0.94	14.23744	2.98421	1.1745E144
0.95	17.62944	3.35278	6.0783E154
0.96	22.66076	3.83863	2.3546E167
0.97	30.85463	4.52555	7.0497E182
0.98	46.50620	5.61987	2.6433E203
0.99	88.78943	7.87682	7.0942E235

m4ns2hfa.dat



14:28 Thursday, September 1, 1994

OBS	ENERGY	MVL
1	0.09	0
2	0.14	0
3	0.19	0
4	0.20	0
5	0.23	0
6	0.29	0
7	0.29	0
8	0.34	0
9	0.37	0
10	0.38	0
11	0.41	0
12	0.43	0
13	0.49	0
14	0.53	0
15	0.54	0
16	0.55	0
17	0.65	1
18	0.68	0
19	0.68	0
20	0.70	1
21	0.70	0
22	0.72	0
23	0.79	0
24	0.84	0
25	0.88	0
26	0.89	0
27	0.91	0
28	1.00	0
29	1.20	1
30	1.20	0
31	1.20	0
32	1.23	1
33	1.24	1
34	1.28	1
35	1.35	0
36	1.56	0
37	1.60	0
38	1.61	1
39	1.90	1
40	1.99	0
41	2.10	0
42	2.39	1
43	2.50	1
44	2.80	1
45	3.20	0
46	3.60	1
47	3.70	1
48	4.33	0
49	4.70	1
50	5.00	1

Class	Levels	Values
MVL	2	1 0

Number of observations used - 50

Probit Procedure

Data Set =WORK.INDATA
 Dependent Variable=MVL

Weighted Frequency Counts for the Ordered Response Categories

Level	Count
1	15
0	35

Log Likelihood for NORMAL -21.74577103

Goodness-of-Fit Tests

Statistic	Value	DF	Prob>Chi-Sq
Pearson Chi-Square	34.1984	43	0.8288
L.R. Chi-Square	36.8999	43	0.7320

Response Levels: 2 Number of Covariate Values: 45

NOTE: Since the chi-square is small ($p > 0.1000$), fiducial limits will be calculated using a t value of 1.96.

Variable	DF	Estimate	Std Err	ChiSquare	Pr>Chi	Label/Value
INTERCPT	1	-0.655907	0.232181	7.980549	0.0047	Intercept
Log10(ENE)	1	2.51433949	0.721711	12.13729	0.0005	

Estimated Covariance Matrix

	INTERCPT	Log10(ENERG)
INTERCPT	0.053908	-0.058109
Log10(ENERG)	-0.058109	0.520866

Estimated Correlation Matrix

	INTERCPT	Log10(ENERG)
INTERCPT	1.000000	-0.346777
Log10(ENERG)	-0.346777	1.000000

Probit Model in Terms of Tolerance Distribution

MU	SIGMA
0.260867	0.397719

Estimated Covariance Matrix for Tolerance Parameters

MU	MU	SIGMA
0.009338	0.004892	0.004892
0.004892	0.013033	0.013033

Probit Procedure
 Probit Analysis on ENERGY

Probability	ENERGY 95 Percent Fiducial Limits		
	Lower	Upper	
0.01	0.21659	0.02020	0.44381
0.02	0.27800	0.03535	0.52662
0.03	0.32572	0.05031	0.58813
0.04	0.36693	0.06553	0.63993
0.05	0.40428	0.08116	0.68615
0.06	0.43904	0.09727	0.72877
0.07	0.47197	0.11392	0.76895
0.08	0.50355	0.13113	0.80743
0.09	0.53410	0.14892	0.84471
0.10	0.56386	0.16730	0.88117
0.15	0.70576	0.26828	1.05981
0.20	0.84360	0.38408	1.24773
0.25	0.98313	0.51290	1.46222
0.30	1.12798	0.65134	1.72153
0.35	1.28120	0.79511	2.04718
0.40	1.44579	0.94058	2.46477
0.45	1.62513	1.08610	3.00540
0.50	1.82334	1.23226	3.70949
0.55	2.04571	1.38139	4.63387
0.60	2.29947	1.53704	5.86372
0.65	2.59487	1.70391	7.53356
0.70	2.94734	1.88833	9.86802
0.75	3.38161	2.09951	13.26971
0.80	3.94090	2.35246	18.53378
0.85	4.71059	2.67515	27.47001
0.90	5.89608	3.13136	45.26276
0.91	6.22458	3.25100	51.09247
0.92	6.60222	3.38552	58.29088
0.93	7.04395	3.53911	67.39604
0.94	7.57232	3.71803	79.27476
0.95	8.22348	3.93209	95.42409
0.96	9.06040	4.19804	118.68686
0.97	10.20689	4.54787	155.25984
0.98	11.95862	5.05543	222.02041
0.99	15.34966	5.96624	390.56947

APPENDIX B

This appendix contains fundus photographs showing visible lesion development and fluorescein angiography for a least one eye at each pulsedwidth. The order of pulsedwidths is from lowest to highest with the color visible lesion photograph first at 1 and 24 hours and then the FA photographs at 1 and 24 hours also.

Order of Photographs

Monkey #639-OD

Figure A.	90 fs-580 nm	1-hour color fundus photograph
Figure B.		24-hour " "
Figure C.		1-hour fluorescein angiography
Figure D.		24-hour " "

Monkey #775-OS

Figure A.	90 fs-580 nm	1-hour color fundus of suprathreshold lesions
Figure B.		24-hour " " "
Figure C.		1-hour fluorescein angiography

Monkey #639-OS

Figure A.	600 fs-580 nm	1-hour color fundus photograph
Figure B.		24-hour " "
Figure C.		1-hour fluorescein angiography
Figure D.		24-hour " "

Monkey #589-OS

Figure A.	3 ps-580 nm	1-hour color fundus photograph
Figure B.		24-hour " "
Figure C.		1-hour fluorescein angiography
Figure D.		24-hour " "

Monkey #773-OD

Figure A.	60 ps-532 nm	1-hour color fundus photograph
Figure B.		24-hour " "
Figure C.		1-hour fluorescein angiography
Figure D.		24-hour " "

Monkey #871-OS

Figure A.	60 ps-532 nm	24-hour MVL with Hemorrhage
Figure B.		24-hour fluorescein angiography

Monkey #866-OD

Figure A.	4 ns-532 nm	1-hour color fundus photograph
Figure B.		24-hour " "
Figure C.		1-hour fluorescein angiography
Figure D.		24-hour " "



639-OD

Figure A. (90 fs-580 nm) One-hour fundus photograph showing L-shaped marker grid surrounding MVL exposure sites. The 16 threshold data lesions range in energy of delivery from 0.52 to 4.8 μ J. Three hemorrhagic lesions occurred at 1.7 to 4.8 μ J, and became apparent ophthalmoscopically within 10 minutes.

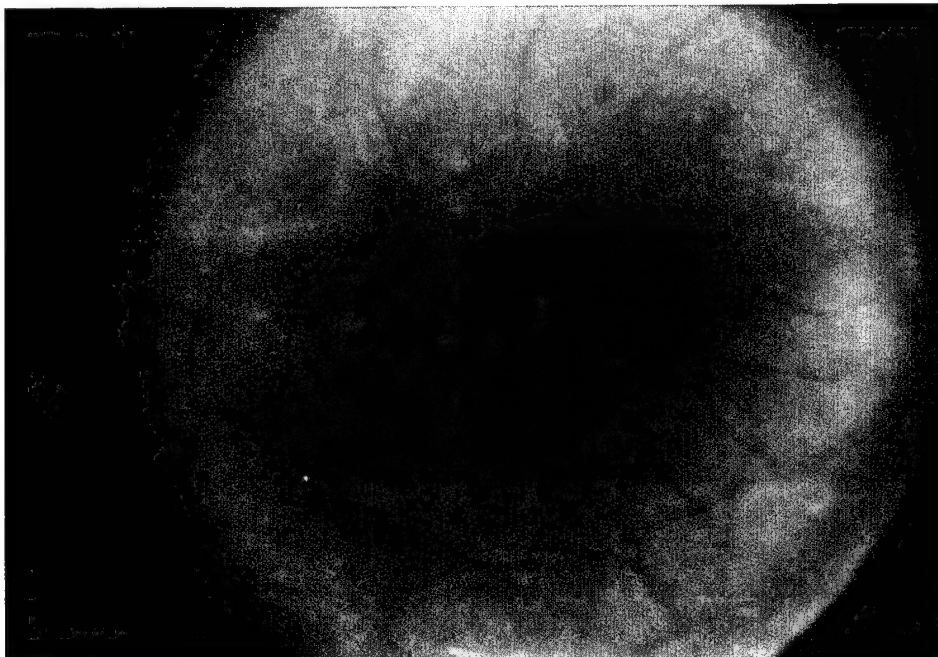
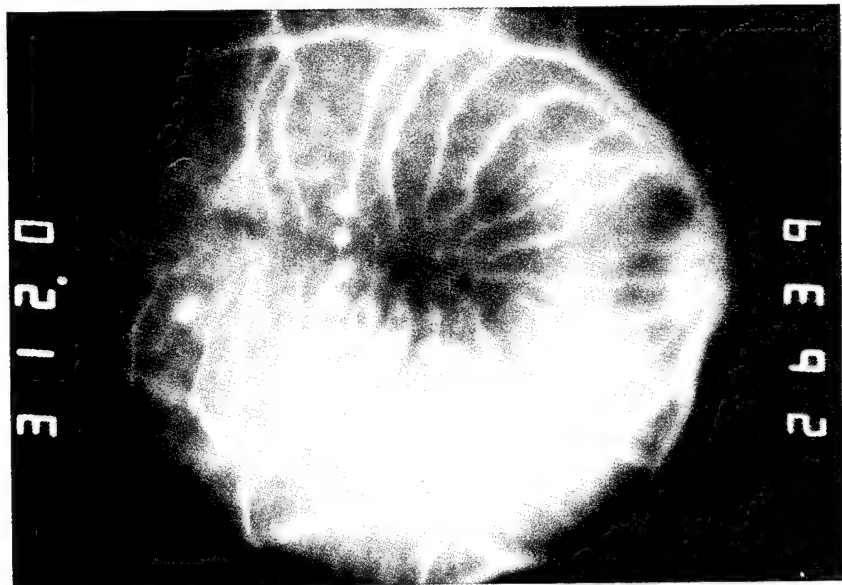


Figure B. 24-hour fundus photograph shows increase in the area of blood leakage from 3 hemorrhages, and more apparent whiteness from MVLs.



639-OD

Figure C. (90 fs-580 nm) One-hour FA showing lesions that demonstrate hyperfluorescence except where blocked by blood.

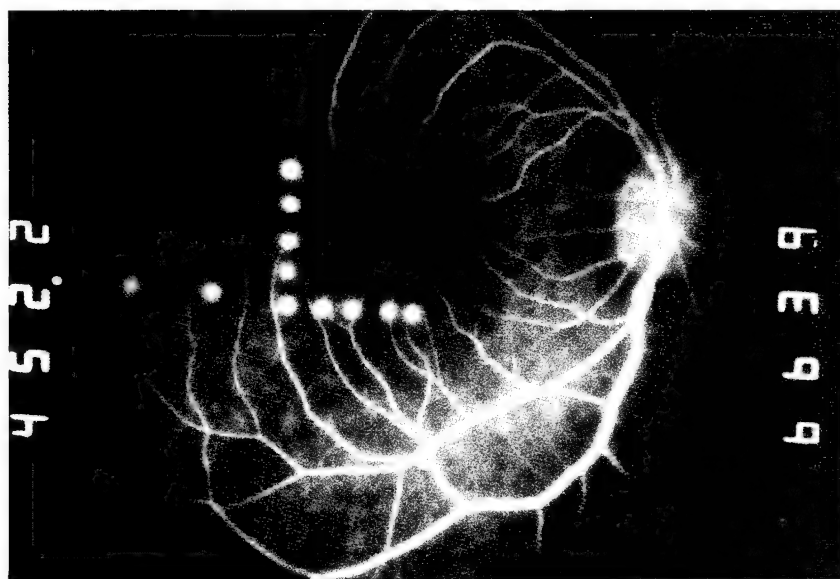
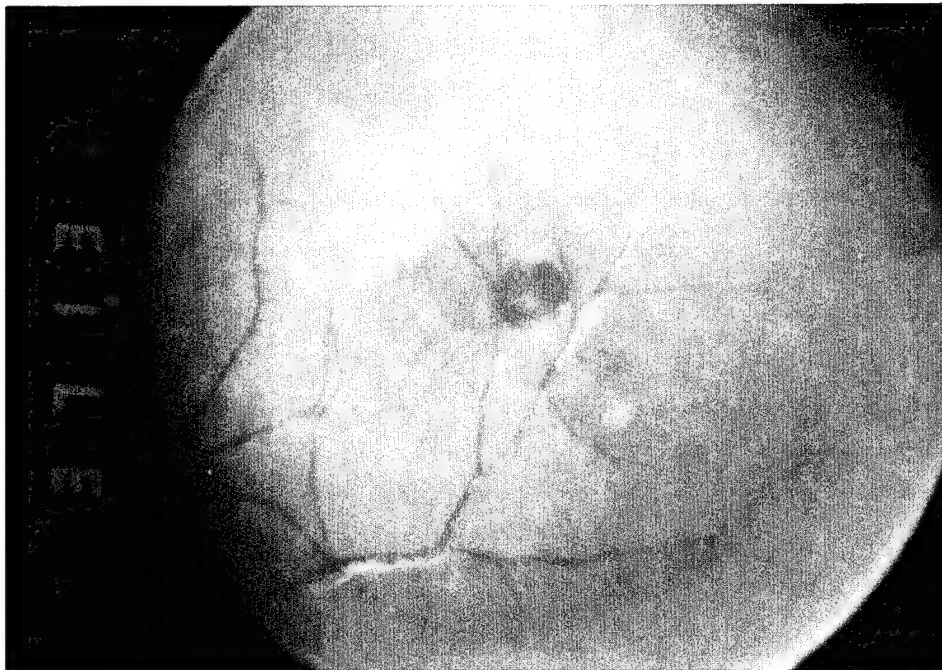


Figure D. 24-hour FA demonstrates fewer lesions that hyperfluoresce compared to those at 1 hour.



775-OS

Figure A. (90 fs-580 nm) One-hour fundus photograph of 6 suprathreshold lesions delivered from 22 to 82 μ J of energy. The hemorrhagic lesion in the macula occurred over a retinal venule with energy delivery of 81 μ J.

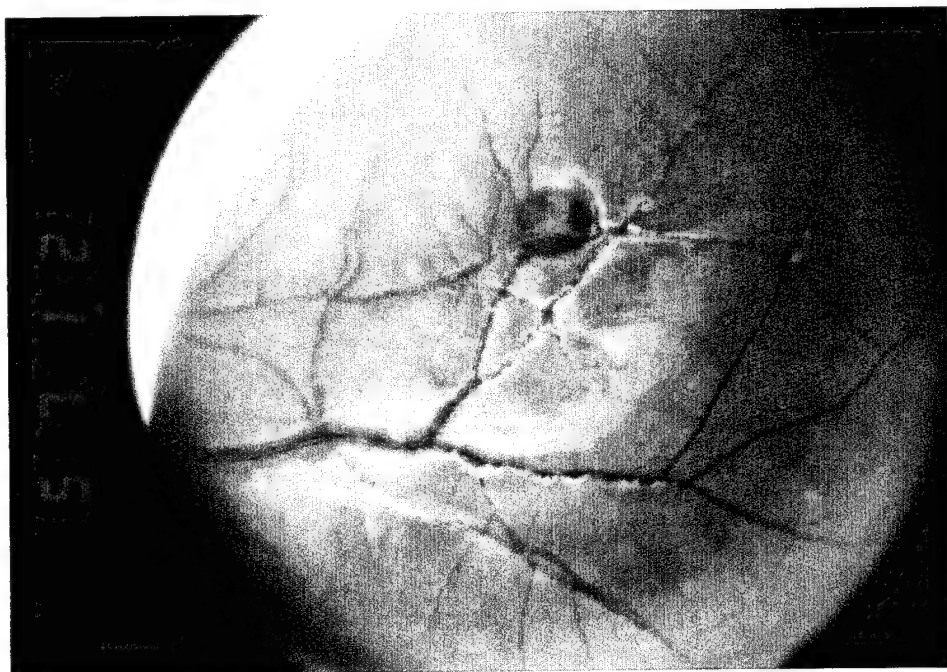
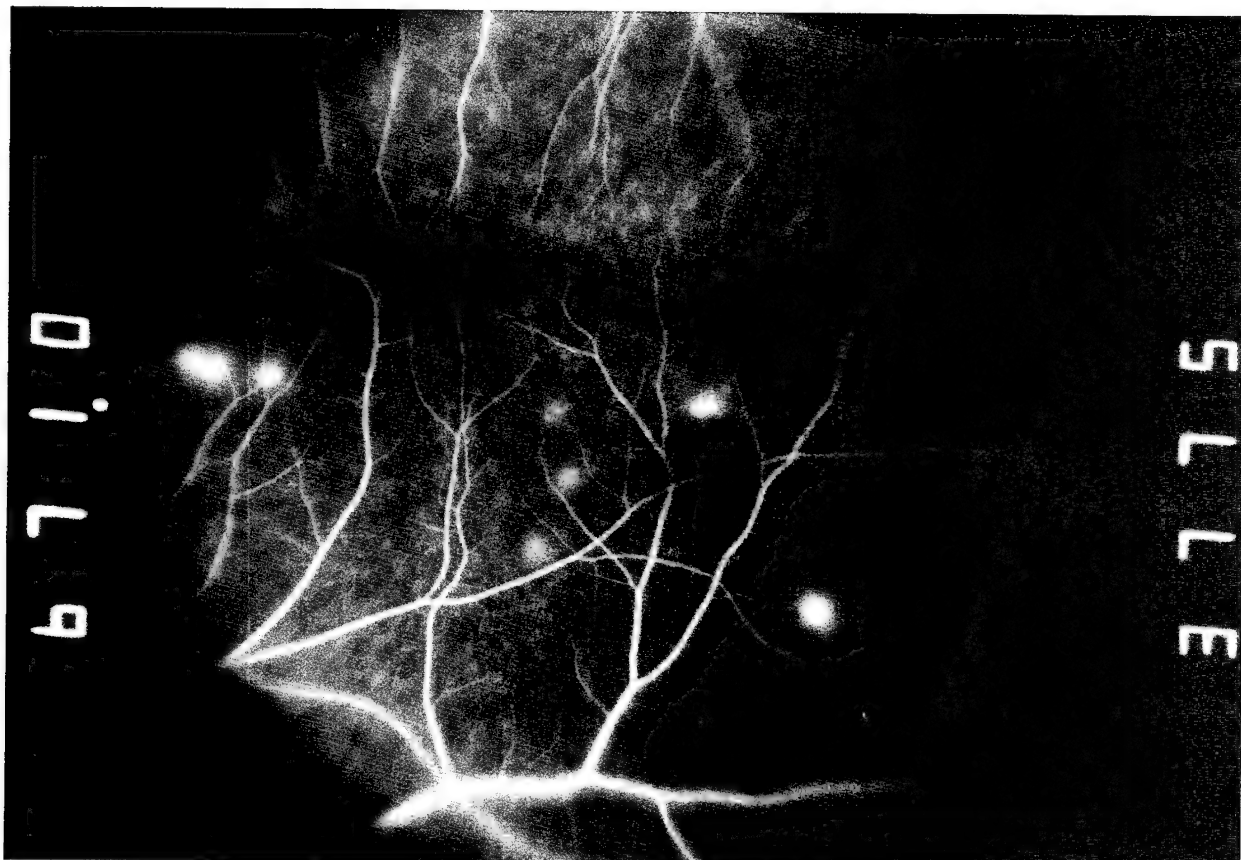
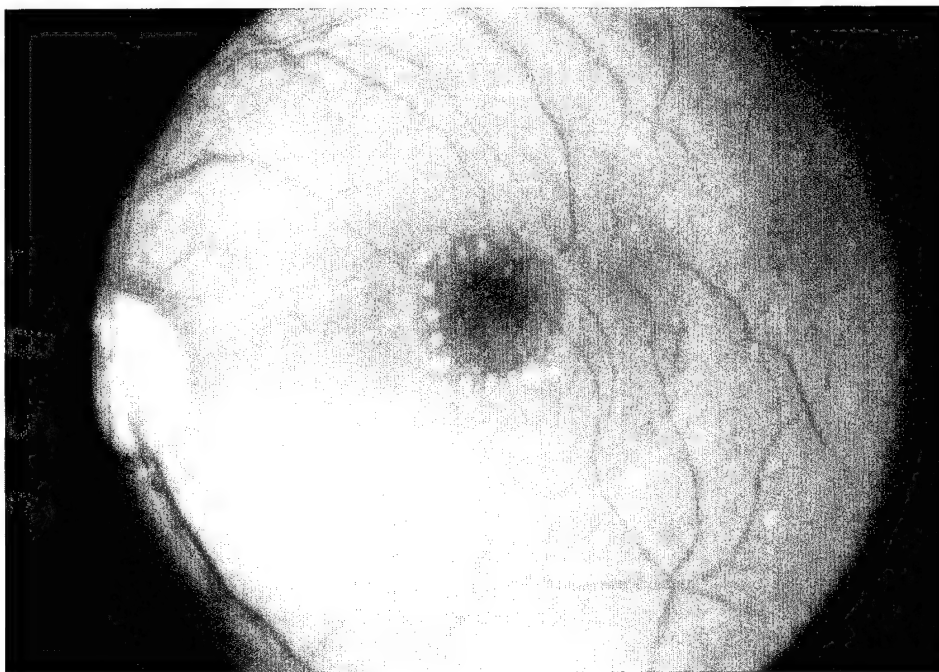


Figure B. 24-hour fundus photograph showing an enlargement of the 81 μ J hemorrhage as well as the non-hemorrhagic suprathreshold lesions



775-OS

Figure C. (90 fs-580 nm) One-hour fluorescein angiogram (FA) showing hyperfluorescence from the non-hemorrhagic suprathreshold lesions, and leakage within the area of blocked fluorescence from the site of the hemorrhage.



639-OS

Figure A. (600 fs-580 nm) One-hour fundus photograph of 25 threshold lesions ranging from 0.10 to 10.2 μ J. Three hemorrhagic lesions occurred between 3.6 to 10.2 μ J and became apparent ophthalmoscopically within 10 minutes.

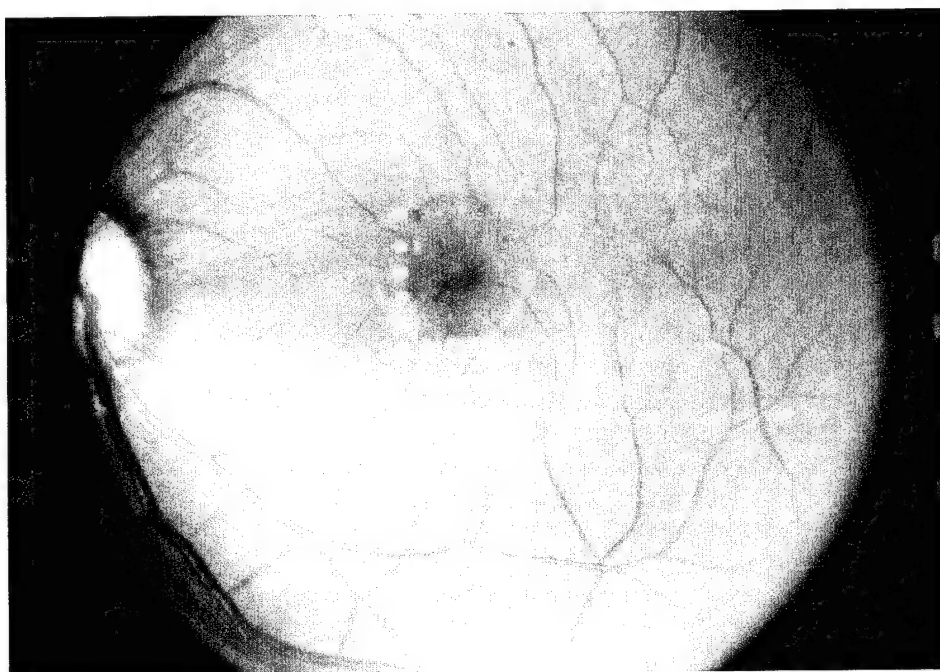
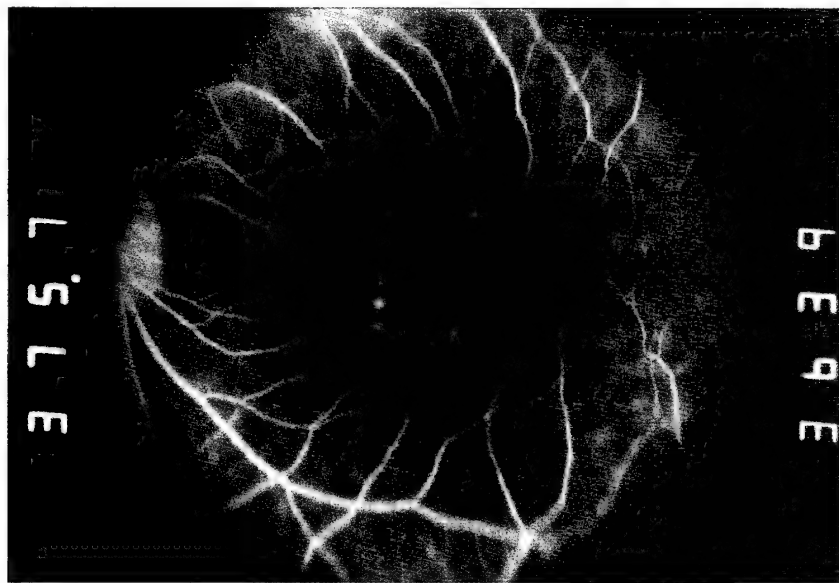


Figure B. 24-hour fundus photograph showing an increase in size of the 3 hemorrhages between 1 and 24 hours.



639-OS

Figure C. (600 fs-580 nm) One-hour FA showing a few sites of visible fluorescein leakage or blockage.

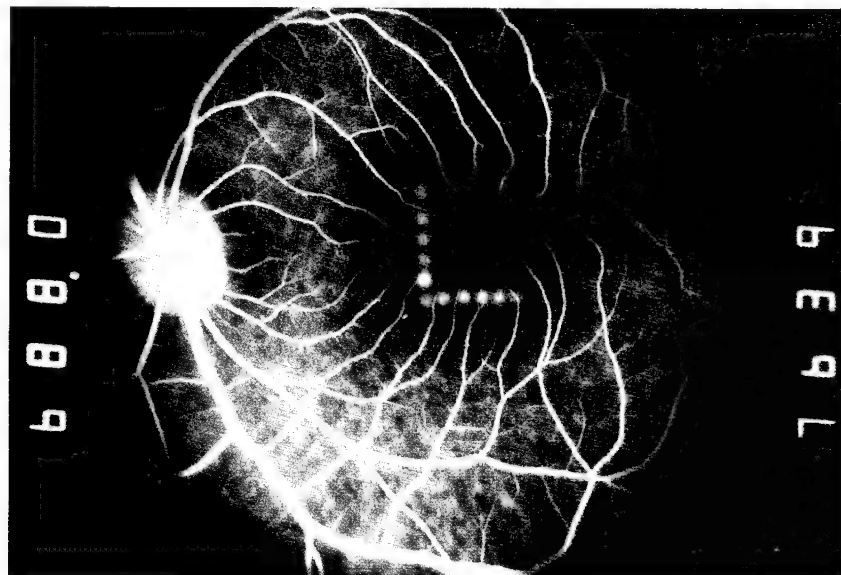
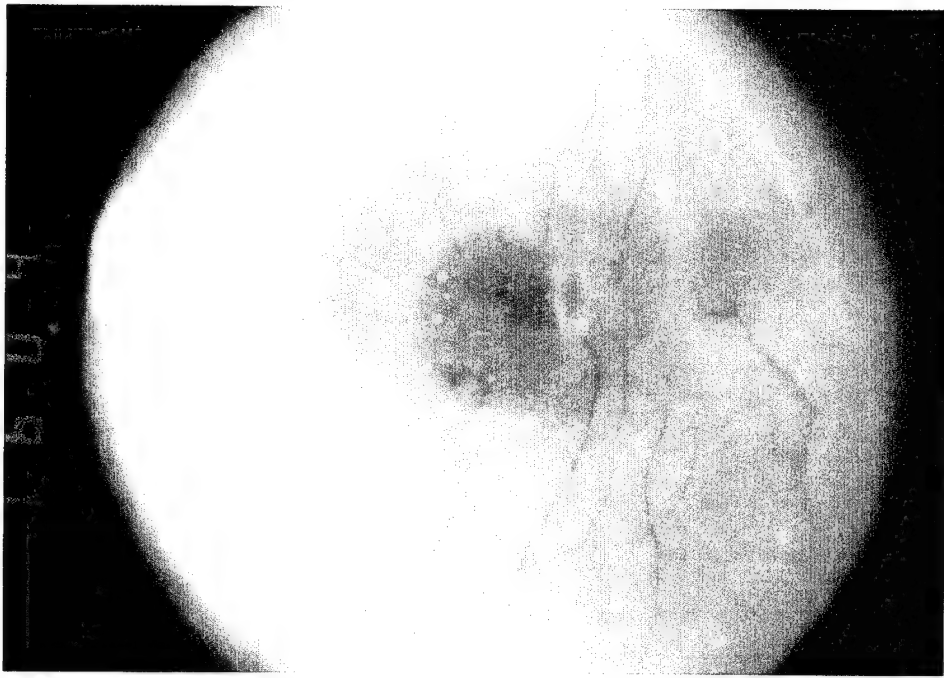


Figure D. 24-hour FA showing that more lesions are visible than in the 1 hour FA. This demonstrates that lesion development between 1 and 24 hours increased significantly. However, fewer lesions are visible in the 24-hour FA compared to the 24-hour fundus photograph, implying that fluorescein angiography is less sensitive than ophthalmoscopic evaluation.



589-OS

Figure A. (3 ps-580 nm) One-hour fundus photograph of 9 threshold lesions ranging in energy of delivery from 0.45 to 9.5 μ J. One hemorrhagic lesion occurred at 9.5 μ J and became apparent within 10 minutes.

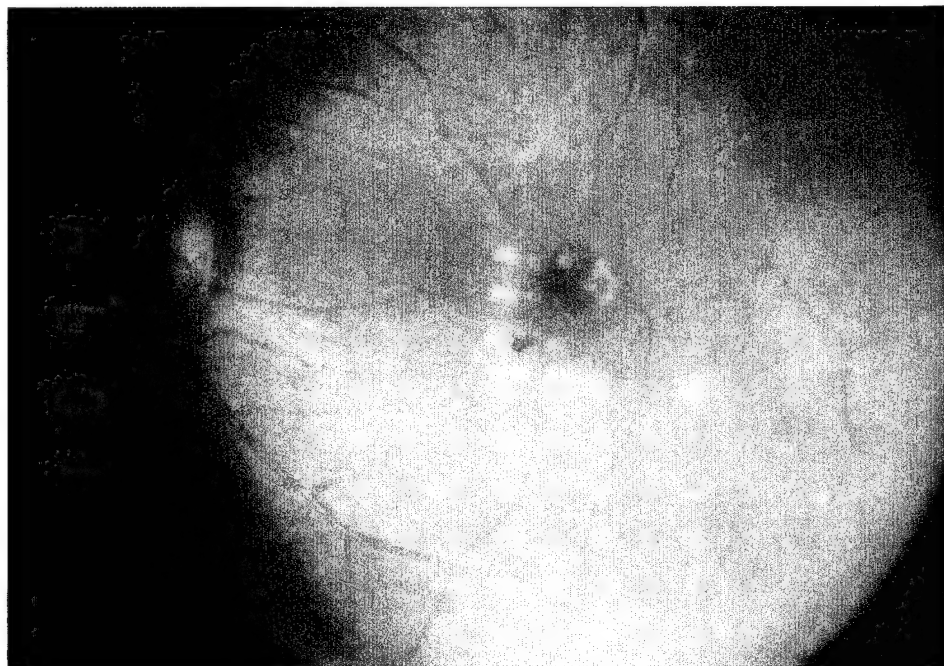
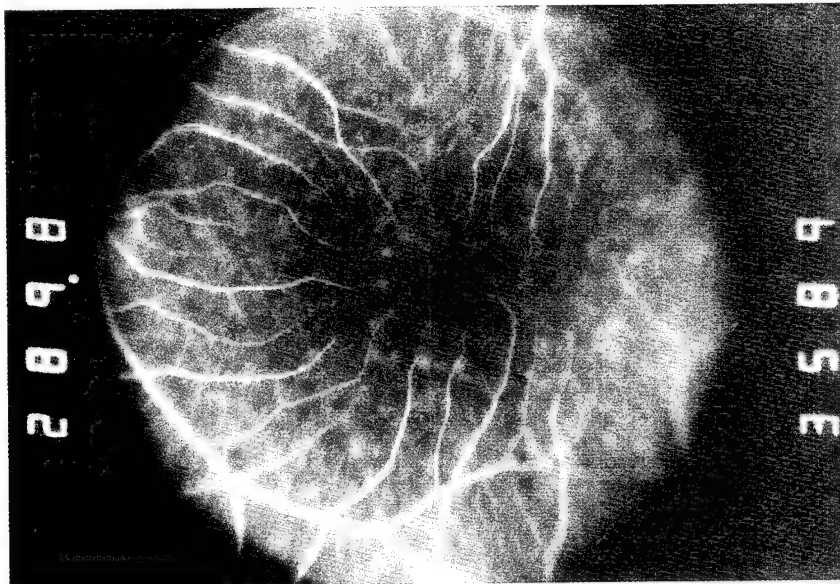


Figure B. All lesions became ophthalmoscopically visible within 24 hours.

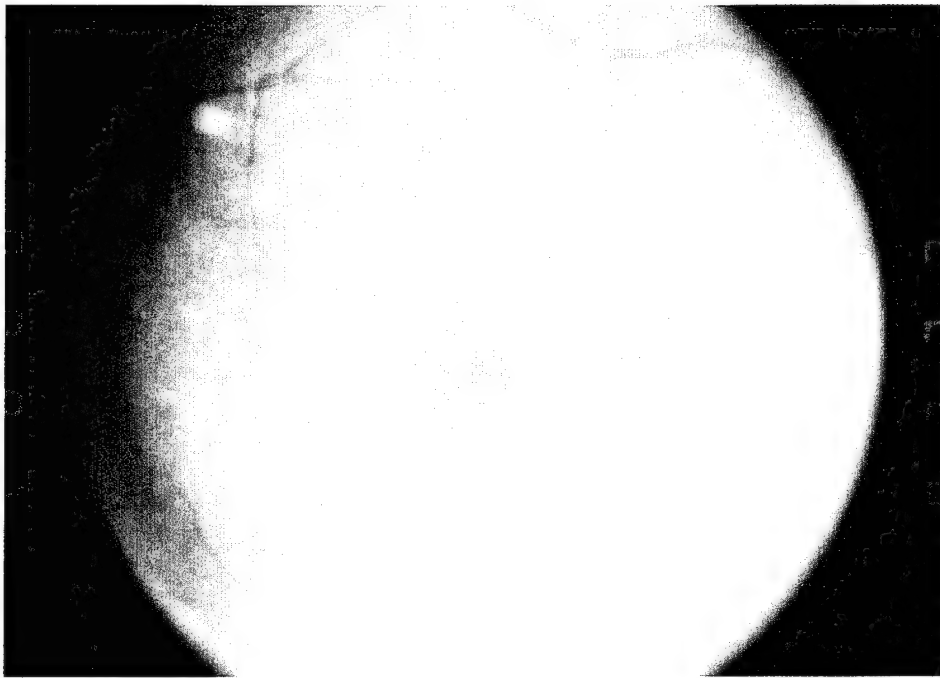


589-OS

Figure C. (3 ps-580 nm) One-hour FA showing the site of blocked fluorescence corresponding to the 9.5 μ J hemorrhage. Fewer lesions are apparent (as compared to Figure A.) showing a decrease in sensitivity FA compared to ophthalmoscopic evaluation. No hyperfluorescence marking the 1.7 to 5.3 μ J lesions is apparent by fluorescein angiography, although it was ophthalmoscopically visible at 1 hour.



Figure D. At 24 hours, FA determination shows all lesions in the middle row and the 1.4 μ J lesion (previously visible ophthalmoscopically) do not hyperfluoresce while all others emit a faint hyperfluorescence.



773-OD

Figure A. (60 ps-532 nm) One-hour fundus photograph of 9 lesions ranging in energy of delivery from 0.26 to 3.7 μ J. All lesions in the bottom row and the 2 lesions at 0.85 and 0.86 μ J became apparent within 1 hour.

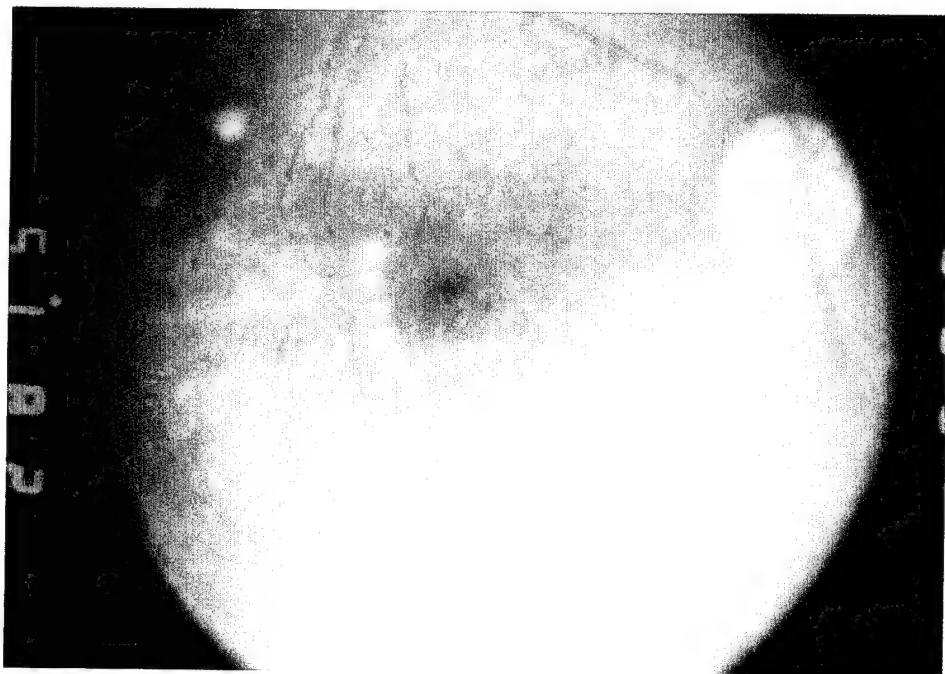
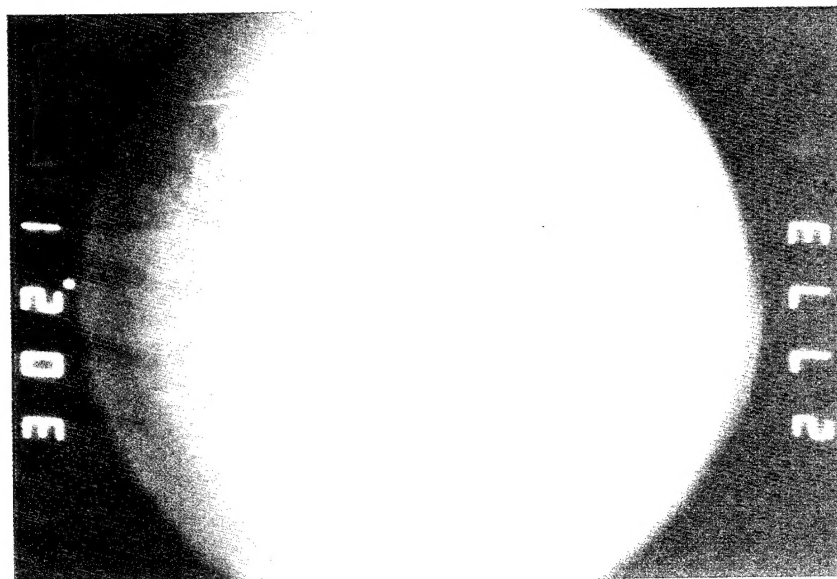


Figure B. At 24 hours, all lesions in the second row became ophthalmoscopically visible.



773-OD

Figure C. (60 ps-532 nm) One-hour FA shows very faint hyperfluorescence from a few of the 9 lesions.

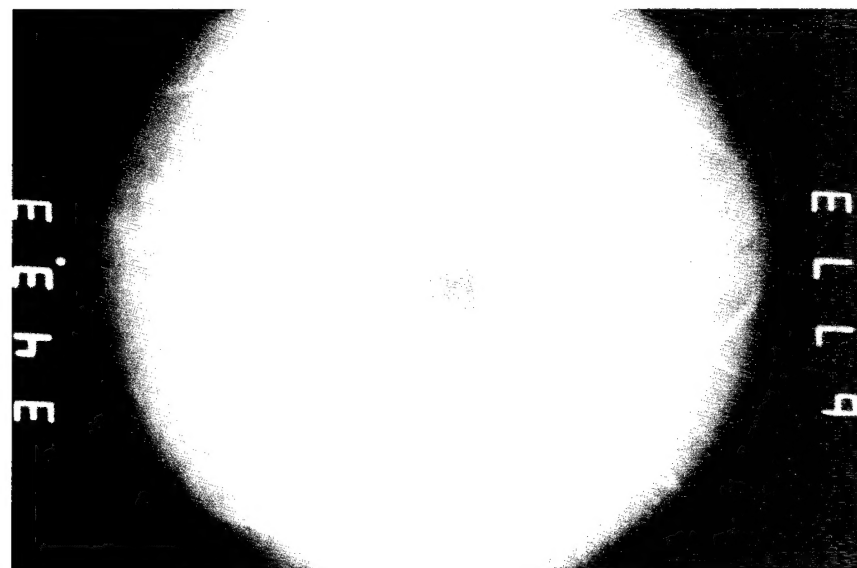
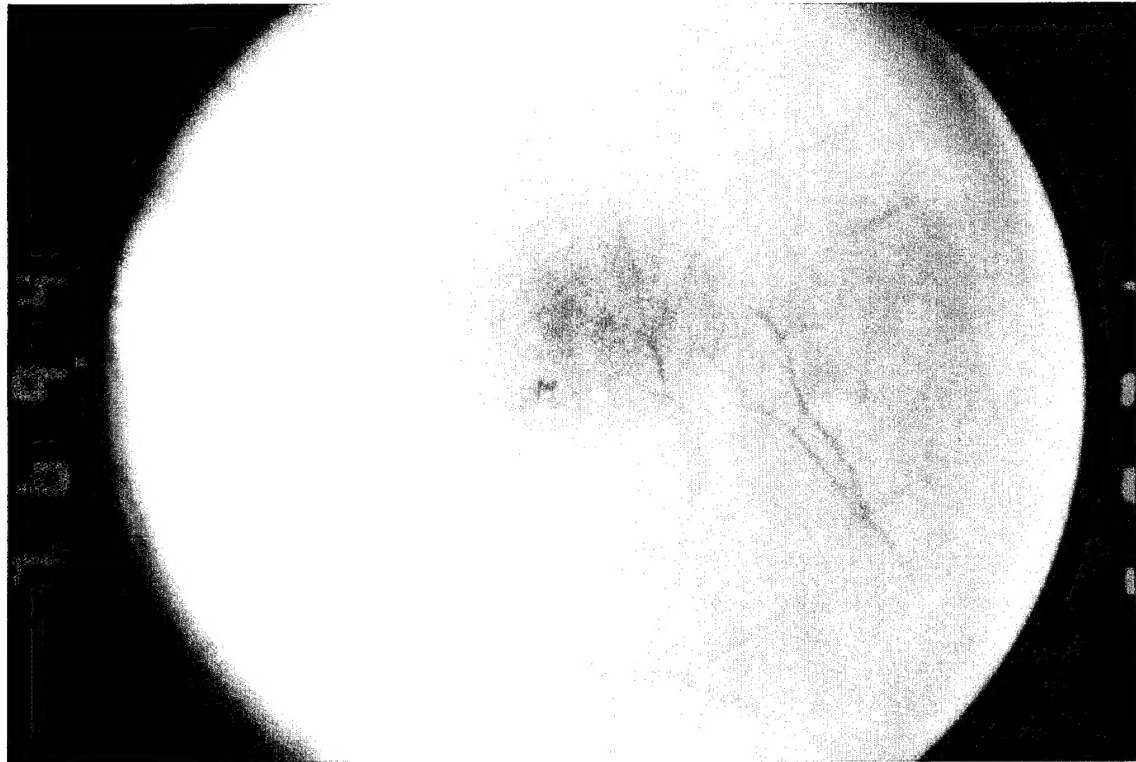


Figure D. The 24-hour FA demonstrates faint hyperfluorescence.



871-OS

Figure A. (60 ps-532 nm) 24-hour fundus photograph of 9 threshold lesions ranging in energy of delivery from 0.75 to 6.6 μ J. One hemorrhage occurred at 6.6 μ J and became apparent ophthalmoscopically within 10 minutes.

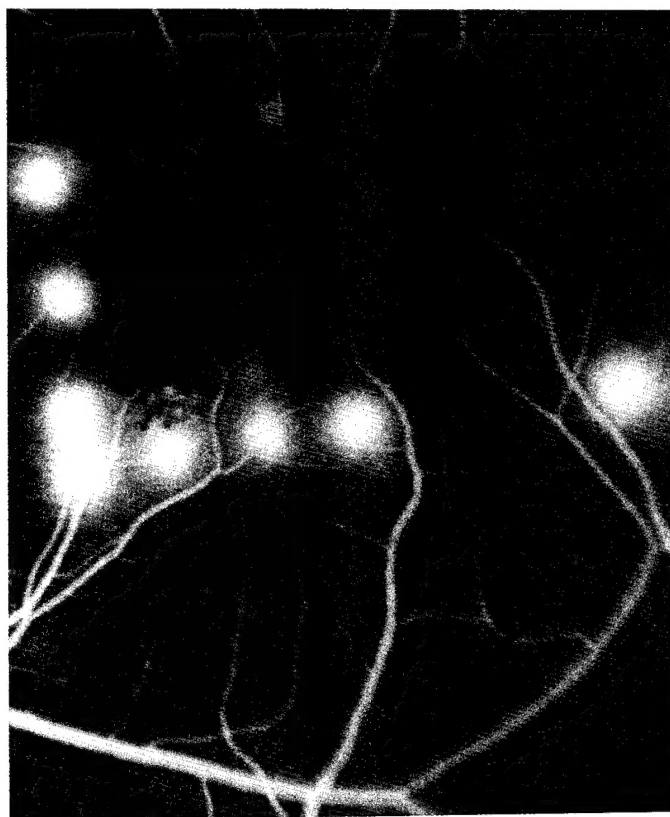
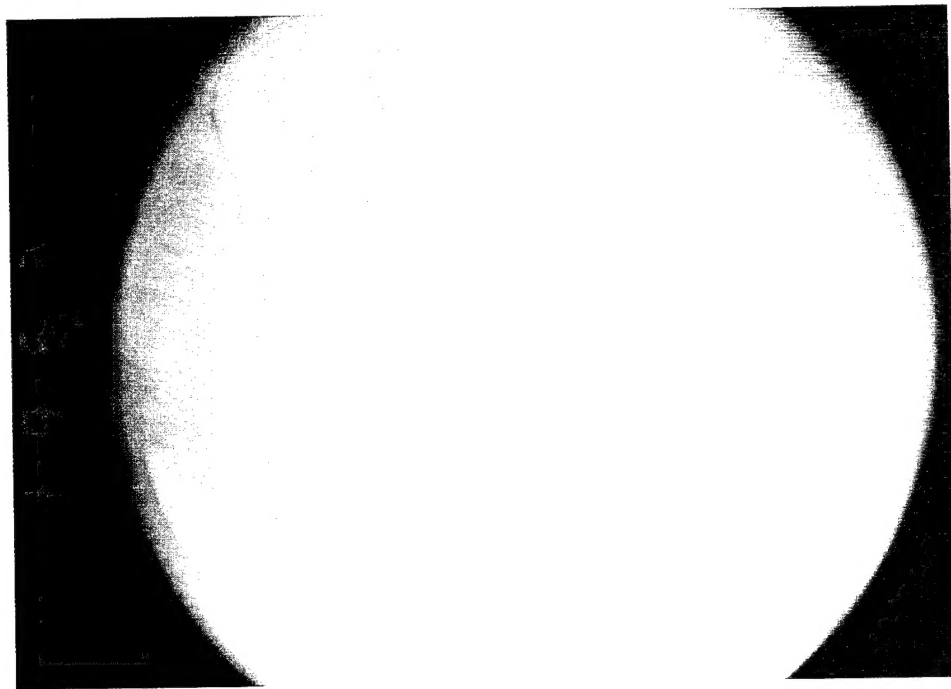


Figure B. The FA at 24 hours shows hyperfluorescence from MVLs.



866-OD

Figure A. (4 ns-532 nm) One-hour fundus photograph of 25 threshold lesions ranging in energy from 0.14 to 5 μ J incident at the cornea (demonstrated on the corresponding fundus map). A number of very faint MVLs became ophthalmoscopically visible within 1 hour.

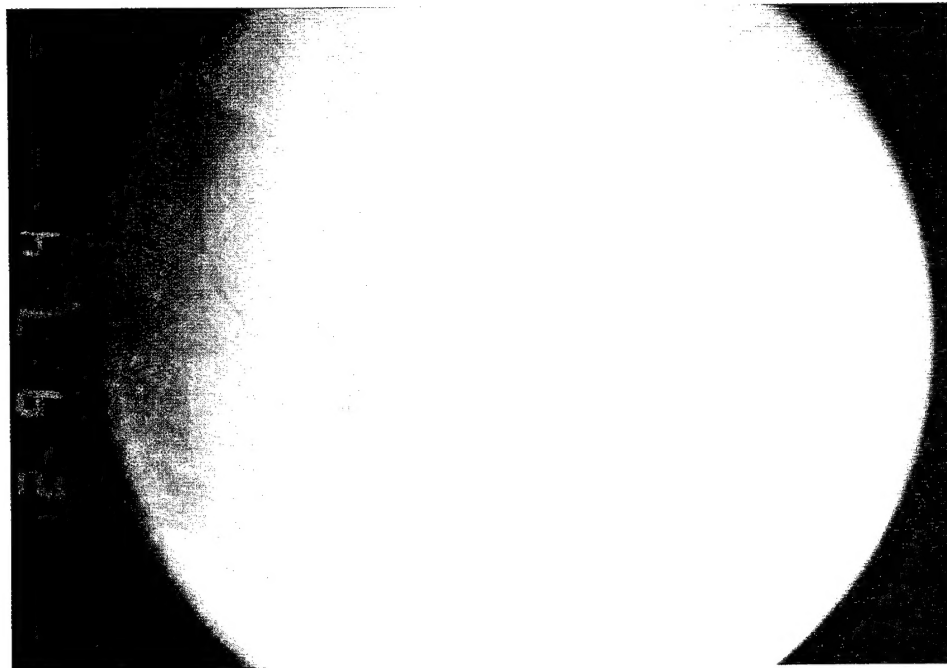
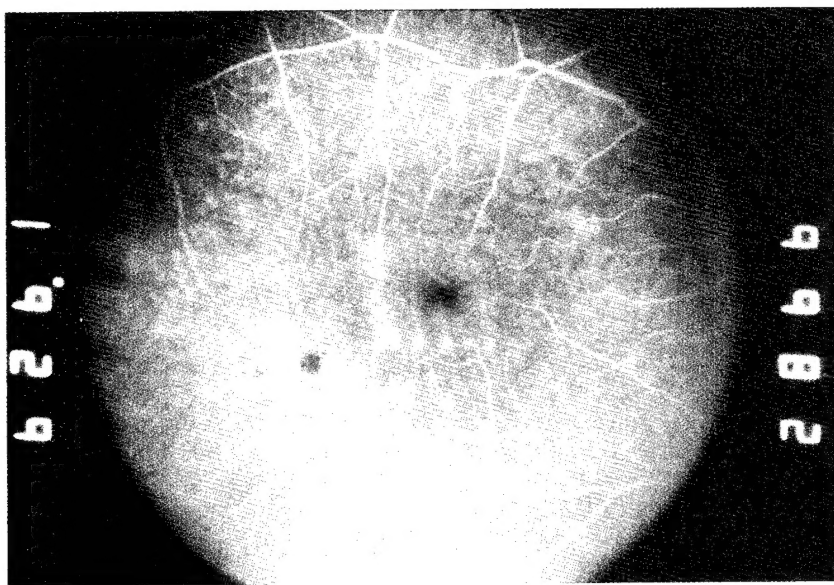


Figure B. The 24-hour fundus photograph shows an increase in the number of MVLs, and an increase in MVL lesion whiteness and diameter compared with the one-hour determination.



866-OD

Figure C. (4 ns-532 nm) One-hour FA, corresponding to Figure A, showing all lesions previously observed ophthalmoscopically.

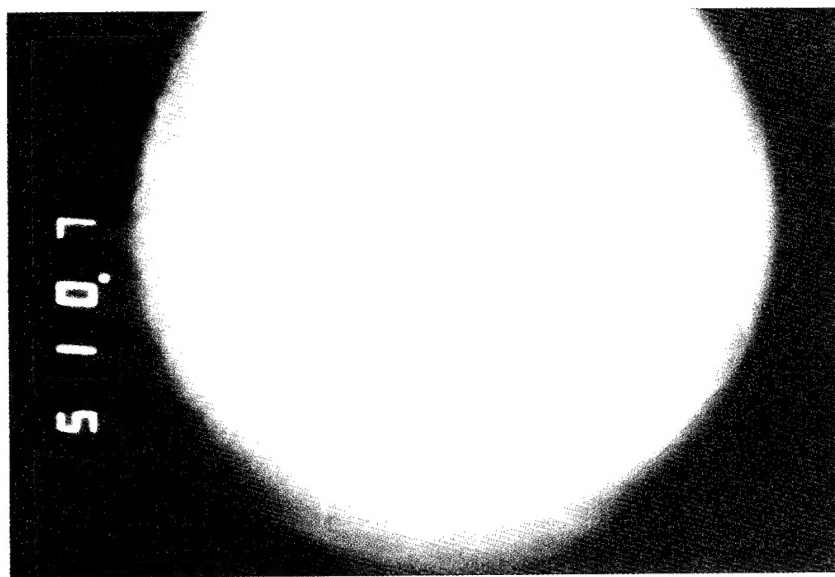


Figure D. 24-hour FA corresponding to Figure B. The MVLs emit faint hyperfluorescence and the angiograph demonstrates that fewer lesions were visible compared with 1 hour.